Alma Mater Studiorum - University of Bologna

Department of Electrical, Electronic, and Information Engineering "Guglielmo Marconi"

Automation Engineering Bachelor Degree's Thesis

Muscle isometric force model: Towards control design

Written by:
Nicholas Baraghini

Supervisor:
Prof.
Lorenzo Marconi

Co-Supervisor:
Mario Spirito

2020

To all the people who supported me along this path.

Muscles are in a most intimate and peculiar sense the organs of the will.

G. Stanley Hall

Abstract

Muscle is a complex physiological system; Medicine and physiology have faced the problem of analyzing it accurately by describing each of its particular functions. From a greater understanding of its performance came the interest to develop a model that could describe and simulate its behavior. Various models have been proposed in the past, from more complex and detailed to less elaborate and more approximate. However, in literature, it was not possible to find out any model that could represent satisfactory characteristics in such a way that it could be used for control purposes. With the future goal of being able to design an antagonist control for a complex muscular system, the need to develop a model, such that could describe the response simply and accurately and being implementable in a control system, arose. After a deep study of the most relevant models, it has been chosen to develop two prototypes. The first one, called Evaluation model, was developed to understand better the phenomena of muscle force production in Isometric conditions; This prototype is designed to emulate muscle response in a simplified way, neglecting effects such as yielding, and fiber recruitment. The second model, defined as Control model, has been developed as a linear product of two nonlinear components. The particular structure of the Control model was conceived to use this prototype for the design of the controller through particular control techniques that require a linear and simple model. Both models were designed in such a way as to be able to simulate the strength response of any muscle belonging to any animal. To this end, the two prototypes have a certain number of degrees of freedom which must then be tuned according to the nature and type of muscle considered. The results obtained were by far satisfactory, obtaining an average representation error with very low empirical data, thus demonstrating the validity and the goodness of the models developed.

Contents

List of Figures

List of Tables

Introduction

The thesis will deal with the development of two models: one, called Evaluation model, it is designed to provide a simple and accurate description of the main phenomena occurring during an active contraction, or a passive stretching of a muscle. The second one, called Control model, is synthesized to afford a prototype implementable for the design of control systems. These models will then be compared with previously created prototypes found in literature. Their behavior was then validated through comparison and an analysis of the error conducted with empirical data, coming from different animals. In the last part of the paper, simulations overtime of the trends assumed by the two models were implemented to describe a simple force-imposed experiment.
In the first chapter, therefore, the muscle is presented as a biological actuator, and its physiology has been reported to understand the mechanical and physiological principle exploited by the muscle to generate force. In the second chapter, then, are described in detail the models found in literature, we have used as a reference to build the two prototypes. Always in the same chapter, it is explained how we carried out the development of the Evaluation model. Furthermore, the two last sections of this chapter deal with the comparison with the empirical data, for validation, and a last comparison with the models developed in other studies described at the beginning of the same chapter. On the other hand, the third chapter deals with the description and the validation of the development of the Control model. In the final part of the third chapter is also described a simulative result used to perform a simulation in time of the behavior of both the prototypes, comparing their trends and analyzing the error of deviation between them. In the last chapter the conclusions are drawn and, parallel and future projects related to this paper are mentioned.

Chapter1

Fundamental Muscle Mechanics

This chapter aims to introduce the muscle system as a machine capable of actively producing tension. Therefore the main mechanical and physiological notions, which were the theoretical basis in the development of the models, are reported.

1.1 Morphology of Skeletal Muscles

Muscle is the soft tissue that builds the human musculoskeletal system. The organ system which gives humans the ability of independent motion.
Skeletal muscle is one of the three types of muscles in a mammalian body, among cardiac muscle and smooth muscle. The main feature of this type of muscle, that made it distinguishable from the other two, resides in the fact that skeletal muscles connect bones. So as a similitude, the skeletal system of a mammal represents its rigid structure, a complex kinematic chain, and the skeletal muscle system represents the actuation system. Through the contraction of a muscle, the relative position of bones changes, and the development of forces and torques happens as a consequence of the muscle activity. Each fiber which composes the muscle contains a massive number of myofibril that are the constitutive elements of the myocytes. Those last elements are the characteristic elements that make up the whole muscle. In turn, each myofibril is made up of thousands of myosin and actin filaments; Those filaments are found to be intertwined in order to create a sequence of actin bands alternated with myosin bands. Myosin filaments show small projections protruding from the threads called cross-bridges. Thus, in other words, cross-bridges are the globular heads of a myosin molecule that projects from a myosin filament in muscle. And those last elements are the key factor which links the two types of filaments of the myofibril and produce the muscle contraction [Sweeney & Hammers (2018)].
Each actin filament is fixed, at one end, to a disc of protein, called Z-disk, which goes across the whole thickness of the myofibril and is connected to other discs of adjacent myofibril cells, imposing a continuous distribution of myofibril along with the thickness of the muscle fiber [McMahon (1943)]. The portion of myofibril between two Z-disk is also called Sarcomere. So in other words, the sarcomere is the basic contractile unit of striated muscle and consists of an A band containing myosin ("thick") filaments, which is flanked by two half I-bands made up of actin ("thin") filaments. This A band is the central region of the sarcomere, composed primarily of myosin filaments, the force-generating motor protein of skeletal, cardiac,

and smooth muscle. Sarcomeres are organized in series to make up a myofibril.

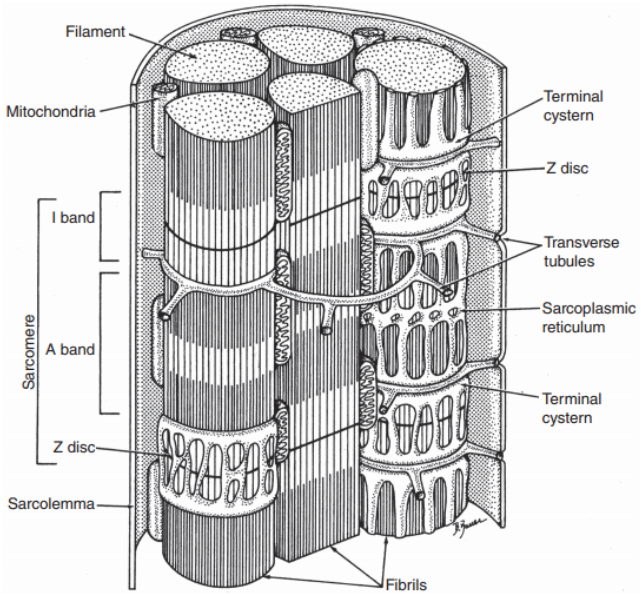

Figure 1.1: The basic architecture of a mammalian striated skeletal muscle fiber, consisting of myofibrillar bundles of paracrystalline myofilaments organized into serially repeating sarcomeres. Action potentials traveling along the sarcolemma and invaginations called transverse tubules to activate the contractile state by releasing calcium from terminal cisternae of the sarcoplasmic reticulum; relaxation occurs as calcium is pumped back into the sarcoplasmic reticulum. Varieties of scaffold structures (not illustrated) maintain the highly regular alignment of all of these structures across the length and breadth of muscle fibers. The figure is taken from Tsianos & Loeb (2017)

1.2 Parallel-Fibered and Pennate Muscles

The force produced by a muscle depends in a significant way on the direction of the fibers concerning the longitudinal axis of the muscle itself.
Then a classification can be made according to fibers distribution with respect tendons' longitudinal axis:

- Parallel fibers. This type of distribution allows a faster and wider movement;
- Oblique fibers, also called Pennate fibers. This configuration allows the delivery of remarkable strength of contraction but imposing a slow movement and of modest amplitude. Pennate muscles can further classified as:
  - *Unipennate muscles*, have the tendon running along one side;
  - *Bipennate muscles*, the tendon passes up the center of the muscle and the fibers attach to it on either side;
  - *Multipennate muscles*, have aponeuroses of the tendon material approaching the belly of the muscle from both ends, and the fibers run only for a short distance from one aponeurosis to another.

Considering a pennate fiber the angle of pennation is defined as the angle between the main axis of the muscle fiber and the action direction of the muscle, in other words the axis on which the force is developed. The pennation angle is always found in the range [0,30°] and it can increase during the motion. The force of distribution of pennate fibers transmitted to the tendon is found to be maximum when the pennation angle is 0 and it decreases when this angle increases [McMahon (1943)]. When muscle fibers are found to be diagonally oriented with respect the axis where the force is developed only a portion of the tension produced by a single fiber will contribute to the total force delivered by the muscle, and the magnitude of the parallel component of force with respect the axis of the resultant will depend on the angle of pennation of the fiber distribution. Accordingly in pennate muscles, the total force delivered by the muscle is less than the sum of all the forces released by all the fibers which build the entire muscle; In general, the delivered force is 90% of the effective force. However, pennate muscles are generally more powerful than parallel-fibered muscles of the same weight, because their organization allows a larger number of fibers to work in parallel. But because all the fibers are shorter, pennate muscles have a shorter working stroke, and therefore a lower end-to-end velocity of shortening.

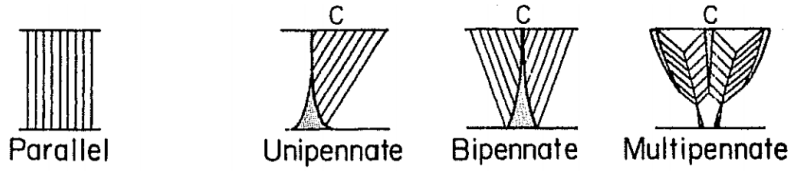

Figure 1.2: The lined labelled C represents the midpoint of the muscle halfway between the origin and insertion.

The model developed does not take into account the pennation of the muscle to make the final product as simple and general as possible.

1.3 General Contraction Mechanism

The start and execution of muscle contraction occurs according a perfectly coordinated sequence of event :

- An action potential travels along a motor neuron to its terminations on muscle fibers;
- At each termination the nerve releases a small amount of neurotransmitter substance called acetylcholine;
- The opening of these channels allows the entry of large quantities of sodium ions into the muscle fiber. This determines the onset of an action potential on the membrane;
- The potential propagates along the muscle fiber membrane in the same way it propagates along the nerve fiber membranes;

- The action potential depolarizes the membrane of the muscle fiber propagating towards the center of the fiber itself, where it causes the release of large quantities of calcium ions from the sarcoplasmic reticulum, stored inside the reticle itself;

- Calcium ions initiate a process that gives rise to attractive forces between the myosin and actin filaments, which cause them to slide over each other, i.e. contraction;

- After a fraction of a second, the calcium ions are brought back into the sarcoplasmic reticulum by a membrane pump for Ca^{++}, where they remain stored until the onset of a new action potential. With the removal of calcium ions, muscle contraction ends;

1.3.1 Contraction at Molecular Level

Considering a sarcomere, defined as the portion of myofibril enclosed by two Z-disks. In a state of relaxation, the ends of actin fibers belonging to different Z-lines do not overlap. On the other hand, in a state of contraction, those actin filaments belonging to different Z-disks will be pulled towards each other by the bond formed with the myosin filament and overlapping will occurs [McMahon (1943)]. Moreover, the Z-lines can be thought linked fixedly with the actin filaments, this lead to the fact that during contraction the distance between two consecutive Z-disks will decrease and so the overall effect is that the muscle is shortening. Thus the muscular contraction happens according to a sliding mechanism of filaments. The relative sliding which takes place between actin and myosin filaments is caused by the interaction of the cross-bridges [Rall (2014)].
Actin filaments contain an additional protein, called tropomyosin, which is wrapped as spirals along the actin filaments. The main task of those molecules is to avoid the interaction of myosin globular heads with the actin filament and so to avoid the formation of cross-bridges.
Therefore, from a molecular point of view, after calcium ions are released in the sarcoplasmic reticulum, due to stimulus on the surface of the muscle fiber, such ions diffuse through the cytoplasm of the thin filament. The calcium ions will bind with the troponin site placed in the tropomyosin molecule causing the unroll of this last one from the thin filament of actin and revealing the active site on it. This leads the globular head of myosin to bind to an actin filament site. This type of connection is called cross-bridge.
Just after the bond has been created the projection of the myosin filament, changes its structure in order to reshape the angle of attachment with the thin filament. This adjustment produces a mutual force between the thick and the thin filaments. Thanks to the force occurring between the two fibers a relative sliding take place for a distance which goes from $50 \cdot 10^{-7}$mm to $100 \cdot 10^{-7}$mm .
During the first part of the cycle, myosin heads carry the hydrolyzed product of the ATP, the Adenosine Diphosphate.
At the end of the work stroke, the cross-bridge releases the molecule of ADP and bind itself with a molecule of ATP present in the cytoplasm, and uses the energy of the Adenosine Triphosphate, by splitting it into a molecule of ADP plus a Phosphate,

to separate itself from the thin filament and coming back to the starting position ready to start a new working cycle.

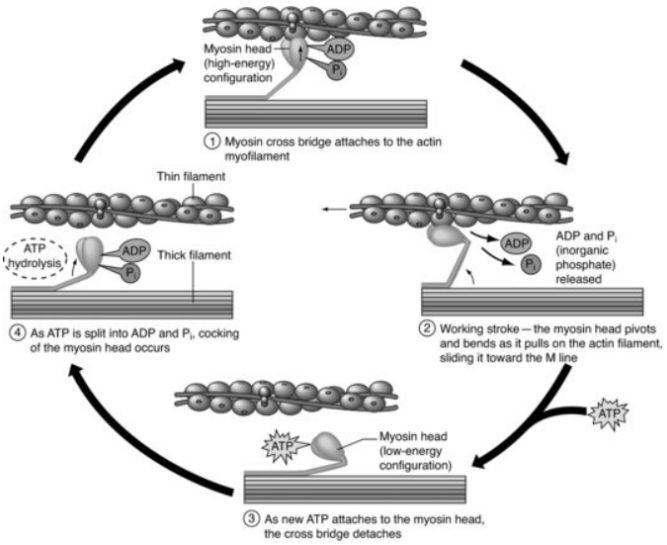

Figure 1.3: Sliding Filament Theory working Cycle. Taken from https://musculoskeletalkey.com/pathophysiology-of-skeletal-muscle-injuries/

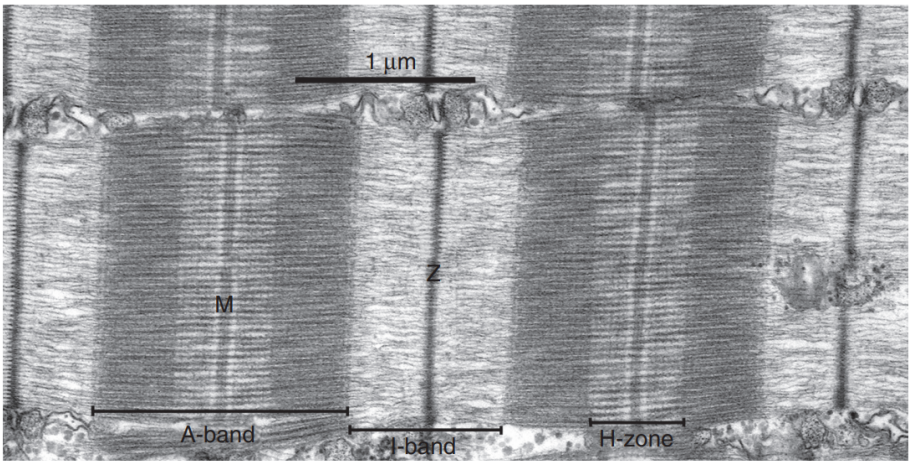

Figure 1.4: Organization of the sarcomere of skeletal muscle. Electron micrograph of a longitudinal thin section through a muscle fiber, with the fiber long axis horizontal. Two complete sarcomeres are shown, and elements of the sarcoplasmic reticulum separate myofibrils in the longitudinal direction. The major bands and lines are indicated, notably, the thin, distinctive Z-line flanked by two low-density half I-bands, with very dense A-bands containing the thick filaments. The relative densities of the bands in this electron micrograph are related to their content of protein. The light band on either side of the M-line shows the extent of the cross-bridge-free regions of the thick filaments. The fine transverse periodicity across the A-band, at 43 nm, is due to the periodic structure of the thick filament backbone, which in turn determines the position of relaxed cross-bridges on the surface of the filaments and is enhanced by the presence of accessory proteins Figure taken from Sweeney & Hammers (2018)

1.3.2 Types of Muscle Contraction

Muscle contractions are described based on two aspects: force and length. When the force in a muscle increases without a corresponding modification in length the contraction is claimed to be isometric. Isometric contractions are necessary for maintaining posture and stabilizing a joint. On the opposite side, if the muscle length changes whereas the muscle tension remains comparatively constant, then the contraction is defined as isotonic contraction. Moreover, the isotonic contraction will be any further classified in concentric contraction, when the muscle generates tension and also the entire muscle shortens, and as eccentric contraction, when lowering the weight from the shoulder to the waist the bicep would also be generating force, but in this case, the muscle would be lengthening. Eccentric contractions work to decelerate the movement at the joint, and additionally, this type of contraction can generate more force than concentric contractions.

1.4 Twitch & Tetanus

A single electrical impulse imposed on the muscle result in a peak of force delivered by the muscle itself referred to as twitch. A train of impulses appropriately spaced in time from each other will generate a sequence of twitches with the same amplitude. By increasing the frequency of the impulses, thus reducing the amount that separates two consecutive electrical impulses, then it can be seen as a rise of the magnitude of the last twitch considered [McMahon (1943)]. In other words, considering two consecutive twitches once the second starts before the first one is over, then the second twitch develops a bigger peak tension. The effect becomes pronounced as the twitches are brought closer together. When a train of stimulations is imposed to the muscle, after a certain transient time from the first impulse, a steady magnitude of tension is measured from the muscle, with a certain ripple superimposed at the stimulation frequency. This type of behavior is called unfused tetanus. By increasing the frequency of impulses the ripple will reduce, the mean force raises until it is reached the frequency at which the ripple is practically null and the mean force cannot be increased any further. In this case, it has been achieved complete tetanus.
Tetanic fusion frequency is about 50 to 60 shocks per second in the mammalian muscle at body temperature.

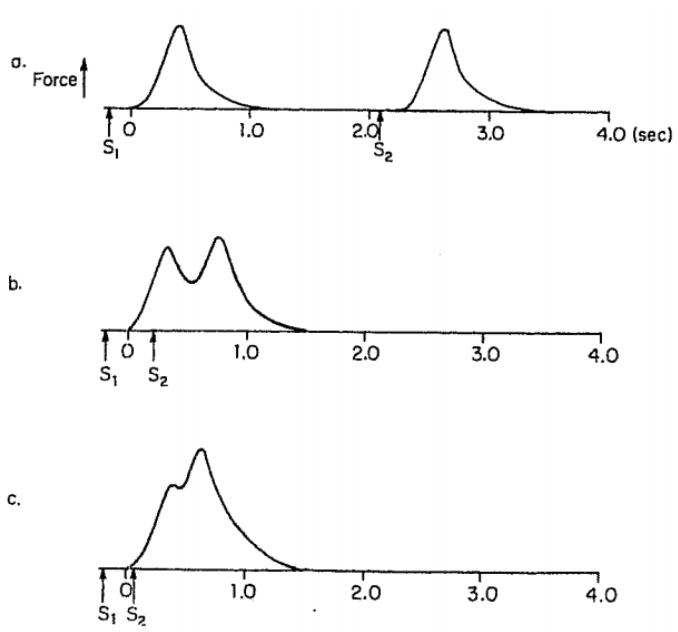

Figure 1.5: Two-Twitch experiments.
(a) When two identical electrical stimuli, S_1 and S_2, are given with a suitable time interval separating them, the two transient force events (twitches) are identical.
(b,c) When the stimuli are moved closer together, the second twitch reaches an higher force maximum than the first McMahon (1943)

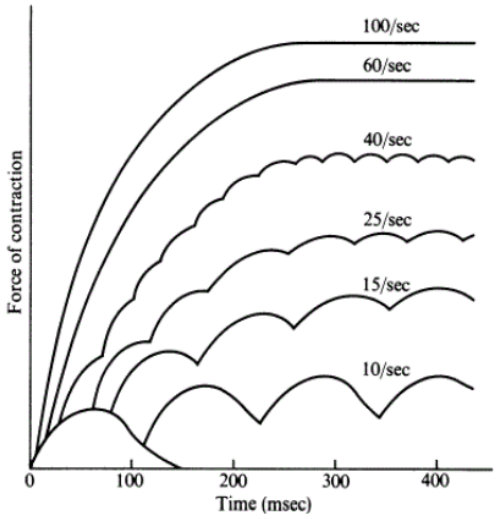

Figure 1.6: Twitch and Tetanus. When a series of stimuli is given, muscle force rises to an uneven plateau (unfused tetanus) which has a ripple at the frequency of stimulation. As the frequency is increased, the plateau rises and becomes smoother, reaching a limit as the tetanus becomes fused. McMahon (1943)

1.5 Spinal Marrow Organization for Motor Functions

Each section of the spinal marrow contains, within the grey matter, a high number of neurons for each spinal nerve. Among those neurons can be distinguished two particular types of neurons called motor-neurons of the anterior horns and interneurons. Motor-neurons of the anterior horns give rise a nerve fibers that starting from the marrow they innervate the muscle fibers of the skeletal muscle. Two types of neurons belonging to the family of the anterior horns' motor-neurons can be identified:

- α-*motorneuron*: the excitation of one of this fiber lead to the excitation of a certain number of skeletal muscle fibers.
- γ-*motorneuron*: this type of motor-neurons transmit their impulses to a particular class of skeletal muscle fibers, called intrafusal fibers. Those muscle fibers are placed in the polar portion of spindles, which are muscle structures involved in the control of muscle tone.

On the other hand, Interneurons, are those neurons which are found in central nodes of neural circuits, enabling communication between sensory or motor-neurons, and the central nervous system.[Guyton & Hall (2006)] So, in other words, interneurons are neurons that cannot be classified either as sensory or motor neurons. An example of interneurons that can be found in the anterior horns of the spinal marrow are the so-called Renshaw Cells. Those type of interneurons are inhibitory neurons which can obstruct motor-neurons close to them. In this way, each excited motor-neurons, through the activation of the Renshaw cell, can inhibit other motor-neurons close to the excited one such that the signal results to be less affected by noise. This mechanism is called lateral inhibition or recursive inhibition. These effects were not considered in this paper, but are discussed in a parallel work conducted, described by F.Curto (2020).

1.5.1 Sensory muscle receptors

Proper control of muscle function requires not only the excitation of the muscle produced by the motor neurons of the anterior horns of the spinal cord but also by the continuous flow of sensory information from the muscle itself to the CNS, so that, at each instant of time, the functional situation of the muscle are known [Guyton & Hall (2006)]. In other words, it is necessary that the CNS knows, every time, the length assumed and the tension developed by the muscle and the rapidity of variation they acquire. In order to provide this type of informations muscles and tendons are provided with two kinds of sensory receptors :

- *Muscle Spindles*: stretch receptors, within the body of the muscle, that primarily detect changes in the length of the muscle;
- *Golgi Tendon Organ*: sensory receptor organ that senses changes in muscle tension. It lies at the origins and insertion of skeletal muscle fibers into the tendons of skeletal muscle;

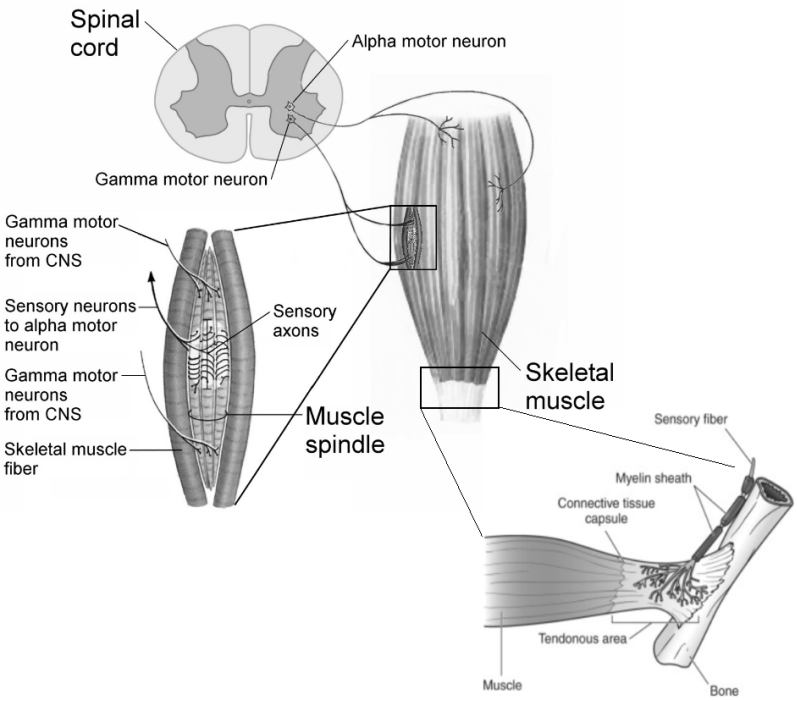

Figure 1.7: Representation which schematizes, in a simplified way, the neuronal communication between spinal marrow and muscle. The figure also shows the structures of the spindles and Golgi tendon organ and their location in the muscle.

In the model that will be introduced in the following chapters, the muscle system considered will show a single input coming from the central nervous system, defined as the activation frequency. This approach allows a simplification of the system and has been validated by previously developed models.

1.5.2 Motor Unit and Fiber Recruitment

Motor unit is composed of a single α-motorneuron, its axon, and of all the skeletal muscle fibers innervated by the motor neuron itself. Whereby once one particular α-motorneuron generates an action potential then all the fibers of the motor unit will be contracted together[D.Purves (2001)]. It's worth point out that, although one motorneuron innervates more than one fibers, each fiber can be innervated only by one motorneuron. However, the entire muscle is composed of several motor units of different types. This kind of diversification allows to modify the period of the contraction force in two ways :

- Recruiting different types of motor unit;
- Changing the number of motor unit involved in the contraction

Indeed, the tension developed by the muscle can be increased by recruiting new motor unit according to a particular mechanism controlled by the central nervous system (CNS), called fiber recruitment.
A weak stimulus directed to a set of somatic motor neurons of the central nervous system activates only the neurons that have a low threshold, which will activate the

slow fatigue-resistant fibers, which develop minimal force as the stimulus reaches the set of motor neurons, it increases in intensity, other motor neurons with a higher threshold begin to fire. Those neurons trigger the motor units, in this case, made by fast fibers fatigue resistance. And since more units are involved by the contraction then the muscle produces a higher overall force. When the stimulus has a faster increase in other motorneurons with the highest threshold trigger motor unit made by fast fibers, and at this point, the contraction force gets close to the maximum value. These last fibers are sensible to fatigue so the maximum contraction cannot be held for a long period.
One way to avoid fatigue in a sustained contraction is asynchronous recruitment of motor units. The nervous system modulates the rate of discharge of motor neurons so that different motor units in turn maintain muscle tension. The alternation of active motor units allows some of them to re-propose contractions, predicting fatigue.

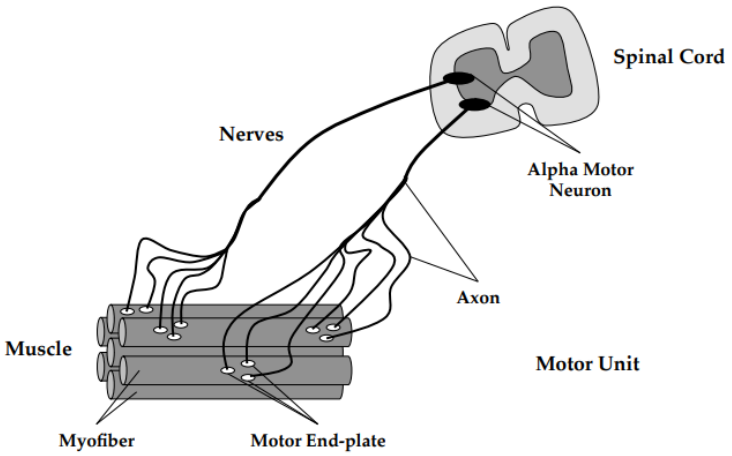

Figure 1.8: Components of a motor unit for muscle contraction. U.Jensen (2016)

It is worth pointing out that in the model that will be developed in the following chapters the principle of fiber recruitment will not be considered, in order to keep this model as simple as possible.

Chapter2

Muscle Modelling

For an accurate representation of the muscle force, muscle models have to be developed from muscle experiments. There exist various experimentally validated models on either macroscopic scale, taking only gross effects into account or a microscopic scale, including even molecular phenomena.

2.1 Tension-Length Curve

Muscle stiffness is one of the main features determining the phenomenon whereby a twitch sequence coalesce into a tetanus. Two separate elements belonging to elastic behavior have been distinguished :

- One due to *passive behavior*, which means a force production due to the internal structure of the muscle itself that do not depend on the electrical impulses imposed to the muscle ;
- The other elastic behavior is due to *active properties*, so linked to a force production caused by the muscle contraction and dependent on the activation frequency imposed;

Passive properties are easily measurable since the muscle do not require to be stimulated. The curve describing this type of behavior gets progressively steeper at a larger stretch, presumably for the same reason because a piece of yarn gets stiffer as it is extended.
When the muscle is excited the force at each length is found to be greater compared to the tension developed when it was in resting condition. So, in addition to the passive force when the muscle is stimulated it contracts to produce an active force. This tension is derived from the interactions of the actin and myosin filaments. The active tension-length curve is described by the Sliding Filament theory and has its maximum at the muscle's normal length in the body.
G.A.F. Huxley and Julian recognized from microscope observations that even in single fiber preparations, the stretch of a sarcomere, and therefore the degree of thick and thin filament overlap, was different at the ends of the fiber from what it was at the center. At length by which the maximum active contractile force is produced, called optimal length, the filament of myosin is found to be perfectly overlapped with the filaments of actin determining the maximum rate of cross-bridge formed.

By stretching or shortening the muscle from the optimal length then the overlapped surface of the thin filament over the thick one diminish in both cases determining then a decrease of the active force production. Furthermore, it can be seen from the plot of the total tension-length curve that at a relatively high stretch length the passive force related to the structural stiffness response of the muscle overcome the active force and become the prominent behavior.

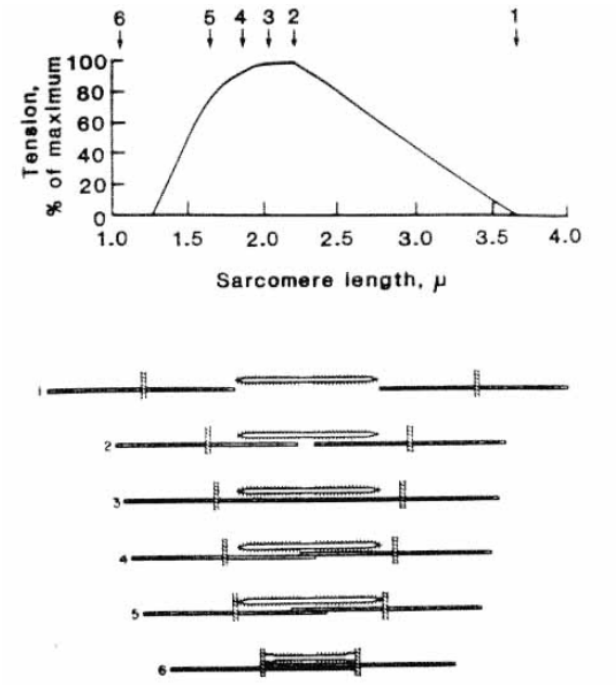

Figure 2.1: Length-tension relationship of a single frog semitendinosus muscle fiber. The numbers 1 through 6 on the length tension curve correspond to the numbers on the schematic diagram of thick and thin filament arrangement. In this way the relationship between thick and thin filaments can be compared to the tension at various sarcomere lengths.. http://educ.jmu.edu/ strength/KIN$_4$25/$kin_4 25_{10} 4_t erms.htm$

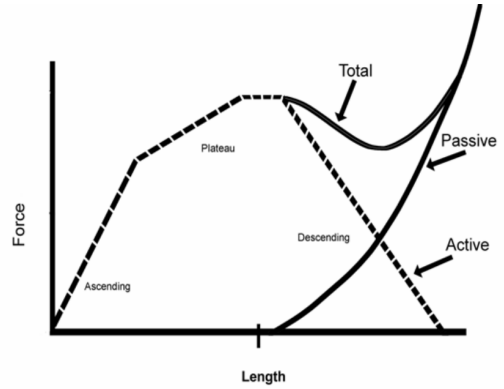

Figure 2.2: The force-length relationship of muscle reflects the sum of the active (dashed line) and passive tension (continuous line) sources of force. The active tension curve is typically classified as having an ascending, plateau, and descending limbs D.V.Knudson (2006)

2.2 The Visco-Elastic Model of Muscle Contraction

H.S.Gasser & A.V.Hill (1924) conducted an important study of muscle mechanics that led to the development of the visco-elastic model of muscle contraction. According to the elastic theory of contraction, upon stimulation, the muscle effectively became a stretched elastic body with the main difference that the force exerted by a purely elastic body when stretched is determined by its length and it is independent of the velocity of shortening. Gasser and Hill verified the force-shortening relationship was a fundamental property of the muscle itself. The effects of the speed of shortening on the force exerted by a muscle was proposed to be due to the fact that muscle consisted of an elastic network containing a viscous fluid.

2.2.1 Force-Velocity Curve

It is a matter of common experience that muscles shorten more rapidly against light load than they do against heavy ones [Rall (2014)]. So, considering a muscle contracting in no-load condition, the shortening velocity measured in this case would be maximum. By increasing the load applied to a muscle the shortening velocity will decrease, slowing down the movement. In such a case the load higher enough to equate the maximum force the muscle can produce the shortening velocity will reduce to zero which leads the muscle in a static condition: Isometric contraction occurs. The decrease in the shortening velocity in the function of the load is due to the fact that the load represents a force which opposes to the tension developed by the muscle in contraction conditions, whereby the net force available to impose a shortening velocity, result to be reduced proportionally to the opposing external force, the load. Particularly important is the rate at which the contractile component shortens before it is time to move far from the initial length. This is shown as a broken line target to the lengthy-time curve just after the rapid shortening phase. When this initial slope is plotted against the isotonic afterload, T, a characteristic curve is obtained which shows an inverse relation between force, T, and shortening velocity, v.

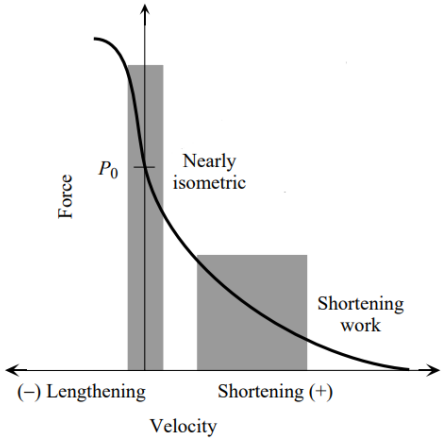

Figure 2.3: Schematic representation of the force–velocity curve for striated skeletal muscle depicting the range of force and velocity over which muscles that generate force isometrically (P0 is the isometric force), or with a brief initial stretch, operate compared with muscles that shorten to perform work and generate mechanical power. Biewener & Gillis (1999)

2.2.2 Hill equation for a tetanized muscle

By measuring the velocity of shortening under different loads applied to an isolated frog sartorius Hill modeled the data he found as a hyperbole [Rall (2014)]:

$$(P + a)(v + b) = Constant \tag{2.1}$$

where :

- P : load during shortening;
- v : velocity of shortening;
- a and b : constants parameters depending on the type of muscle

Introducing then the maximum isometric tension P_o then Hill's equation can be rewritten as :

$$(P + a)(v + b) = b(P_o + a) \tag{2.2}$$

Neglecting the constant a and b on the left side of the equation, it assert the concept of power delivered by the muscle during muscle contraction. It is worth noting that the power delivered is then constant during contraction since higher the load lower will be the shortening velocity and vice versa; But this consideration has its validity only in case the muscle is tetanized,for which the equation is obtained.

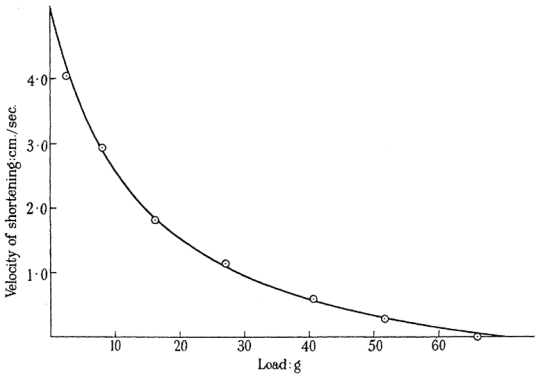

Figure 2.4: Relationship between load and velocity of shortening in isotonic contractions of isolated frog sartorius muscle at 0 °C. Figure taken from A.V.Hill (1938) Biewener & Gillis (1999)

Two approaches for the Hill equation. One called an empirical approach, is based on the experiments of "quick release": the muscle is locked at a length L_o and it is excited with a frequency that leads the muscle to reach the steady-state in tetanus such that it will develop the maximum isometric tension P_o. After a certain period of time, the muscle is released leaving it free to contract. In this case, the muscle will assume a contraction speed which will be recorded and plotted in a tension-length graph.
A second approach to the Hill equation, which can be called a theoretical approach, consists of making energetic consideration. And in relation to this approach Hill himself faced the problem of going to study the thermal power the muscle releases during contraction. Fundamental energy required by the muscle to contract comes to the metabolism of the ATP molecule, as shortly described in Chapter 1. By a rearrangement of the Hill equation then it is possible to obtain the relation of the mechanical power :

$$Pv = v\frac{bP_o - av}{v + b} \tag{2.3}$$

From this equation, it can be noticed that the output in terms of power delivered by the muscle assumes maximum at values of tension and velocity which are between a third and a fourth of their maximal values.

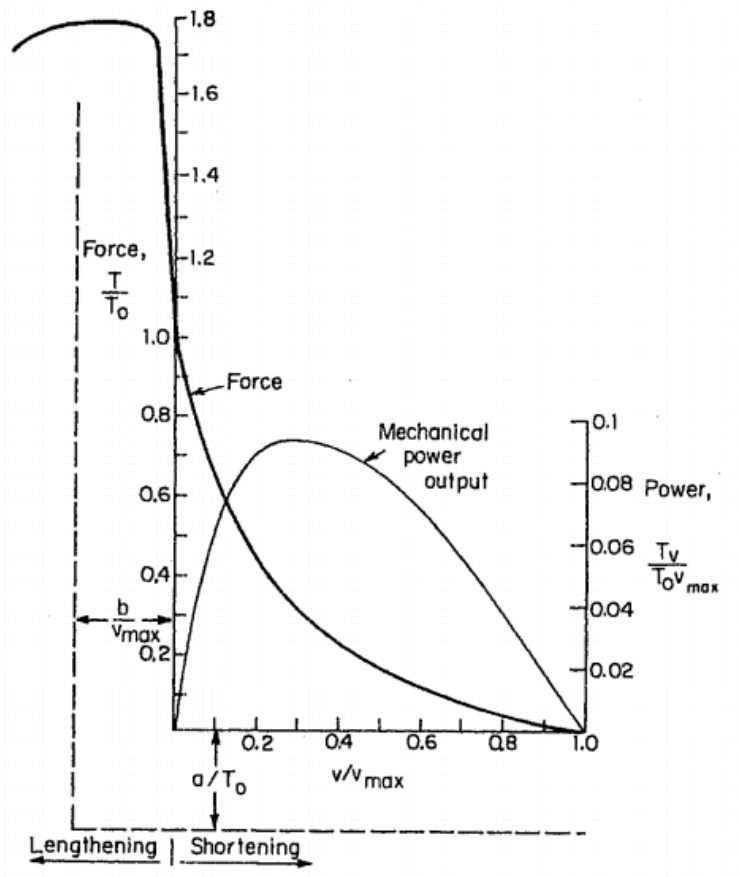

Figure 2.5: Hill's force-velocity curve. Near zero shortening velocity, the lengthening part of the curve has a negative slope approximately six times steeper than the shortening part. The externally delivered power was computed from the product of tension and shortening velocity. Figure taken from McMahon (1943)

2.2.3 Hill's Three-Elements Model

Hill's equation does not provide a full description of muscle behavior. For this reason, Hill developed a model that is among the ones that better approximate the muscle behavior keeping considerable simplicity in the expression [A.V.Hill (1997)]. From the study of the muscle behavior length against time two main phases can be distinguished: a first phase where the response is practically instantaneous and a second one where it is slower, from which taking the tangent of each point the shortening velocity can be computed; In order to better describe this behavior Hill modeled the muscle with lumped parameters. Three elements were introduced, two for the active force and one for the passive :

- *Series Elastic Element*: it assumes a behavior very similar to a spring that reacts, instantaneously, to the force imposed by the load. This element is introduced in order to approximately model the tendon;

- *Parallel Elastic Element*: it goes to represent the non-linear muscle elastic response of the connective tissue of the myolemma and the residual interaction of the myofibril;

- *Contractile Component*: this component is modeled as an instantaneous force generator where it is applied in parallel a damper in order to introduce a viscous delay on the response, for better represent the empirical data;

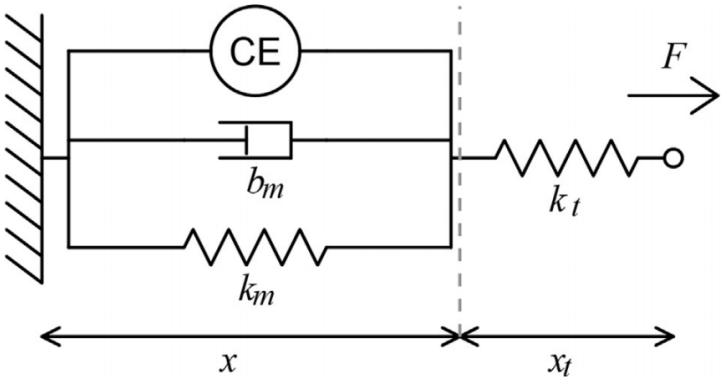

Figure 2.6: The Hill muscle model is modeled as an active contractile element in parallel with a damper and spring element. These components are attached in series with a stiffer spring element approximating the tendon McMahon (1943)

Therefore, with reference the figure 2.6, by knowing the lumped parameters of the stiffness k_m, of the parallel elastic element, k_t, of the series elastic element, the parameter related to the damper b_m and the relation which determines the active contractile component; Then the positions x(t) and $x_t(t)$ can be computed and the overall position of the muscle determined, under the external force applied F.
Most authors would identify the contractile element with the sliding actin-myosin molecules, and the generation of active tension with the number of cross-bridge between them. Many suggestions have been made to describe the structural behavior of the lumped elastic elements of Hill's three-elements model, But none of them is definitive. The basic difficulty with Hill's model is that the division of forces between the parallel and the contractile elements and the division of extensions between the parallel and the contractile and series elements are arbitrary. These divisions cannot be made without introducing auxiliary hypothesis. Consequently, empirical evaluation of the properties of the elements, such as the active contractile relation the definition of the parameters k_m, k_t, and b_m will depend on the auxiliary hypothesis imposed. For further progress then, the Hill's equation needs to be explained in order to determine whether the contractile element is entirely stress-free and freely distensible in the resting state or not and to search for methods to predict the constants involved in Hill's equation and in the constitutive equations of the parallel and series elements. For these purposes, the basic theory of sliding elements was proposed by A.F.Huxley and H.E.Huxley in 1954.

2.3 Model Developed By I.E.Brown, E.J.Cheng and G.E.Loeb

In this section, we will introduce the model developed I.E.Brown et al. (1999):

2.3.1 The Model

The model developed by I.E.Brown, E.J.Cheng and G.E.Loeb contains :

- *An active contractile element* (CE): it represent the force produced under a certain stimulation;
- *A passive elastic element* (PE): it represents the muscle fascicle passive elastic resistance.

Although the complete model they introduce also contains an elastic element in series, this element is not studied, as it is considered negligible for the operating conditions of their preparation.
In order to develop a model which is adaptable to muscles with different architectures, the inputs and outputs of the model itself need to be normalized; Under this perspective, then, defining L_0 the fascicle length at which maximal tetanic isometric force can be elicited, all data collected from the experiments were normalized upon the maximal tetanic isometric force developed by the muscle, F_0, and the so-called optimal length L_0.
A mathematical summary of their model :

$$F = F_{CE} + F_{PE} \tag{2.4}$$

$$F_{CE} = R \cdot Af \cdot FL \cdot FV \tag{2.5}$$

$$F_{PE} = F_{PE1} + R \cdot Af \cdot F_{PE2} \tag{2.6}$$

where :

- F : total force produced by the muscle fascicles;
- F_{CE} : force produced by the CE element;
- F_{PE} : force produced by the PE element;
- R : is defined as the recruitment factor of muscle cross-sectional area and is unitless quantity which range from 0 to 1.(the data collected from their study the recruitment factor assumed always the maximum value, 1)
- Af : is defined as the activation-frequency relationship and as for the recruitment factor also this parameter is a unitless value between 0 and 1, where at Af = 1 correspond the tetanic stimulation. from a physiological point of view Af provides a measure of the fraction of available cross-bridges that are cycling in all recruited muscle fibers.
- FL : is defined as the the tetanic force-length relationship and has units of F_0 so then $0 \leq FL \leq 1$;
- FV : is defined as the tetanic force-velocity factor, unitless and at the isometric condition, it assumes the value 1. This multiplication factor shapes the isometric force, dictated by the FL relationship, according to the contraction speed assumed during the movement;

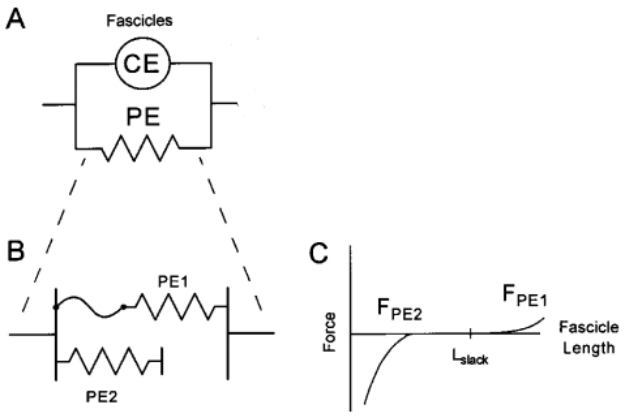

Figure 2.7: A.The contractile element (CE) operates in parallel with the passive elastic element (PE) to represent the fascicles.
B.C. Passive elastic element. PE1 is the well recognized non-linear spring that resist stretch in the passive muscle, while PE2 is a non-linear spring resisting constriction during active contraction at short lengths.

2.3.2 Components Description

The approach they used to develop the Force-Length relationship was to collect data from five feline caudofemoralis, applying 5 stimulus frequencies ranging from 15 to 120 pulses per second at each of six lengths from 0.65 to $1.25L_0$. Through a fitting process (Levenberg-Marquardt algorithm), then, they found out the proper equation. Furthermore, isometric passive FL relationships (for PE1) were collected in every animal, in the isometric state, 30ms after stretching to at least 15 different lengths. These data were used after the experiment to remove the passive component of total recorded force, leaving the active component which goes to describe the behavior of the contractile element CE.
In their model, they also included a second passive force, F_{PE2} that resisted constriction at lengths shorter than 0.75 the optimal length. So, in other terms, the passive element they developed, PE, has two spring-like components with characteristics that are non-linear functions of the length. Taken from a functional point of view, when the slack is pulled out of the ideal, bendable, fixed-length linkage that connects spring PE1, it exerts a tensile force. On the other side, at shorter fascicle lengths, the constriction spring PE2 comes into play with a separate spring function that resists constriction. Physiologically, PE2 represents the effects of compressing the thick filament at sarcomere lengths that are shorter than the thick filament. Consequently, the relations they found out for the two passive components are in the form:

$$F_{PE1}(L) = c_1 \cdot k_1 \cdot ln(e^{\frac{L-L_{r1}}{k_1}} + 1) \tag{2.7}$$

$$F_{PE2}(L) = c_2 \cdot (e^{k_2 \cdot (L-L_{r2})} - 1), \qquad F_{PE2} \leq 0 \tag{2.8}$$

Where c_1, c_2, k_1, k_2, L_{r1} and L_{r2} are parameters to be determined that change according the muscle architecture and the type of twitch behavior (slow-twitch muscle or fast-twitch muscle) it is intended to model.
Then, accordingly, to what previously stated, both the F_{PE1} and F_{PE2} are subtracted to the empirical data in order to obtain the active force response of the

muscle; And from these results the relation the isometric force-length relation has been found out :

$$FL(L) = e^{-|\frac{L^{\beta}-1}{\omega}|^{\rho}} \tag{2.9}$$

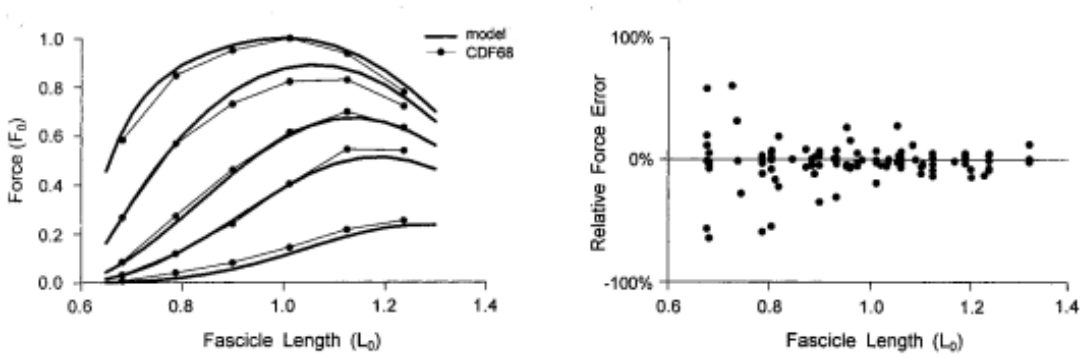

Figure 2.8: (C) Isometric FL data. The best-fit model is plotted with these data for comparison.
Table containing the data extracted from this plot can be seen in Table 2.1
(D)It is shown the relative force errors of the model respectively where relative error is defined as $Err_{rel} = \frac{F_m \pm F_d}{F_d}$. where F_m is the force predicted by the model and F_d is the real force coming from empirical data

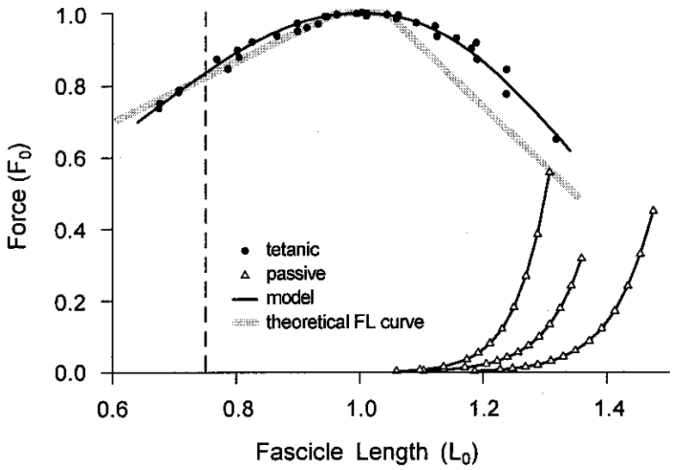

Figure 2.9: Active isometric tetanic FL data and passive (F_{PE1}) FL data. Data are indicated with circles (tetanic) or triangles (passive) while the best-fit curves are drawn with a thin black line (equations (2.9) and (2.7))

They analysed then the effects of the activation frequency Af at different length and built the equation :

$$\begin{cases} Af(\alpha, L) = 1 - e^{-(\frac{\alpha}{a_f \cdot n_f})^{n_f}} \\ n_f = n_{f0} + n_{f1} \cdot (\frac{1}{L} - 1) \end{cases} \tag{2.10}$$

As will be shown later, this approach, that is to find a relationship of a parameter that describes the frequency of excitation as a function of the frequency of impulses and the length assumed by the muscle itself, differs from the approach we embraced in the implementation of the evaluation model.

The equation (2.5), that describes how they modeled the active force produced by the contractile element, also contains a parameter FV(V,L), which modulates F_{CE} based on the velocity assumed by the muscle during a movement; so as to find the proper relation of FV, in the function of the length L and the speed V, they performed displacement control experiments during the stimulation of the muscle; In other words, they measured the change in the force production of the muscle during an imposed displacement with a constant velocity [Brown & Loeb (1999)]. The relation they built from the fitting of those empirical data is piecewise function defined as:

$$FV(V,L) = \begin{cases} \frac{V_{max}-V}{V_{max}+(c_{v0}+c_{v1}\cdot L)V}, & V \leq 0 \\ \frac{b_V - a_V \cdot V}{b_V + V}, & V > 0 \end{cases} \tag{2.11}$$

Due to the lack of reliable and general experimental data, the model we developed does not contain this multiplicative factor which varies according to the speed of movement. In any case, this does not preclude the fact that in the event data should be found, which allows a good fitting of the Tension-Velocity relationship of the muscle, this cannot be added to the model developed.

A schematic description of muscle model sub-elements is presented

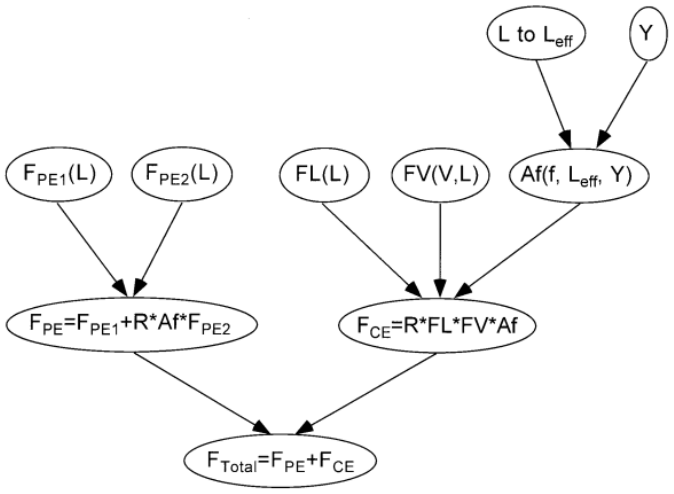

Figure 2.10

For a complete understanding of the elements presented by this scheme, it is recommended to consult the article I.E.Brown et al. (1999) and references

2.4 Model Developed By J.M.Winters

J.M.Winters developed a model of the muscle oriented towards postural control [J.M.Winters (1995)]. The basic structure of its model comprises a first stage where the neuro-controller input is properly filtered. Followed by the Hill-based muscle model, with the peculiarity to also consider the behavior of the spindles and the Golgi tendon organ, which are then used to build length and force feedback loop.

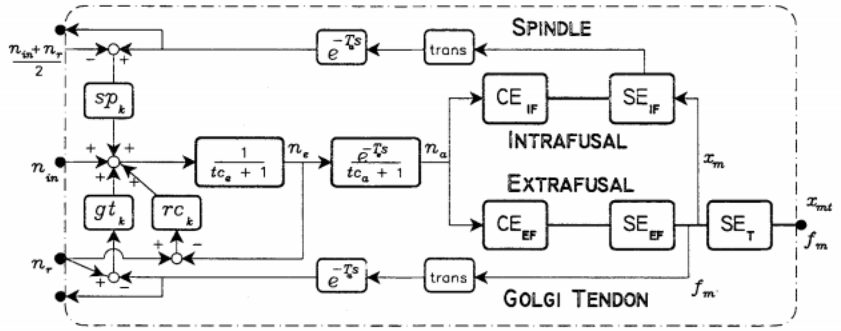

Figure 2.11: Schematic of the overall fourth order, nonlinear muscle-reflex actuator. CNS inputs are n_{in} the feedforward excitation drive, and $n_{r'}$ the reference state term related to the general level of coactivation and excitability for a system of muscles. The thicker connection lines represent bi-causal mechanical interaction, the thinner lines uni-causal information flow. Notice the bi-causal coupling between the muscle and its environment, and between the two CE-SE elements. The force generated by the IF system is assumed to be insignificant, thus the uni-causal information flow of kinematic information from the EF to IF muscle.Figure taken from J.M.Winters (1995)

Neglecting for the moment the modeling of Spindles and GTOs, which will be considered in future works. Winters described the tension-length relation by a normal distribution shaped by the activation frequency n_a and the length assumed by the contractile component CE, l_{CE} :

$$F_a(l_{CE}, n_a) = n_a \cdot e^{-(\frac{x_{CE}-flmax}{fl_{sh}})^2} \tag{2.12}$$

where $fl_{max} = fl_{oo} + fl_{shft}(1 - n_a)$ and $x_{CE} = \frac{l_{CE}}{l_{mo}}$.

J.M.Winters defines :

- l_{mo} as the muscle rest length;
- fl_{oo} as a dimensionless parameter locating peak of the "Gaussian" relation used for to fit the active component of F_P defined for case of peak activation;
- fl_{sh} as a dimensionless shape parameter for F_P "normal distribution" curve;
- fl_{shft} a dimensionless activation-dependent shift in maximum value on F_P relation;

It can be noticed the similarity in the approach adopted to describe the active contractile force relation, with the model developed by I.E.Brown, E.J.Cheng, and

G.E.Loeb. Where, also in this case the effects of the activation frequency on the force have been modeled through a parameter, which assumes values between 0 and 1, that changes the magnitude of the curve according to the activation state in which the muscle is located.
The passive relation for the CE lengths above the rest length has been modeled by the exponential fit which is common for biological tissues under extension. On the other side for lengths which stand under the rest length, $x_{CE} < 1$ (by definition), J.M.Winters assumed the intervention of a negative (repulsive) force, that can subtract from the active force :

$$F_P(l_{CE}) = \begin{cases} (\frac{1}{e^{p_{sh-l}}-1})^{(e^{\frac{p_{sh-l}\cdot(x_{CE}-1)}{e^{p_{ex-l}}}}-1)-1}, & x_{>}1.0 \\ \langle -(\frac{1}{e^{p_{sh-s}}-1})^{(e^{\frac{p_{sh-s}\cdot(1-x_{CE})}{e^{p_{ex-s}}}}-1)-1}, (0.0001 - F_a)\rangle, & x_{\leq}1.0 \end{cases} \tag{2.13}$$

In this case the author defines the parameters :

- p_{sh-l} as a dimensionless shape parameter, passive F_P lengthening
- p_{ex-l} as a dimensionless parameter (relative to l_{m0} that locates point of passive F_P exponential, where it crosses ± 1.0 on dimensionless force axis in lengthening condition;
- p_{sh-s} as a dimensionless shape parameter, passive F_P shortening
- p_{ex-s} as a dimensionless parameter (relative to l_{m0} that locates point of passive F_P exponential, where it crosses ± 1.0 on dimensionless force axis in shortening condition;

The inequality for shorter muscle lengths is due to the fact that, since the overall muscle does not push, there is a negative passive repulsive force that is constrained not to be any higher than the current active attachment force F_a. A similar approach was adopted by I.E.Brown, E.J.Cheng, and G.E.Loeb wherein the model they also introduced a negative passive force, that resisted constriction at lengths shorter than the optimal one (equation (2.8)). An important difference between the passive force in shortening conditions introduced by Winters and the one introduced by Brown, Cheng, and Loeb, relies upon the fact that, in the model developed by Brown, Cheng and Loeb the negative component of the passive force is in the function of the activation frequency and no saturation at 0 occurs. Instead in the model developed by Winters the negative passive force does not depend on the stimulation frequency and so then a saturation to 0, for lengths below the optimal one, is needed, otherwise the total force provided by the muscle, for a certain range of lengths below the optimal one, will assume negative values: a behavior which is not compliant with empirical data.

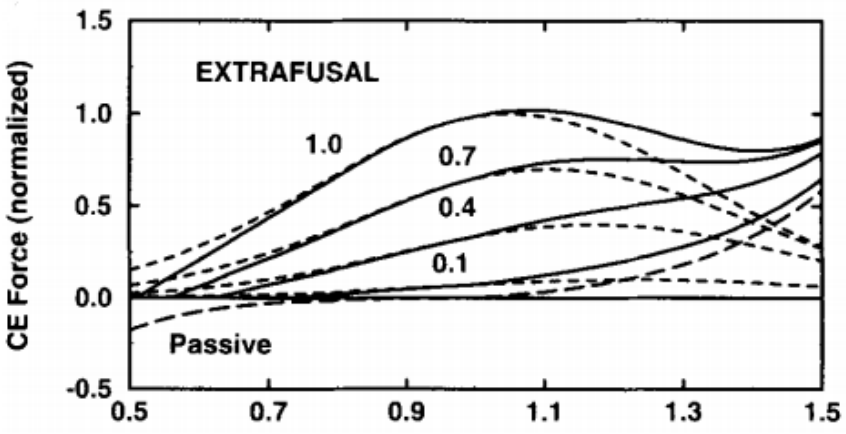

Figure 2.12: Assumed a dimensionless CE force-length curve as a function of the activation input n_a. The local passive (activation independent) contribution is added to the active contribution to determine the net relation. Figure taken from J.M.Winters (1995)

2.5 Evaluation model: Isometric Force Prototype

Muscles are complex physiological systems, the models found in the literature, try to minimize the error between the empirical data and the measurements provided by the developed model. So, consequently, they show great complexity in form. In order to better understand the physical phenomena and the dynamics of the muscle, considered as an actuation system, the need for a developing a model arose. Therefore we have set ourselves the goal of developing a new model that would describe the behavior of muscle contraction, maintaining simplicity as the main characteristics. In other words, we sought a simple, flexible model, that qualitatively describes the contractile force delivered by a muscle, whose coefficients can be then properly tuned, in order to meet the quantitative trend provided by empirical data. The approach followed to build the so called 'Evaluation model' was a bottom-up approach. This means that we started considering the total force developed by the muscle decomposed in active isometric force and passive force. And with the assumption, validated by previous studies, the superposition principle was exploited to assemble these found components, and obtain the final relation of the evaluation model. Therefore the model it is described in the following subsections contains a certain number of degrees of freedom, defined in the form of matrices and vectors, which allow the model to adapt to experimental data from different animals that show different muscle structures. The matrix representation was adopted in order to make the model easier to read and to simplify the process of determining the parameters.

2.5.1 Active Isometric Force Data Fit

Active force can be defined as the component of total force delivered by the muscle, that describes the state of contraction only. So, in other words, thinking that the behavior of the muscle can be theoretically subdivided into two parts: one, which has a close dependence on the frequency of excitement imposed on the muscle, and the other independent on the muscle stimulation but only a function of length; Active force is then the component of force dependent on the stimulation frequency and length of the muscle.
Acceptable experimental data that could allow for an adequate curve fitting, consistent with the real behavior of the muscle were found in the article I.E.Brown et al. (1999) reported in the figure 2.8;
The graphed data were then extracted from the image by using an online software specialized in this purpose called WebPlotDigitizer [Rohatgi (Rohatgi)]. The experiment carried out by Brown, Cheng and Loeb considered five different frequencies of activation at which the force production was then measured at six different lengths assumed by the muscle :

	Isometric Force				
Length	15pps	30pps	40pps	60pps	120pps
0.68012902	0.007564544	0.032042009	0.0852463	0.26959046	0.583284981
0.78529314	0.040622791	0.119666338	0.2755992	0.56726357	0.847932571
0.89782767	0.080920015	0.242054885	0.4612702	0.72909253	0.95105952
1.01046188	0.141896853	0.404801067	0.6120925	0.82028999	1.000070549
1.12463178	0.215931322	0.541848223	0.6950237	0.82710332	0.935329531
1.23676704	0.253667028	0.536748964	0.6303053	0.71744110	0.775225898

Table 2.1

The Table 2.1 report the data extracted from the figure 2.8 : In the first column are found, in ascending order, the values of the lengths at which I.E.Brown, E.J.Cheng, and G.E.Loeb sampled the force data; In the following five columns are listed the relative force values produced by the muscle at the length specified by the row and at the impulse frequency specified by the column;
These empirical data were then transported in Matlab. The tool made available by this software, named Curve Fitting Toolbox, makes available a series of algorithms designed to optimize the fitting process of sequences of numerical data. Therefore, for this reason, data represented in the table 2.1 were then modeled in curves using this tool.
Following the definition provided for active force, the force-length relationship was conceived as a function dependent on the activation frequency, α, and on the length assumed by the muscle: $F_A = F_A(\alpha, \mathrm{L})$; The fitting procedure adopted to find out this relation can be schematized as:

1. Considering the activation frequency constant at a single value, it has been found the curve that describes the trend of empirical data, along the length dimension, so, in function to L. In this case the shape chosen to model the data was a Gaussian function. Inspired by the works in literature, a Gaussian function was chosen can lead to the fact that it is one of the best relations that can describe well and in a simple way (in terms of number of coefficients) the trend of real values that tend to concentrate around a single average amount. And as it can be seen from the figure 2.1 the force production of a muscle in contraction condition can be thought it tends to concentrate at lengths close to the optimal one, L_o;

2. The first step was then extended, also, to the other frequencies. It is important to point out that the shape of the curve fitted, in function to the muscle length at a particular frequency of activation, must be kept constant when considering a second curve, in function to L, but at a different frequency. This means that the shape of the Normal distribution was imposed on all the curves fitted in function to L;

3. From the previous step, five bell functions were obtained, each one related to a particular impulse frequency. Considering the coefficients of each Gaussian function. They were collected in order to obtain vectors containing values of the same coefficient but related to different frequencies of activation.

4. The fitting was then carried out for each vector defined in the previous step in order to achieve in having each coefficient of the Gaussian function represented by a certain relation dependent on the activation frequency;

5. The final result of the fitting process was, then, to reassemble the Normal distribution in L with the coefficients as a function of the activation frequency;

Therefore the active isometric Force-length relation is then defined as :

$$F_A(\alpha, L) = a_1(\alpha) \cdot \mathbf{e}^{-(\frac{L-a_2(\alpha)}{a_3(\alpha)})^2} \tag{2.14}$$

where:

$$\begin{cases} a_1(\alpha) = \frac{c_{1,1}\alpha^2+c_{1,2}\alpha+c_{1,3}}{\alpha^2+c_{1,4}\alpha+c_{1,5}} \\ a_2(\alpha) = c_{2,1}e^{c_{2,2}\alpha} + c_{2,3}e^{c_{2,4}\alpha} \\ a_3(\alpha) = c_{3,1} + c_{3,2}\cos c_{3,4}\alpha + c_{3,3}\sin c_{3,4}\alpha \end{cases} \tag{2.15}$$

Consequently the matrix C can be defined as the matrix containing the coefficient $c_{i,j}$, with i = 1,2,3 and j = 1,2,...,5 :

$$\mathrm{C} = \begin{pmatrix} 1.134 & 0.723 & 0.050 & 11.330 & 643.260 \\ 0.574 & -0.021 & 0.848 & 0.001 & 0 \\ 0.452 & -0.017 & -0.124 & 0.049 & 0 \end{pmatrix}$$

C will, therefore, depend on the structure of the muscle to be modeled, thus varying from animal to animal and from muscle geometry to muscle geometry. As will be shown in the next chapter, from a suitable setting of the matrix C, the trend of the curve found will follow, maintaining an almost minimal error, the trail followed by

the empirical data.

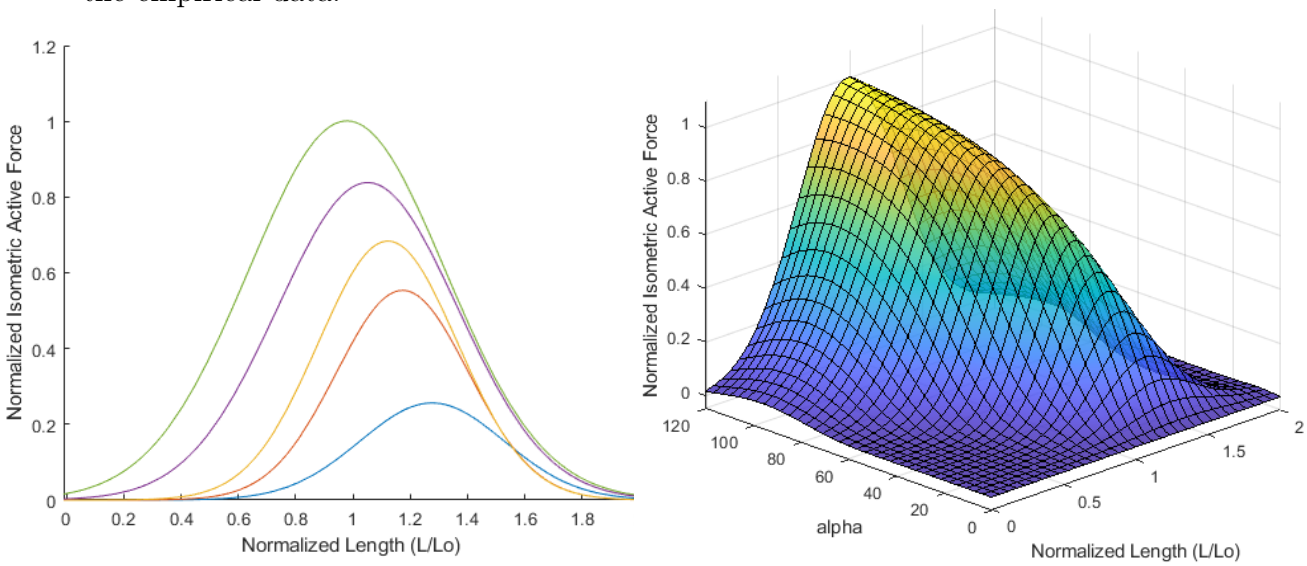

Figure 2.13: Plots of the Isometric Active Force. On the left side, it is shown the comparison of the trend assumed by the curve at fixed activation frequencies, $\alpha = \{15, 30, 40, 60, 120\}$pps. On the right side it is shown the surface generated by the $F_A(\alpha, L)$

2.5.2 Passive Force Data Fit

It has been defined as Passive force, the total force component that can be considered independent of the muscle activation. From this definition, then, the passive force takes into account the mechanical properties of the relaxed skeletal muscle. The importance and the effects of this component on muscle behavior can be:

- Passive muscle tension resist joint motion, so it places fundamental constraints on movement and motor control systems;
- The capacity of muscles to generate active forces is modulated by passive muscle forces;
- The way in which muscles deform under both passive and active conditions influences the sensitivity of muscle Spindles and Golgi Tendon Organ to joint movement and muscle force;

Under the suggestion of J.M.Winters' model, the approach adopted in modeling passive force was to decompose the behavior into a passive stretching force and a passive shortening force. In this way, the two passive tension relationships have been simplified in expression and the total passive force has been expressed as a piecewise function. Actually, this was the basic idea on which the fitting of data is based on. However, using appropriate functions that take null values in the range where those function should not be considered, which means that the passive stretching force assumes null values for length below the optimal one and the passive shortening

force assumes null values for lengths greater than the resting length (L_0), then the total passive force can be constructed as the sum of these two contributions:

$$F_P(L) = F_{PS}(L) + F_{PL}(L) \tag{2.16}$$

2.5.2.1 Positive Passive Force

Valid data of the passive force for lengths above the optimal, were found from the plot 2.9 taken from the article I.E.Brown et al. (1999).
It is important to point out that Passive FL relationships from different animals did not tend to normalize well with respect to each other. The explanation for this discrepancy is unclear, although it is possible that there were differences in architecture between the three muscles used in the experiments, even if animals studied belonged to the same species, were of the same sex, and around the same age. In this case, the data considered, were referred to the passive force in the middle, among the three represented. Considering it as an average behavior:

Length	Passive stretching Force
1.05901495	0.005759696
1.10245475	0.007008571
1.16991643	0.014819131
1.20441578	0.023784025
1.22205030	0.032336545
1.23815292	0.044192152
1.25527815	0.057366308
1.27266092	0.075820955
1.28953465	0.099557353
1.30666827	0.134735305
1.32406161	0.180914734
1.34171602	0.241616249
1.35835454	0.318602251

Table 2.2

The table 2.2 contains the data extracted, where are provided the stretch lengths (lengths normalize to L_0) at which the measurement of the passive force was performed and the related stretching force value.
The procedure adopted to fit those data was practically identical the one exploited to fit the active isometric force data:

- Data extracted from the plot 2.9 were transferred in Matlab;
- Through the use of the Curve fitting tool made available by Matlab, a simple best-fit curve was found. Note that differently from the active isometric force,

the passive force does not show any dependence on the activation frequency, and so no nested fitting procedure is needed;

- The final result of the fitting procedure was a Sigmoid function dependent only on the muscle stretching length. This particular function was chosen for its characteristic 'S' shape; So that, according to a proper shifting along the axis of the lengths, it is possible to obtain null passive force at shortening conditions, and it can be obtained a certain plateau after a certain stretching length; Maintaining the correct behaviour described by the empirical data. The plateau at high stretching conditions was introduced to represent the cleavage of the muscle structure under high stress conditions.

Therefore the Stretching Passive Force-length relation is then defined as:

$$F_{PL}(L) = p_{l1} + \frac{p_{l2} - p_{l1}}{1 + 10^{p_{l4} \cdot (p_{l3} - L)}} \tag{2.17}$$

where it can be defined the vector p_l, whose elements, p_{li} with i = {1,2,3,4} , represent the coefficients of the Sigmoid function:

$$p_l = \begin{pmatrix} 0.003807353 \\ 2.165815210 \\ 1.453883205 \\ 8.166335117 \end{pmatrix}$$

As for the parameter matrix C of the active isometric force relation (2.15), the vector p_l depends on the internal composition of the fiber and on the muscle's structure. But the relation found can be considered general since by appropriate tuning of these coefficients the curve can fit the empirical data with good accuracy.

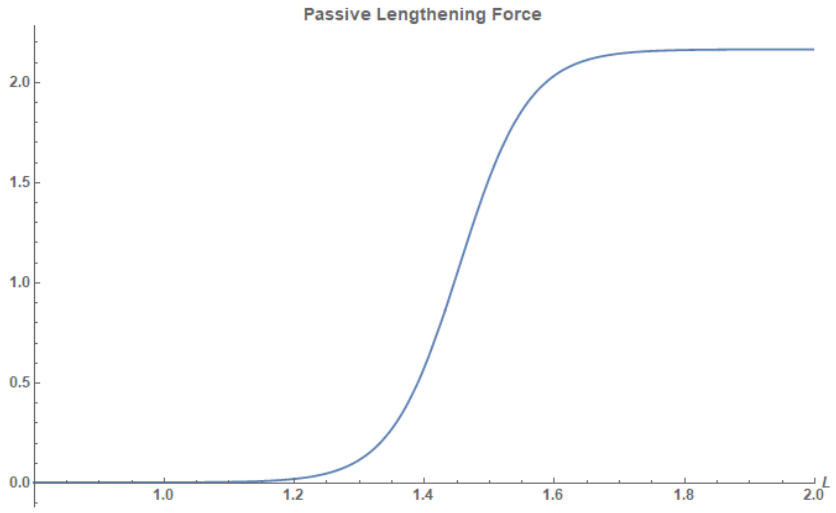

Figure 2.14: Plot which represent the trend of the modeled positive Passive Force.

The reason why a Sigmoid function was chosen to represent the passive force in positive tension condition is mainly due to plateau it introduces after a certain length. The mechanical meaning of the plateau behavior above a certain stretching

length was conceived from the fact that by imposing a lengthening to the muscle fibers above a particular length then, those fibers, due to will no longer show an elastic behavior with the imposed displacement but they will assume a complex behavior dictated from the composition of the fibers and the structure of the muscle. This behavior will be then assumed until the length related to muscle torn will not be reached. Since data that could describe quantitatively the phenomenon just explained, were not found, the model of the passive force in lengthening condition provides only an approximated and qualitative description of the passive force developed at high lengths of stretching.

2.5.2.2 Negative Passive Force

Considering just the isometric active force and the lengthening passive force the model resulted to be incomplete. By making a zoom of the plot represented in figure 2.13, at shortening length, close to 0, it was noticed that the force was not null as it should be. Therefore as it was done by I.E.Brown, E.J.Cheng, and G.E.Loeb or J.M.Winter, a negative passive force was introduced. From a mechanical and physiological point of view, this particular component suggests the action of a repulsive force that during an active contraction reduces the total tension developed by the muscle. This can be due to the interaction and the constriction, of two actin filaments, belonging to two consecutive Z-lines, during the shortening of a sarcomere (figure 2.1). And so the reaction force provided by the actin filament that tries to oppose the constriction force generated by the active cross-bridges can result in large scale as a repulsive negative passive force.
Unfortunately, empirical data which goes to isolate and measure only this particular component of the passive force were not found, as in the case of lengthening passive force. So in order to find out a relation that could describe at least the trend of the shortening passive force, the model developed by J.M.Winters (1995) was consulted. Considering only the shortening passive force developed, the data were extracted from the plot he provided in his article, figure 2.12. Subsequently, the process to fit the data obtained was assumed equal to the approach adopted to find the passive force in elongation, described in the previous section. So the data transferred were modeled exploiting the Curve Fitting Toolbox provided by Matlab. The relation it has been developed is in the form :

$$F_{PS}(L) = p_{s1} \cdot e^{p_{s2} \cdot L} \tag{2.18}$$

where in this case the vector of coefficients is:

$$p_s = \begin{pmatrix} p_{s1} \\ p_{s2} \end{pmatrix} = \begin{pmatrix} -7.320 \\ -7.399 \end{pmatrix}$$

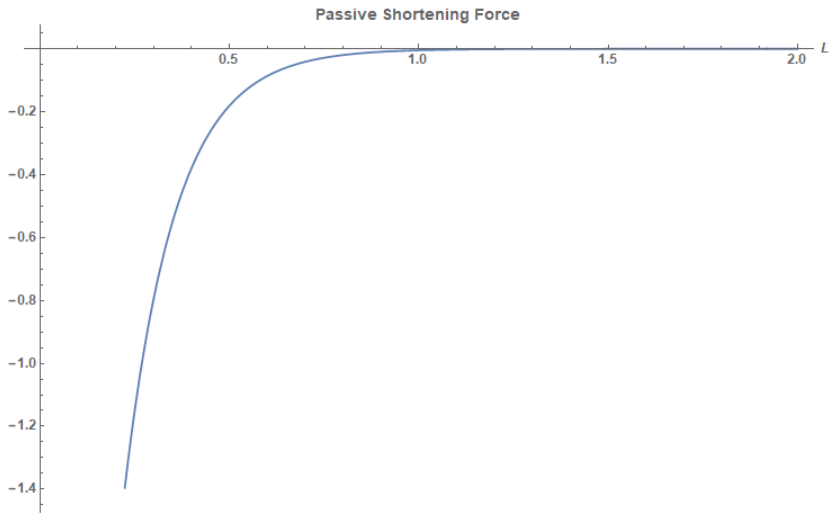

Figure 2.15: Plot showing the trend of the modelled Shortening Passive Force.

It is worth and important to notice that differently from the component of the passive force in lengthening condition, the negative passive force, as it was theoretically conceived, cannot exist without the action of the active contractile force. In other words, since the repulsive passive force in shortening condition is thought as the reaction force of the active force then if the active force itself is null then also the shortening passive force will be null too. This consideration will be exploited in the following section when all the three force components are assembled to find out the relation of the final Evaluation model.

2.5.3 Final Model

The final expression of the evaluation model is therefore, conceptually speaking, the result of the sum of the three tension component defined in previous sections :

- The isomeric active force, $F_A(\alpha, L)$ [in (2.15)];
- The passive force, decomposed in its two components:
  - The passive force in lengthening condition, F_{PL} [in (2.17)];
  - The passive force in shortening condition, F_{PS} [in (2.18)];

On a practical level, it has been seen that the sum of the three curves, alone, is not enough; Since below a certain shortening length, the resulting total force would assume negative values. Such behavior is deductively wrong, as negative forces delivered by a muscle would mean the muscle could generate also stretching forces that, because of the cross-bridge mechanism previously described, it does not find any empirical validation. This error is certainly introduced by the passive shortening force adopted. In order to clean up this conceptual error, it has been considered the solution approach adopted by J.M.Winters (1995), where the total force delivered

by the muscle model is saturated to zero in case the force is supposed to assume negative values. Therefore the Evaluation Model can be defined as:

$$F_{EM}(\alpha, L) = \begin{cases} F_A(\alpha, L) + F_{PL}(L) + F_{PS}(L), & F_{EM} > 0 \\ 0, & F_{EM} \leq 0 \end{cases} \tag{2.19}$$

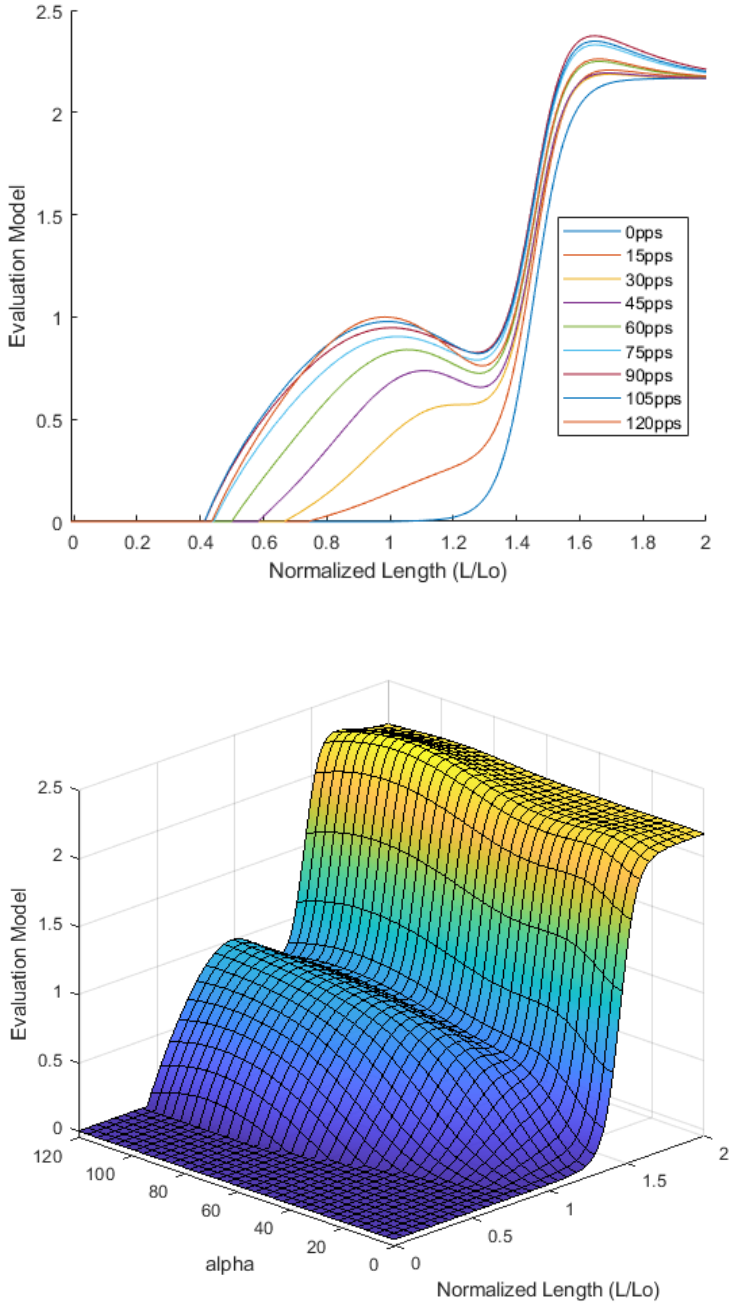

Figure 2.16: Plots of Evaluation Model's trend. On the top, it is shown the comparison of the trend assumed by the curve at fixed activation frequencies, $\alpha = \{15, 30, 45, 60, 75, 90, 105, 120\}$pps. On the bottom it is shown the surface generated by the $F_{EM}(\alpha, L)$

2.6 Validation of the Evaluation Model Developed

The comparisons made between the various models presented in the next section help to understand if the developed Evaluation model shows an acceptable trend that does not diverge with the ones modeled by previous verified studies.
In this section, the main objective is to show that the Evaluation model we built is also compatible with the experimental data.
It should be pointed out that, among the various articles consulted, none of them reported empirical data that isolated and measured the passive shortening tension. So, until now, only the trend of the passive lengthening force can be validated with the experimental data found from those articles.

2.6.1 Data provided by I.E.Brown, E.J.Cheng and G.E.Loeb

In the article I.E.Brown et al. (1999), are found empirical data of the Active isometric force and the Passive force in lengthening condition carried out on a Caudiofemoralis muscle and then properly normalized.

2.6.1.0.1 Active Force Validation

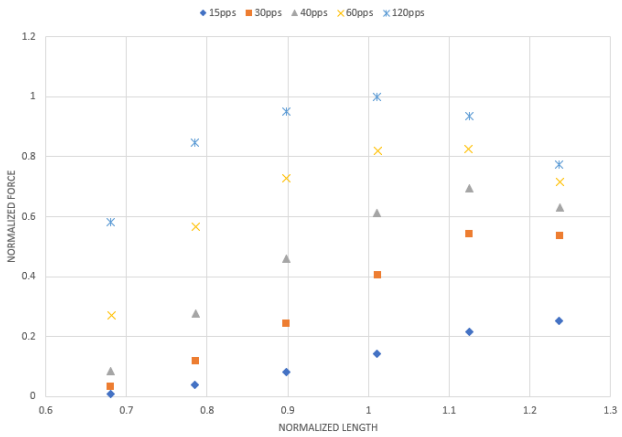

Figure 2.17: Here, are reported the data related to the Active Isometric tension extracted from the article I.E.Brown et al. (1999). The measurements were carried out at different frequency of activation: $\alpha = \{15(\text{rhombus}), 30(\text{squares}), 40(\text{triangles}), 60(\text{x}), 120(\text{stars})\}$pps, at lengths L = $\{0.68, 0.79, 0.90, 1.01, 1.12, 1.24\}L_0$

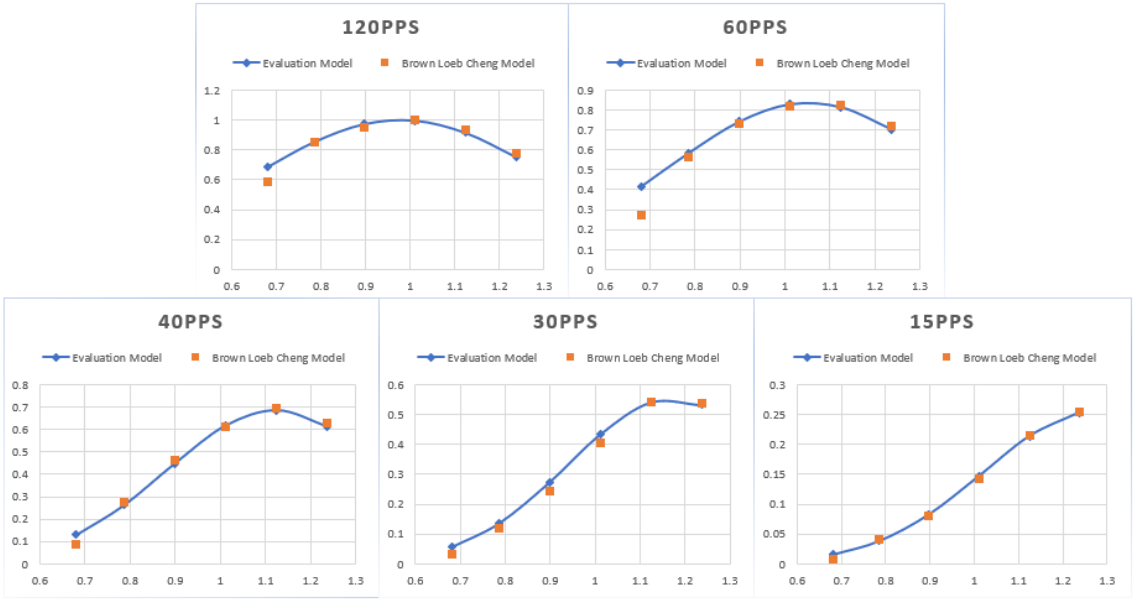

Figure 2.18: Plot comparison between the empirical data of the experiments on the Active isometric force conducted by Brown, Cheng and Loeb, at different frequencies of activation as shown in the figure 2.17

As regards the comparison with the data of the experiments on the isometric active force, it is possible to notice a remarkable precision of the evaluation model in reproducing the real behavior of the muscle in isometric condition. Computing the error at the j-th activation frequency as:

$$Err_{Active,j} = \sum_{i=1}^{n} \frac{|F_A(\alpha_j, L) - Measured\_Data(\alpha_j, L)|}{n} \tag{2.20}$$

Where in this case n = 6, since it is defined as the number of sampled lengths; $F_A(\alpha, L)$ is the active force component of the evaluation model, and $Measured\_Data(\alpha, L)$ is the empirical force data, measured at a frequency α, and at a length L.

Activation Frequency	Active Force Error
15pps	0.33%
30pps	1.79%
40pps	1.78%
60pps	3.63%
120pps	2.90%

Table 2.3: Error of the deviation from the empirical data and the force values computed by the Evaluation model

As it can be seen from the table 3.5, the error computed for all the three sampled frequency of activation, results to be very small, with an average that goes around

the 2.08%. However, these results are not surprising, since they are exactly it has been used to build the isometric force of active contraction relation. So, as a conclusion, it can be said that the fitting of the curve was performed satisfactorily, with a practically negligible implementation error.

Always on the same article [I.E.Brown et al. (1999)] there were also provided additional active isometric force data, but, related only to the tetanus frequency of activation (120pps).

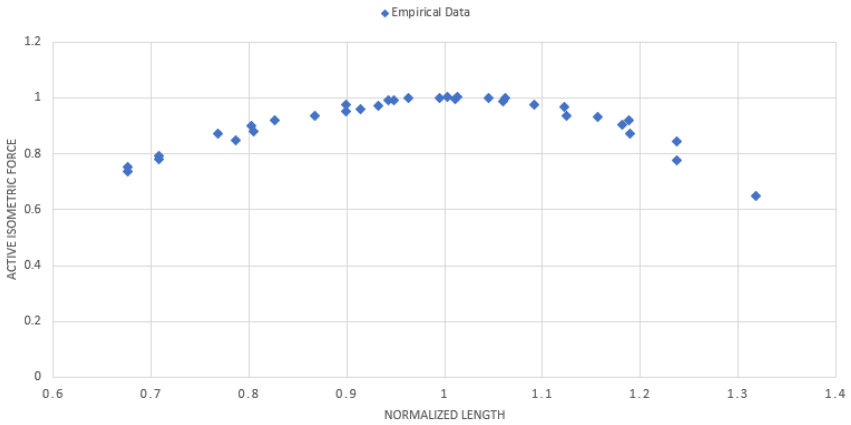

Figure 2.19: Empirical data of the Active isometric force in tetanus condition measured by Brown Loeb and Cheng.

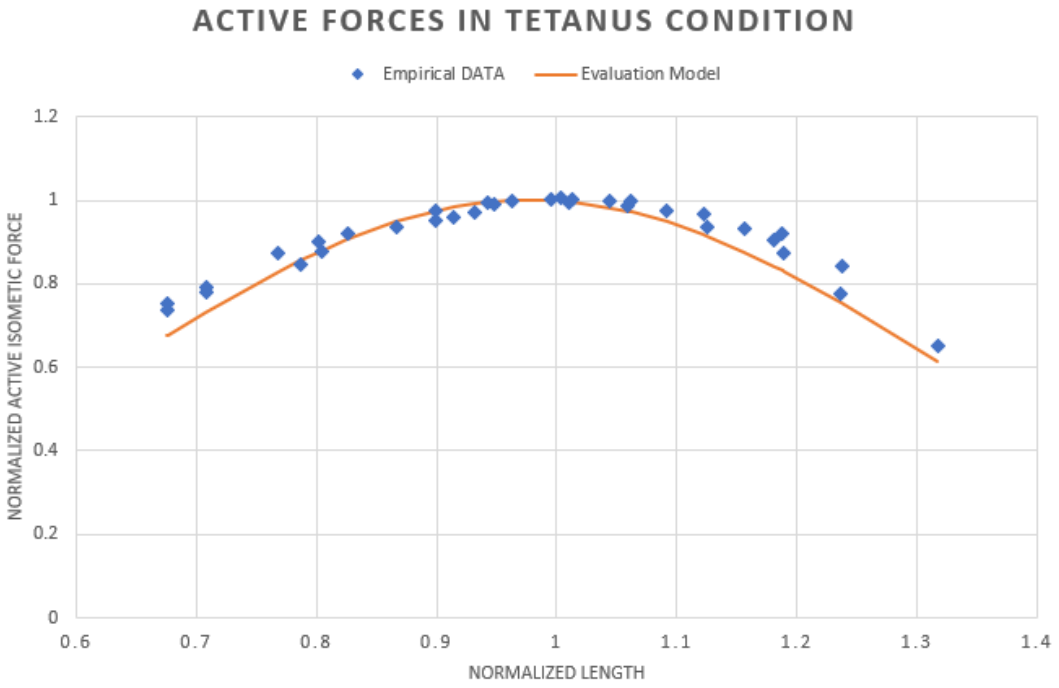

Figure 2.20: Plot comparison between the empirical data of the experiments on the Active isometric force conducted by Brown, Cheng and Loeb at tetanus conditions.

In this case, since the set of data is wider with respect to the one provided by the figure 2.17 then the error, which is computed with the same equation (2.20),

amount of 2.91%. And this can be taken as a first remarkable result that can prove the validity of the model developed since these data were not be used by the fitting procedure which built the evaluation model.

2.6.1.0.2 Passive Force Validation

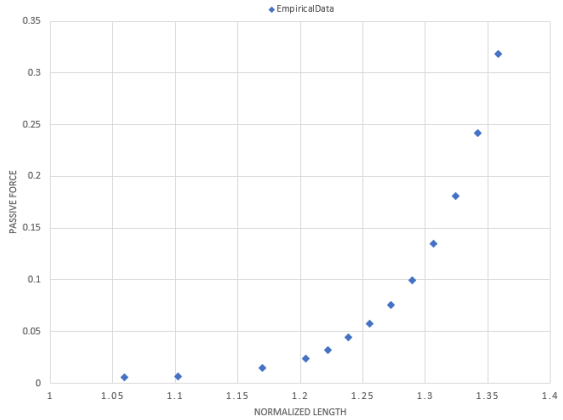

Figure 2.21: Here, are reported the data related to the Passive extracted from the article I.E.Brown et al. (1999).

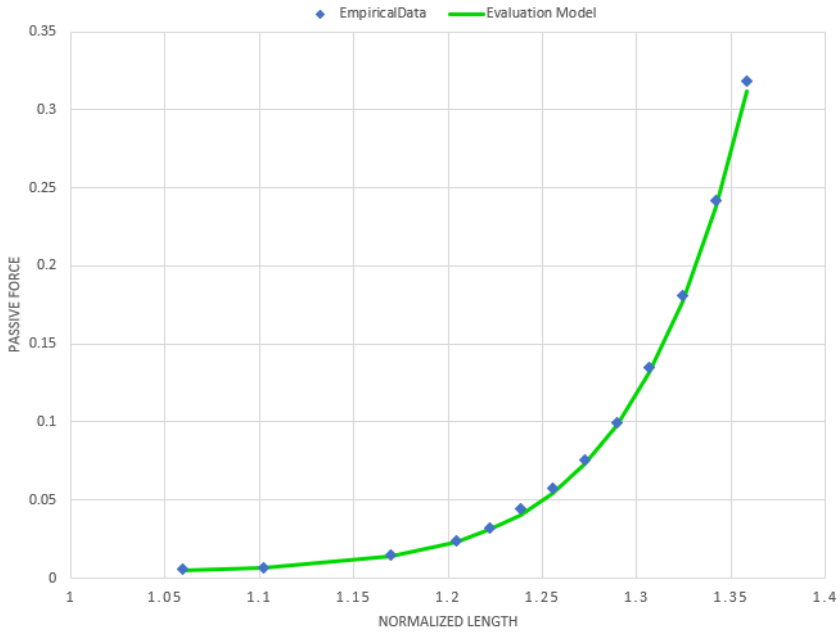

Figure 2.22: Plot comparison between the empirical data of the experiments on the passive force conducted by Brown, Cheng and Loeb, shown in the figure 2.21

Also in this case, as in the case previously studied for the active force, the error, computed according to the formula:

$$Err_{Passive} = \sum_{i=1}^{n} \frac{|F_{PL}(L) - Measured\_Data(L)|}{n} \tag{2.21}$$

Where n in this case is equal to 13, as the number of sampled lengths, $F_{PL}(L)$ is the lengthening passive force component of the evaluation model, and Measured_Data is,in this case, referred to the empirical data related to the lengthening passive tension measured by Brown, Cheng and Loeb. The amount of error in percentage results to be of about the 0.25%. However, for the same reason pointed out when was analysed the validation of the active isometric tension, this remarkable result allows to conclude that the of the passive force curve was done with a good precision, as good as to consider practically negligible the error.

2.7 Comparison Between Models

It may be of interest to make a comparison with previously developed models, in order to evaluate the main differences and the commonalities that are present between them. The model considered to carry out the comparison is the model developed by I.E.Brown et al. (1999) and the model developed by J.M.Winters (1995), previously described in the sections above.

2.7.1 Comparison With the Model developed J.M.Winters

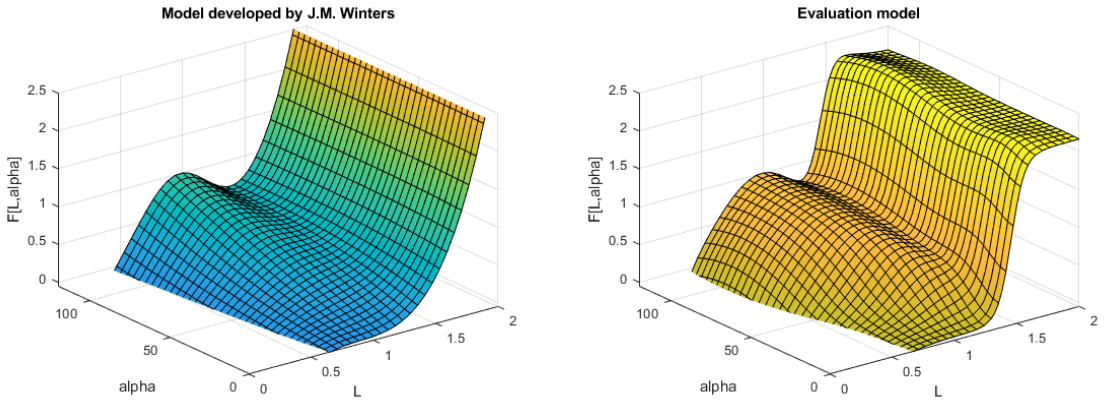

Figure 2.23: Plot 3D of the model developed by Brown, Cheng and Loeb(on the left) flanked by the 3D graph of the evaluation model(on the rigth)

The general procedure of comparison adopted was :

- Define an array composed by a certain number of sampled lengths;
- Compute the values of tension related to each length belonging to the array defined through the model developed by J.M.Winters and the Evaluation model defined in the previous sections;
- Compute the error between the output forces provided by the two models;

2.7.1.1 Active Force Comparison

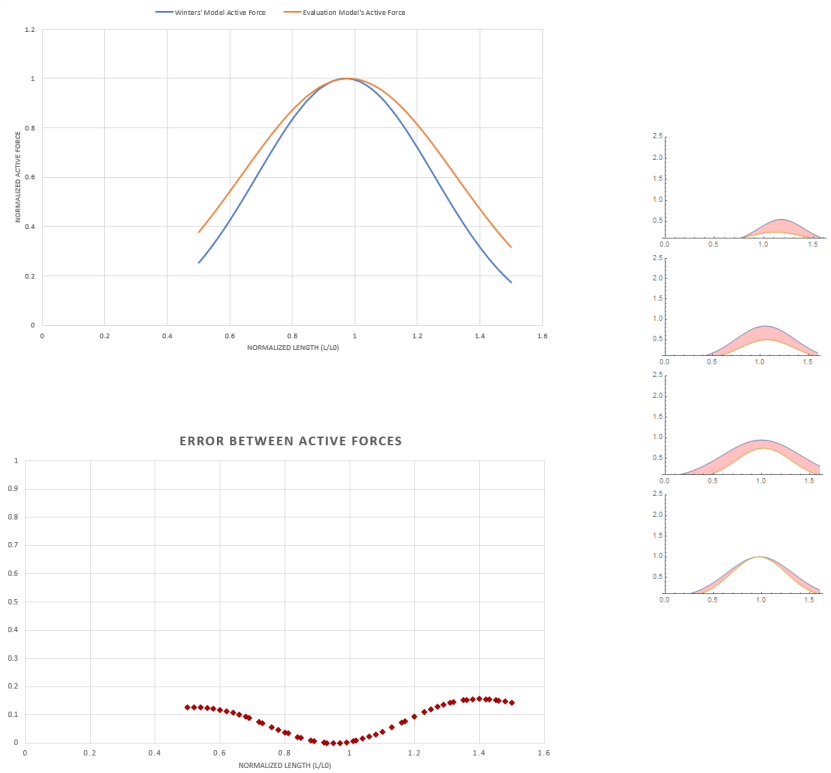

Figure 2.24: Trend of the Active Isometric component of the Evaluation Model in comparison with the Active Force modeled by Winters. On the left it is shown the comparison of the two models describing the muscle in tetanus conditions; Then it is also reported on the bottom-left side the trend of the error computed at the sampled lengths. On the right side, it is shown the comparison of the two models in different frequencies of activation: α = {25, 50, 75, 100}pps.The error in this plot is represented as a red area.

As it can be seen from figure 2.24, the trend of active forces is almost identical. Furthermore is worth notice that for lengths close to the optimal one the error drops to 0 under conditions of tetanic stimulation. By observing the development of the error, varying the stimulation frequency, it is qualitatively seen that the error, in a neighborhood of the optimal length, increases with decreasing frequency.
The close match between the two functions comes to the fact that both the active component of the model developed by J.M.Winters and the active component of the evaluation model is thought as Normal distributions: function (2.12) and (2.13), respectively. A difference can be seen in how the activation frequency affects is taken into account from the two models: Winters defines a parameter belonging to the interval [0,1], that do not modulate all the parameters; On the other hand, we have considered a set of coefficients all function of the activation frequency which is not normalized but it belongs to the range [0,120]pps.

2.7.1.2 Passive Force Comparison

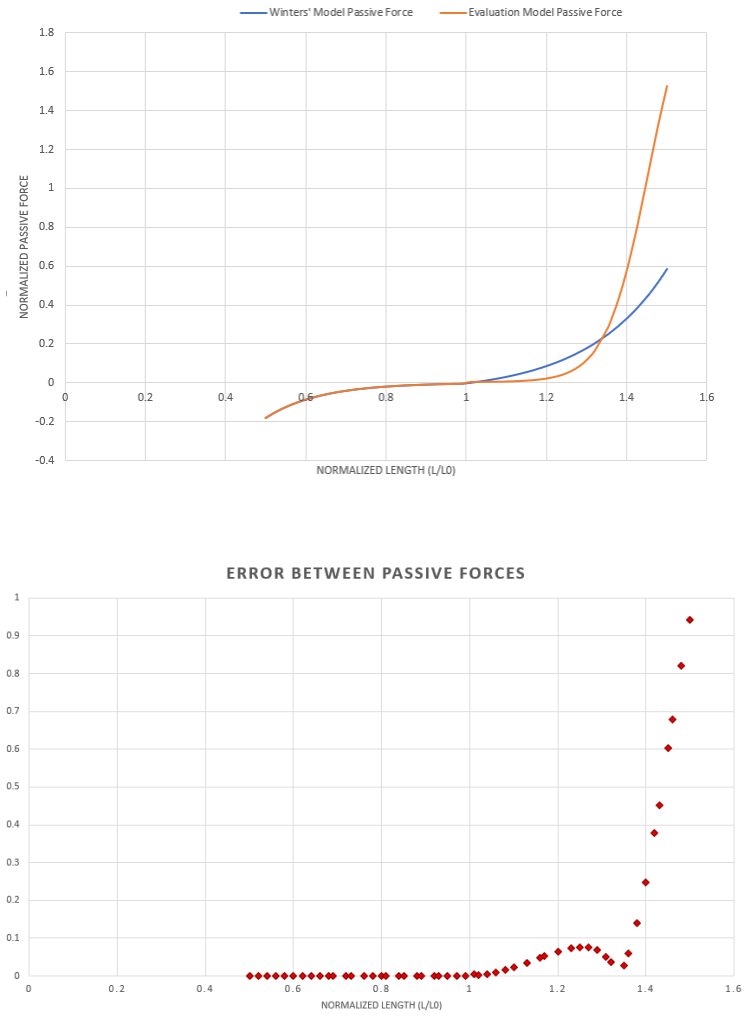

Figure 2.25: Trend of the Passive Forces of the Evaluation Model in comparison with the model developed by Winters. It is also reported on the bottom representation of the trend of the error computed at the sampled lengths.

with reference the figure 2.25, it is shown that the error between the two passive forces becomes relevant at high stretching length. Recalling the concept that passive forces do not normalize well, and, this behavior shows strict dependency on the structure of the muscle considered then the error that occurs between the two lengthening passive forces can be considered of secondary importance compared to the error that takes place between the two active isometric forces.
In this case, the relation provided by J.M.Winter for the passive force results more complex than the one provided by our Evaluation model: equation 2.13 and 2.16; It can be seen from the comparison of the two equations that Winters developed both the lengthening and the shortening passive forces with the same complex function but with different parameters, according to the length's range the muscle is found

to work. So for this reason it has been needed a piecewise function to assemble the total passive force. In the other case, we have defined two functions, passive shortening force, and passive lengthening force, so that their contributions could become null in the range where those functions should not be valid. Consequently, the passive force we developed is not defined as a piecewise function but as a sum of two contributions of forces, which simplifies the implementation of the model.

2.7.1.3 Total Force Comparison

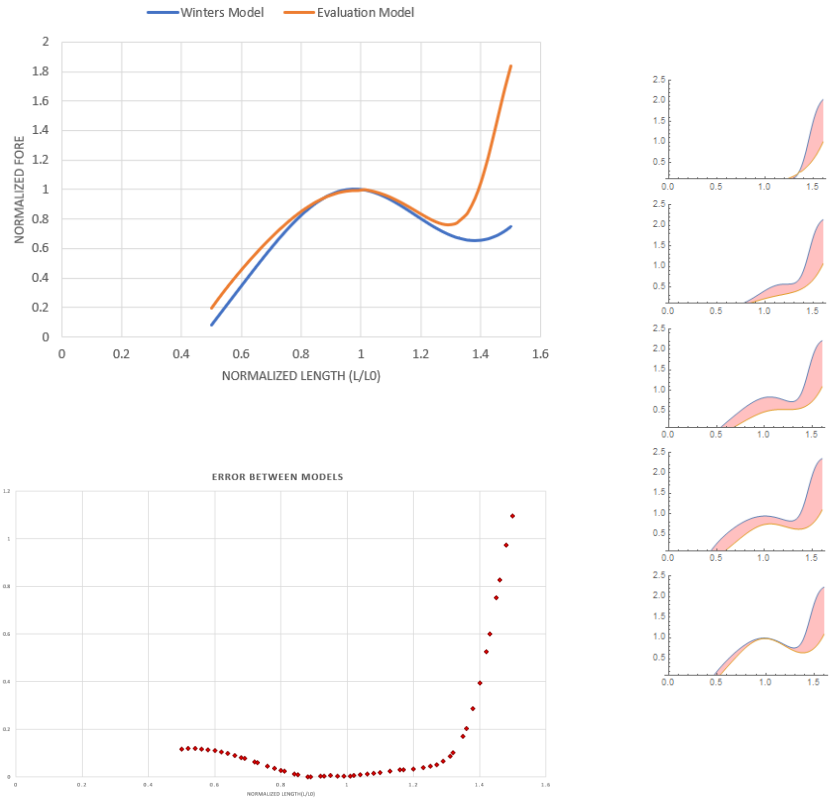

Figure 2.26: Trend of the Evaluation Model in comparison with the model developed by Winters. On the left it is shown the comparison of the two models describing the muscle in tetanus conditions; Then it is also reported on the bottom-left side the trend of the error computed in the sampled lengths. On the right side it is shown the comparison of the two model in different frequencies of activation : $\alpha = \{0, 25, 50, 75, 100\}$pps.The error in this plot is represented as a red area.

As we stated in the previous comparison the highest error can be seen to occur at high stretching lengths where the passive forces take place. In both, Winters and the Evaluation model developed, the total force delivered by the muscle is the result of the sum between the active isometric force and the passive force. But, recalling the consideration that the muscle cannot produce a stretching force and so the force generated by the muscle cannot be negative; In the model developed by Winters the total force is prevented to assume negative values by imposing that the passive shortening force compensates the active force so that the total force

production results to be 0; In our case, the evaluation model, it is saturated at 0 when the passive force is higher, in magnitude than the active force. In this way, the developed evaluation model should be easier to implement.

The error was computed as the :

$$Err := \frac{\sum_{i=1}^{n} |F_{EM}(\alpha, L_i) - F_{Winters}(L_i, \beta)|}{n}, \qquad n = number\,of\,L\,samples \tag{2.22}$$

where $F_{Winters}(L_i, \beta)$ is the total force developed by Winters' model, resulting from the sum of the equation (2.12) with equation (2.13). The frequency β can be defined as $\frac{\alpha}{120pps}$, since in the model Winters normalizes the activation frequency as a parameter belonging to the interval [0,1], and 120pps correspond to the tetanized frequency for the Evaluation model developed.
In this case considering the array of lengths previously defined the error between the Evaluation model and the model developed by Winter, considering a tetanized muscle, is about the 15.22%; Computing the error related to intermediate frequencies it can reach the 35% of deviation.

2.7.2 Comparison With the Model developed I.E.Brown, E.J.Cheng, and G.E.Loeb

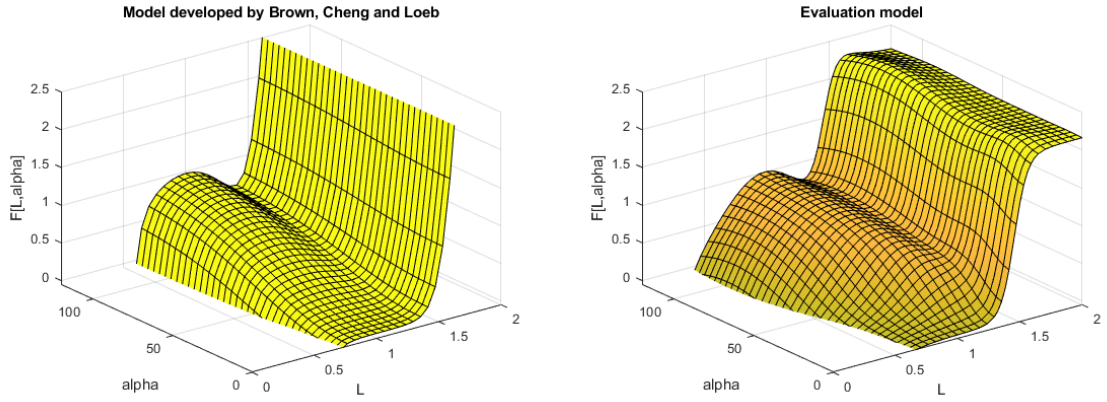

Figure 2.27: Plot 3D of the model developed by Brown, Cheng and Loeb(on the left) flanked by the 3D graph of the evaluation model(on the rigth)

In this case, the comparison for this model was carried out by directly consider the functions defined. Mainly because the plot provided by I.E.Brown, E.J.Cheng, and G.E.Loeb in their article I.E.Brown et al. (1999) is not complete and any trend of the shortening passive force is provided. However, in the same article, they provide a complete definition of all the numerical parameter in order to allow correct implementation of the model. For this reason, through the usage of Wolfram Mathematica Inc. (Inc.), which is a computing system optimized for the symbolic calculus the comparison took place at a symbolic level allowing a more detailed analysis of data.

2.7.2.1 Active Force Comparison

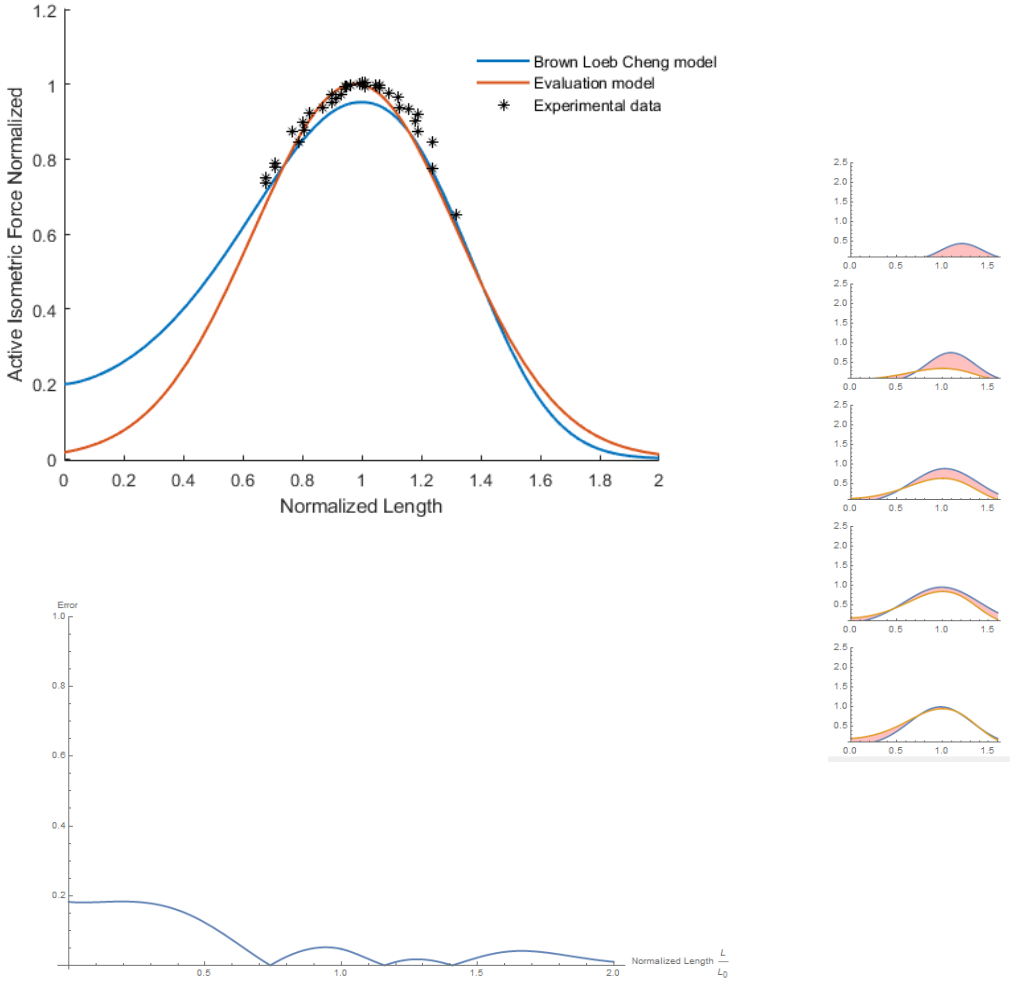

Figure 2.28: Trend of the Active Isometric component of the Evaluation Model in comparison with the Active Force modeled by I.E.Brown, E.J.Cheng, and G.E.Loeb. On the left it is shown the comparison of the two models describing the muscle in tetanus conditions; Then it is also reported on the bottom-left side the trend of the error computed at the sampled lengths. On the right side, it is shown the comparison of the two models in different frequencies of activation: $\alpha = \{25, 50, 75, 100\}$pps. The error in this plot is represented as a red area.

Considering the relation (2.15) and (2.5) which are respectively the Evaluation active isometric force component and the Active contractile force of the model taken by Brown, Cheng, and Loeb. Regarding this last equation, the Active isometric force, from the F_{CE} relation was obtained by setting the recruitment factor to 1 (as they suggest to do) and setting the force-velocity relationship, FV(L), to 1 too; Since at isometric condition the contribution provided by the speed of motion must be null for definition, and so the FV(L) should not provide any modulation to F_{CE}, in isometric condition. Consequently, the Active Isometric Force relation can be found by the I.E.Brown, E.J.Cheng and G.E.Loeb's model taking the product between the

Activation frequency relation (2.10) and the force-length curve (2.9).
As it can be seen from the top-left plot represented in the figure 2.28, the trend by the two curves are mainly the same despite the fact that in this case the relation of the Active isometric force provided by Brown, Cheng, and Loeb is not defined as a Normal distribution. With reference to the plot of the error between the two curves, where the error function is defined as :

$$Err_{active} := |F_A(\alpha, L) - F_{CEisometric}(\alpha, L)| \tag{2.23}$$

the maximum error, occurs at shortening length far from the optimal one, while a modest divergence can be distinguished at lengths near the optimal one that become practically negligible at lengths spanning to length higher the resting length. As in the comparison analyzed previously with the J.M.Winters model, also in this case, where the error on average can be considered minimal, the substantial difference between the isometric active force model developed by Brown, Cheng and Loeb, and the evaluation model, from our point of view, lies in the simplicity of expression. Brown, Cheng, and Loeb developed a very accurate model which takes into account also complex behavior as the yielding of the muscle; however, since their model is focused on the model also those complex attitudes of the muscle then the result is a complex model which is not of interest from a control point of view. So the active isometric force we developed, does not take into account all the complex performance of the muscle but just considering the most prominent is able to model with a good accuracy the muscle behavior as the model developed by I.E.Brown, E.J.Cheng and G.E.Loeb can do, but at the same time keeping a more flexible and simpler expression which allows the model to be easier implemented.
As noticed in the comparison with the Winters model in the previous subsection, also, in this case, the error at lower frequencies is higher than the error at higher ones, as it can be seen qualitatively in the right plot of the figure 2.28.

2.7.2.2 Passive Force Comparison

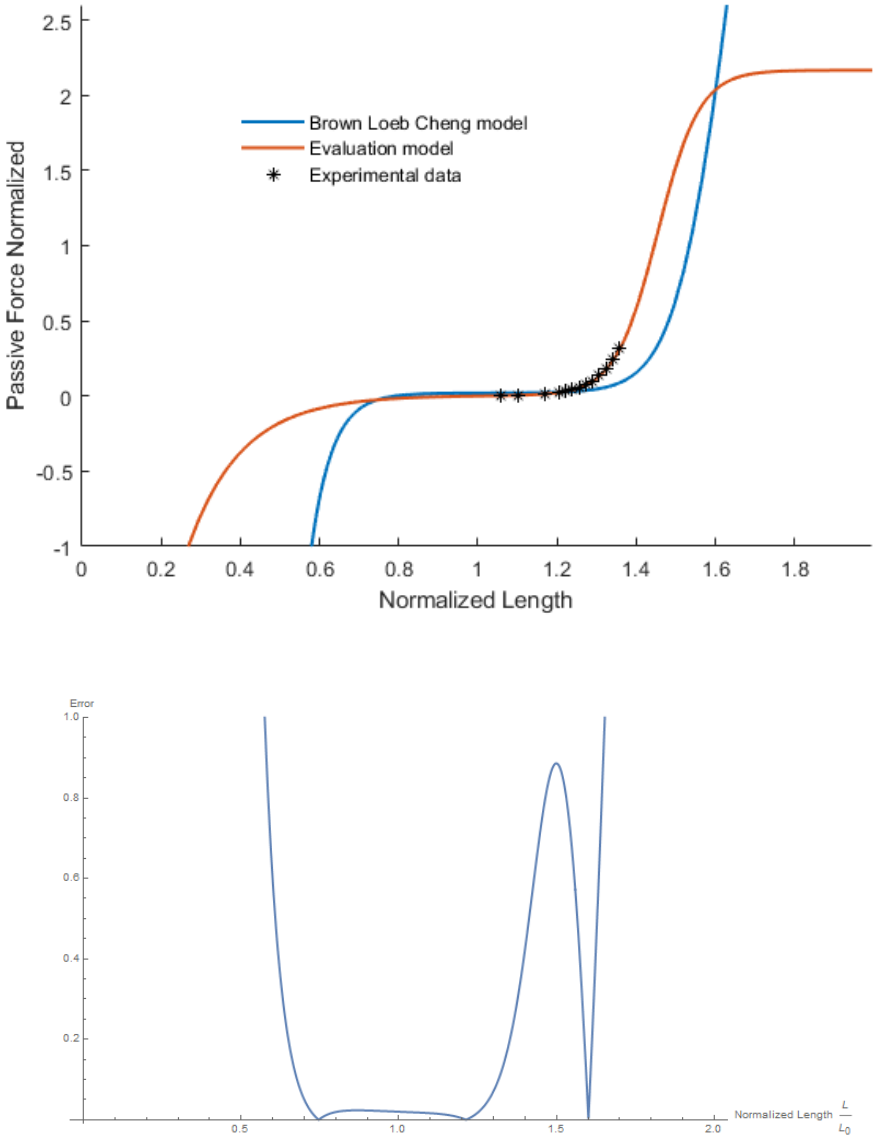

Figure 2.29: Trend of the Passive Forces of the Evaluation Model in comparison with the model developed by I.E.Brown, E.J.Cheng, and G.E.Loeb. It is also reported on the bottom representation of the trend of the error computed at the sampled lengths.

As explained several times in the previous sections, the comparisons between passive forces are always to be considered with caution since the passive tensions are closely related to the mechanical properties, and therefore dependent on the structure of the sample muscle, used to develop the model; The generalization of these effects is almost unreachable. However, a trend analysis can be conducted in detail. And in this case, as you can see in figure 2.29, the trends of the two forces are practically identical. A substantial difference can be seen for shorter lengths than

the optimal one where the shortening passive adopted by I.E.Brown, E.J.Cheng, and G.E.Loeb assumes a steeper behavior than the passive force considered in the evaluation model. While, on the other hand, in stretch conditions, it can be noted that the slope of the two passives is almost identical and therefore the error introduced by this part of the curve is only an offset error. Obviously, above a certain length, the passive of the evaluation model has a plateau, in order to qualitatively represent the compliance of the muscle fibers; This behavior is not described by the I.E.Brown, E.J.Cheng and G.E.Loeb model and therefore the error above a certain length assumes values tending towards infinity, which means that the two models become incompatible. However, this incompatibility can be neglected as no experimental data have been found to favor one model over another and therefore the behavior in this region can be said to be unknown.

2.7.2.3 Total Force Comparison

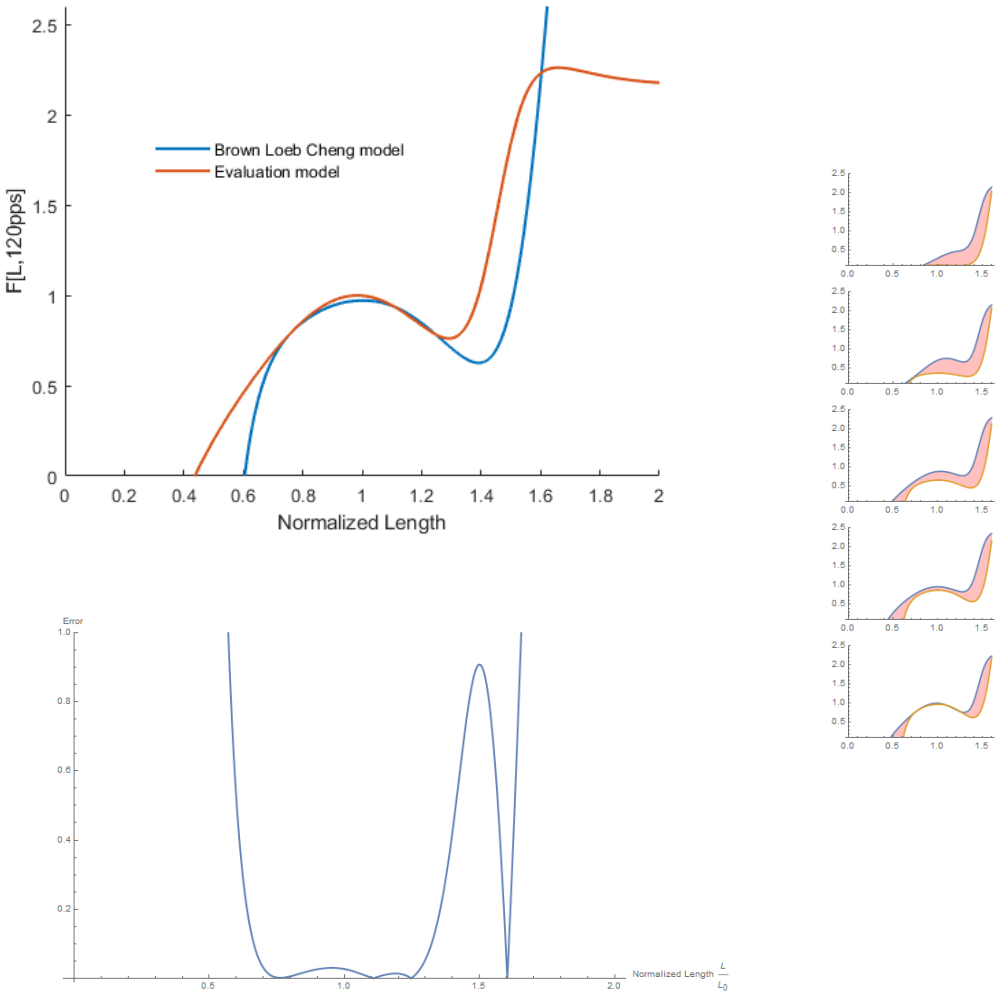

Figure 2.30: Trend of the Evaluation Model in comparison with the model developed by I.E.Brown, E.J.Cheng, and G.E.Loeb. On the left it is shown the comparison of the two models describing the muscle in tetanus conditions; Then it is also reported on the bottom-left side the trend of the error computed in the sampled lengths. On the right side it is shown the comparison of the two model in different frequencies of activation : $\alpha = \{0, 25, 50, 75, 100\}$pps.The error in this plot is represented as a red area.

The evaluation model and the I.E.Brown, E.J.Cheng, and G.E.Loeb model show the same trend where the error is introduced for the most part at lengths far from the optimal one. And this behavior is a direct consequence of the divergence introduced by both, the active and the passive forces. As was stated in the comparison between the two active isometric lengths the modeled introduced by Brown, Cheng, and Loeb although it is a complete and accurate model it also shows a high complexity. Therefore the strengths points of the evaluation model developed are simplicity, flexibility and despite considering only the most relevant aspects of the muscle, and therefore are neglected all the complexities that it presents, this model shows a fair accuracy in describing the behavior of the muscle. Moreover, as has also been noted in the comparison with the J.M.Winters prototype, for lengths close to the optimal one, the model shows a very high affinity with the prototypes found in literature.

Chapter3

Control Model

In the previous chapter, a model was developed in which it could simulate muscle behavior while simplifying the phenomenon of muscle contraction as much as possible. The developed model maintains a relatively simple form, in comparison to the other models found in literature, and through an appropriate tuning of its degrees of freedom, it is able to simulate empirical data with a considerable accuracy. However, this model is still too complicated from a control point of view. In other words, if it is needed to implement certain control techniques that require simple models, the developed evaluation model is too complex to be used in such a purpose. This complexity can be attributed to the fact that muscle contraction is itself a non-linear and convoluted phenomenon, and therefore, any development of a model that maintains a certain accuracy, in fitting empirical data, should be a nonlinear function. For these reasons, a second model was developed. Defined as Control model, the objective of the design was to obtain a model that can be used for control purposes born from an interpretative point of view of the elastic behavior of the muscle which is a function of the excitement imposed and the state of the system itself. The control model was conceived as a product of two components:

- $K(\alpha, L)$: a polynomial function of L which coefficients are polynomial functions of α;
- $(L - L_0(\alpha))$: where L_0 is defined as a polynomial function of α going to represent the rest length: the length by which the muscle provides zero output force; And this length scale with the activation frequency as it can be seen from the plots of figure 2.16

Once the Evaluation model was proven to be accurate, the control model was built exploiting the data computed from the Evaluation model. The procedure adopted to find the polynomial equations of each component of the Control model was:

- Computing, through the Evaluation model the value of the rest length, L_0, considering a certain set of frequencies $\gamma = \{\alpha_1, \alpha_2, ..., \alpha_n\}$ where the value of the i-th activation frequency α_i must belong to the interval [0,120]pps;
- The set of rest length $L_0(\gamma)$ is then fitted by a polynomial function;
- Knowing the function which models the rest length, and knowing the function which models the force production of the muscle (the Evaluation model),then

the function $\bar{K}[\alpha, L]$ can be defined as the ratio between the Evaluation model force F_{EM} and the function $(L - L_0(\alpha))$:

$$\bar{K}(\alpha, L) = \frac{F_{EM}(\alpha, L)}{L - L_0(\alpha)} \tag{3.1}$$

- Considering a set of Lengths $\widetilde{L} = \{L_1, L_2, ...L_m\}$, then it is computed a set of $\bar{K}_i(\alpha_i, \widetilde{L})$.

- The set $\bar{K}_i(\alpha_i, \widetilde{L})$ is then fitted as a polynomial function in order to find the relation in L of the function K at a frequency α_i. It must be notice that at $L = L_0(\alpha_i)$ the function $\bar{K}_i(\alpha_i, \widetilde{L_0})$ shows a singolarity towards $+\infty$.The peculiarity of this function lies in the fact that this singularity involves only lengths very close to the length L_0; This means that exist a neighborhood of $\bar{K}_i$ where the values remain contained at normal, acceptable dimensions. Therefore it is possible to impose continuity in the fitting of the polynomial by sampling the data of $\bar{K}_i$ in the neighborhood of L_0 and neglecting these points of discontinuity; It will then be the fitting procedure that will create a curve without this singular trend.

- Repeating the previous point for each α_i belonging to γ then a set of a polynomial function of K is found, $K(\gamma, L)$. It is important to point out that each polynomial function K_j must be to the same order to a second polynomial function K_i for each i and j.

- Collecting all the coefficients of the polynomials $K(\gamma, L)$; for each coefficient related to the same power order of the parameter L, is performed a fitting procedure in order to model its dependency on the activation frequency with a proper polynomial function $k_i(\alpha)$. So that the result can be found in the form:
$$K(\alpha, L) = k_1(\alpha) \cdot L^z + k_2(\alpha) \cdot L^{z-1} + ... + k_s(\alpha) \cdot L^{z-p} \tag{3.2}$$

- Finally the Control model can be obtained by assembling all the polynomial functions found in order to model the force production of the muscle according the relation :
$$F_{CM}(\alpha, L) = K(\alpha, L) \cdot (L - L_0(\alpha)) \tag{3.3}$$

A good result was obtained by representing the component $K(\alpha, L)$ as a polynomial of the 4th order in function of the length, where each coefficient was a polynomial of the 6th order in function of the activation frequency :

$$K(\alpha, L) = k_1(\alpha) \cdot L^4 + k_2(\alpha) \cdot L^3 + k_3(\alpha) \cdot L^2 + k_4(\alpha) \cdot L + k_5(\alpha) \tag{3.4}$$

where the i-th coefficient of $K(\alpha, L)$ is in the form :

$$k_i(\alpha) = h_1 \cdot \alpha^6 + h_2 \cdot \alpha^5 + h_3 \cdot \alpha^4 + h_4 \cdot \alpha^3 + h_5 \cdot \alpha^2 + h_6 \cdot \alpha + h_7 \tag{3.5}$$

Building then the matrix H which elements are the degrees of freedom of the function $K(\alpha, L)$ defining the element $h_{i,j}$ the j-th coefficient of the polynomial function $k_i(\alpha)$, i-th coefficient of the function K:

$$\mathrm{H} = \begin{pmatrix} -10^{-9} & 5.50 \cdot 10^{-7} & -1.15 \cdot 10^{-4} & 1.20 \cdot 10^{-2} & -6.21 \cdot 10^{-1} & 14.92 & -86.43 \\ 6.48 \cdot 10^{-9} & -3.30 \cdot 10^{-6} & 6.55 \cdot 10^{-4} & -6.46 \cdot 10^{-2} & 3.27 & -76.20 & 471.34 \\ -1.50 \cdot 10^{-8} & 7.27 \cdot 10^{-6} & -1.38 \cdot 10^{-3} & 1.31 \cdot 10^{-1} & -6.40 & 144.62 & -931.85 \\ 1.49 \cdot 10^{-8} & -6.94 \cdot 10^{-6} & 1.28 \cdot 10^{-3} & -1.17 \cdot 10^{-1} & 5.51 & -121.02 & 798.66 \\ -5.34 \cdot 10^{-9} & 2.42 \cdot 10^{-6} & -4.33 \cdot 10^{-4} & 3.86 \cdot 10^{-2} & -1.77 & 37.72 & -251.74 \end{pmatrix}$$

As regards the polynomial which model the trend of the rest length $L_0(\alpha)$, a parabola was found to fit well the data provided by the Evaluation model. Then the rest length function can be found in the form:

$$L_0(\alpha) = r_1 \cdot \alpha^2 + r_2 \cdot \alpha + r_3 \tag{3.6}$$

where it can be defined the parameter vector R:

$$\mathrm{R} = \begin{pmatrix} r_1 \\ r_2 \\ r_3 \end{pmatrix} = \begin{pmatrix} 5.61 \cdot 10^{-5} \\ -1.10 \cdot 10^{-2} \\ 9.44 \cdot 10^{-1} \end{pmatrix}$$

Once the functions K and L_0 have been defined, the equation of the isometric force of a muscle with normalized length and tension parameters, modeled by the Control model, is obtained through the equation (3.3). The trend is shown in the figure below:

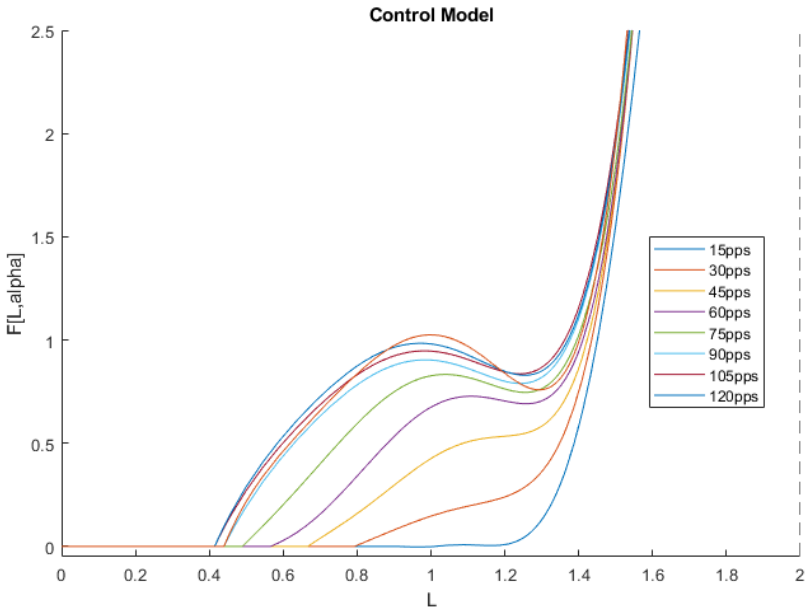

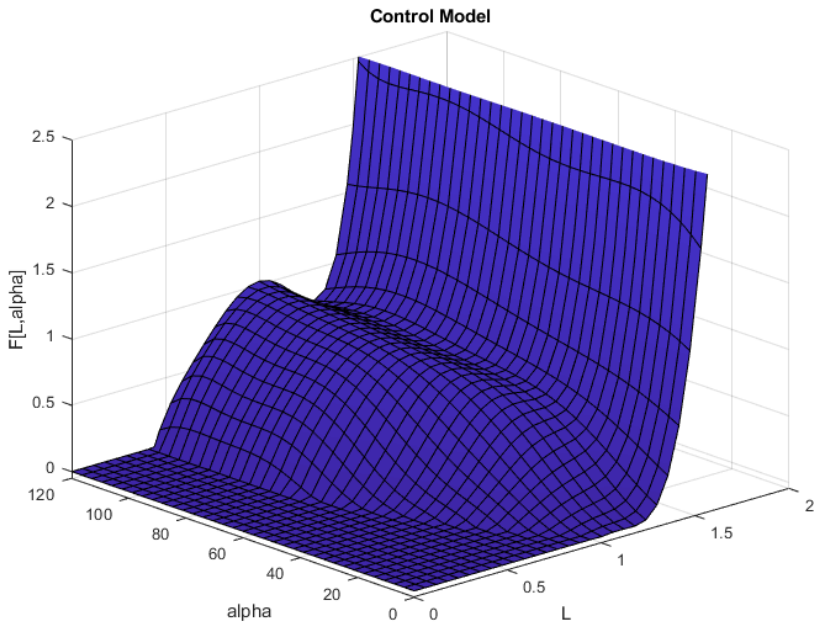

Figure 3.1: Plots of the Control Model's trend. On the top, it is shown the comparison of the trend assumed by the curve at fixed activation frequencies, $\alpha = \{0, 20, 40, 60, 80, 100, 120\}$pps. On the bottom it is shown the surface generated by the $F_{CM}(\alpha, L)$

As it can be seen from both the graphs of figures 3.1 also for the control model, as has been proposed for the evaluation model, shows saturation at zero in case F_{CM} is supposed to assume negative values. On the other hand, for high stretches imposed, the final control model is not capable to model the plateau proposed, in the theoretical line. The main reason to neglect the plain trend at high stretch lengths was the fact that modeling the complete behavior introducing also the plateau would worsen a lot the performance of the Control model itself. Since this behavior is only theoretical and not validated, and those lengths are generally not reached by the muscle, that is working in normal conditions, then in the development of the control model, it was preferred to neglect such behavior in such a way to increase accuracy and reduce the complexity of expression.

3.1 Comparison Between Control Model and Evaluation Model

As already specified in the previous section, the control model does not show any plateau at high stretch lengths; Therefore a divergence between the Control model and Evaluation model can be expected for lengths at a certain distance from the optimal one. However, it may be of interest to compare the trend of the control model with those of the evaluation model. From the first section of this chapter, the Evaluation model can be assumed to be a good reference to perform a comparison and to validate the control model. Therefore analyzing the deviation that exists between the control and the evaluation model, can also be roughly considered as the error that the control model makes in modeling the real muscle force-production phenomenon.

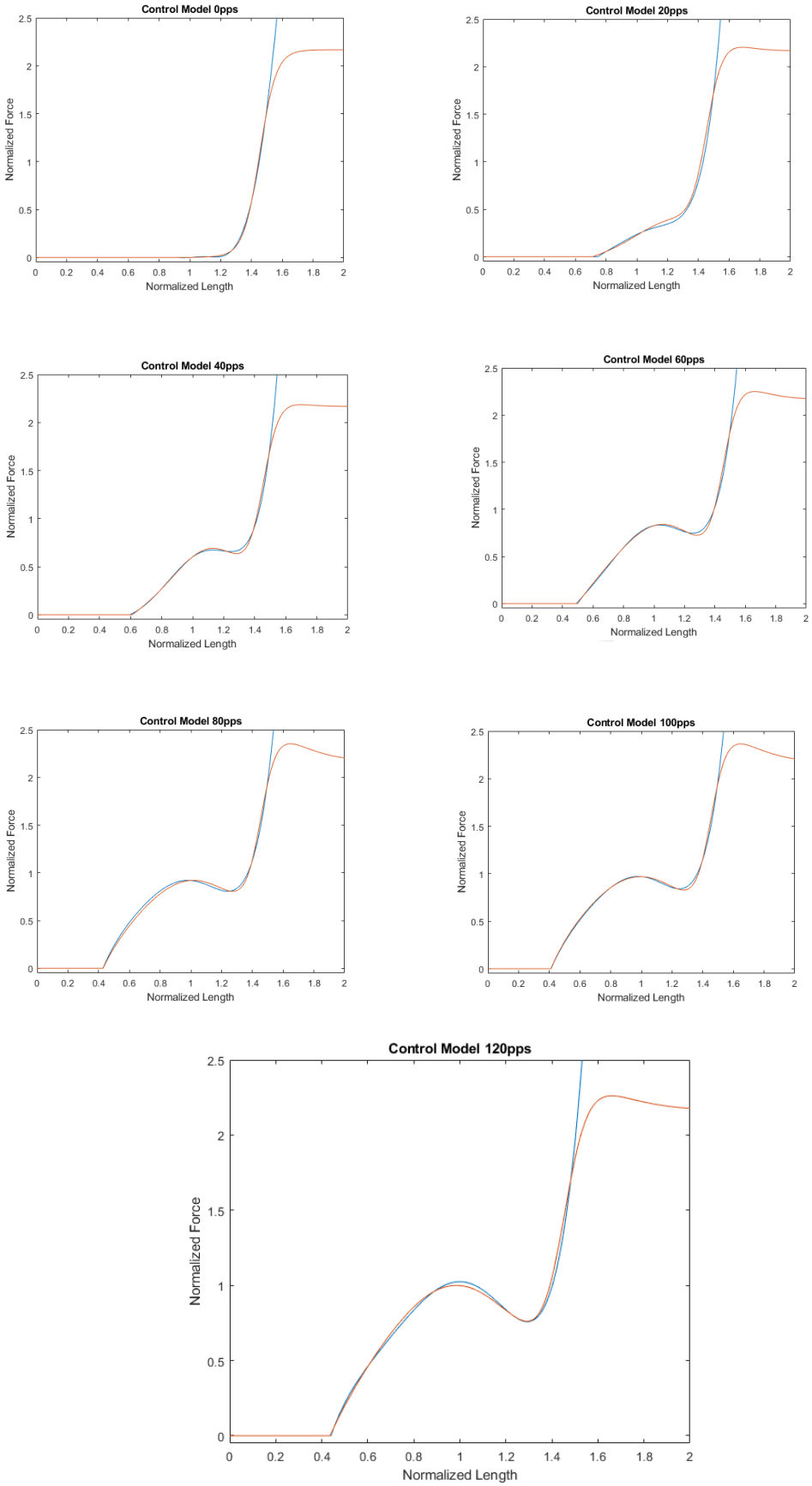

Figure 3.2: Plots comparison between Control model(blue line) and Evaluation model(orange line) at different activation frequency: $\alpha = \{0, 20, 40, 60, 80, 100, 120\}$pps

From the comparison graphs of figure 3.2 carried out at various excitation fre-

quencies it can be seen that the error between the control model and the evaluation model is very low, so much so that the two curves almost coincide for lengths between $[0,\ 1.5]L_0$. So it can be of interest to see the trend of the error, to understand where the control model shows the largest divergences:

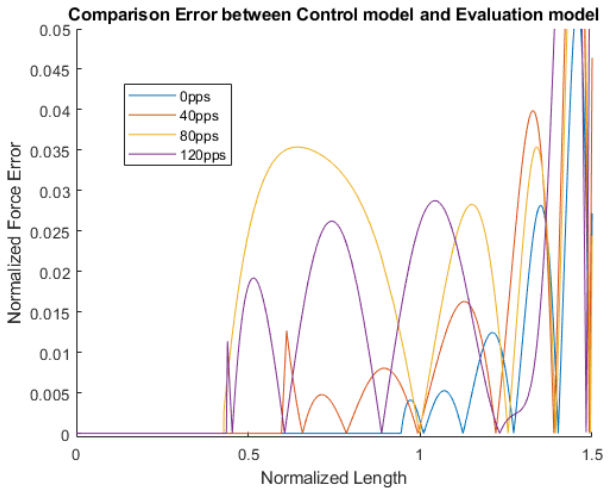

Figure 3.3: trend of the Error coming from the comparison between the Control model and Evaluation model at different activation frequency: $\alpha = \{0,\ 40,\ 80,\ 120\}$pps

From figure 3.3 it can be seen that the trend of the error is strongly irregular along with the frequencies. However, in the interval of normalized lengths which goes from 0 to $\frac{3}{5}L_0$ the Error is to be bounded between 0 and 0.1. This means that in the range on which the control model is supposed to be valid, for any length belong to the interval the error will surely be found below the 10%. Computing the error as the area enclosed between the two models curves for seven frequencies :

Frequency	0pps (Passive force)	20pps	40pps	60pps	80pps	100pps	120pps (Tetanus)
Error in %	0.78%	0.58%	1.21%	0.78%	1.96%	0.57%	1.60%

Table 3.1

From the table above it can be seen that the Error along the interval considered is remarkably low with a maximum percentage that goes around the 2% at medium-high frequencies.
From these unexpected results, then it can be concluded that the two models can be considered practically identical, in the range of working conditions (no overstretch of the fibers occurs). So then the main difference relies on the implementation: in case it is needed to describe the main behavior of the muscle, then the Evaluation model is more suited to this purpose since it shows a more compact expression and fewer degrees of freedom to tuned with respect the control model. On the other hand, if the model should be used for control purposes then the Evaluation model results to be difficult to analyze and so then the Control model is needed.

3.2 Analysis of the Error between Control model and Empirical data

In the previous section, it has been found out that the error between the Control model and the Evaluation model is very low, as the two curves can be considered identical. However, behind this consideration, there is the assumption that the muscle considered is a cat Caudiofemoralis. This because the Control model was build considered the Evaluation model with parameters tuned for a Caudiofemoralis of a cat. Can be then of interest to analyze the Error that occurs between the Control model and the empirical data of other muscles belonging to other animal and if a proper tuning of the degrees of freedom of the Control model leads to a remarkable reduction of the error as it was seen for the Evaluation model.

3.2.1 Data coming from I.E.Brown, E.J.Cheng and G.E.Loeb experiments

Before comparing the experimental data obtained from other muscles of other animals, it may be of interest to calculate the error between the Control model and the empirical data from where the evaluation model was developed.

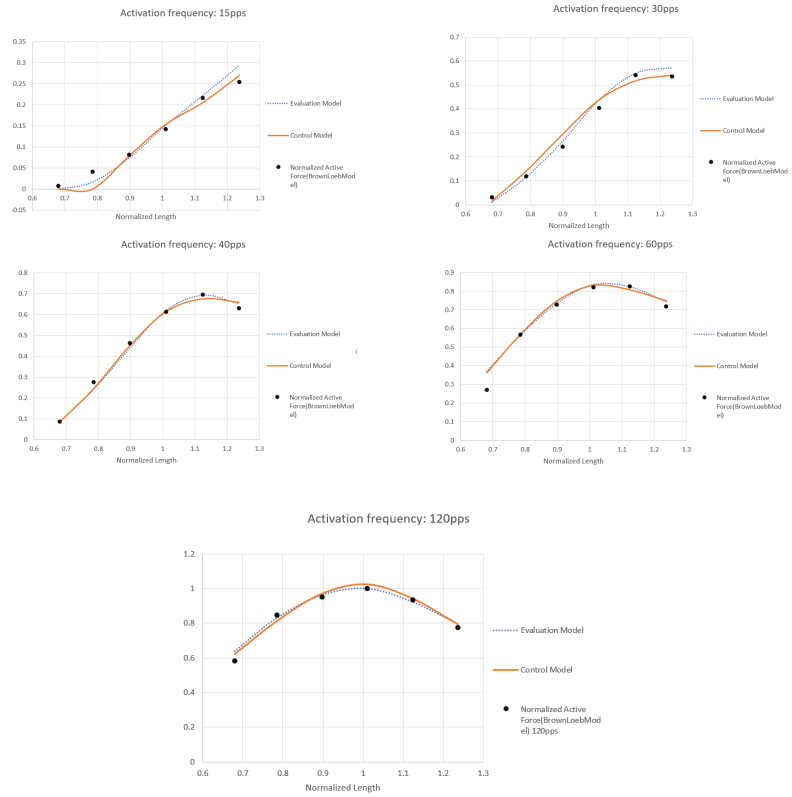

Figure 3.4: Plot comparing the trend of the Evaluation model(blue dotted line), the trend of the Control model(orange continuous line) and the trend along the length axis of the Empirical data collected by I.E.Brown, E.J.Cheng and G.E.Loeb experiments(I.E.Brown et al. (1999)), at different activation frequencies.

It should be pointed out that, the empirical data of figure 3.4 are referred to the active isometric component of force; However, this comparison can be considered valid only because in the range of lengths considered ($[0.6, 1.3]L_0$) the passive forces can be assumed to be null, and so the Control model and the Evaluation model outputs can be thought as active forces.
Computing the average error between Control model and the experimental data :

Frequency	15pps	30pps	40pps	60pps	120pps (Tetanus)
Error in %	1.47%	2.51%	1.55%	2.87%	2.33

Table 3.2

As it has been shown, in the section where the two models are compared, the control model has a very low error compared to the trend of the evaluation model, and this leads as a consequence that also the error with the experimental data from where the evaluation model was fitted, is seen to be very low. In fact, from the table 3.10 it can be seen that this does not exceed 3%, in the length range considered.

3.3 Open Loop Simulations

To analyze the behavior of the models developed in simulation, a simple experiment was considered:

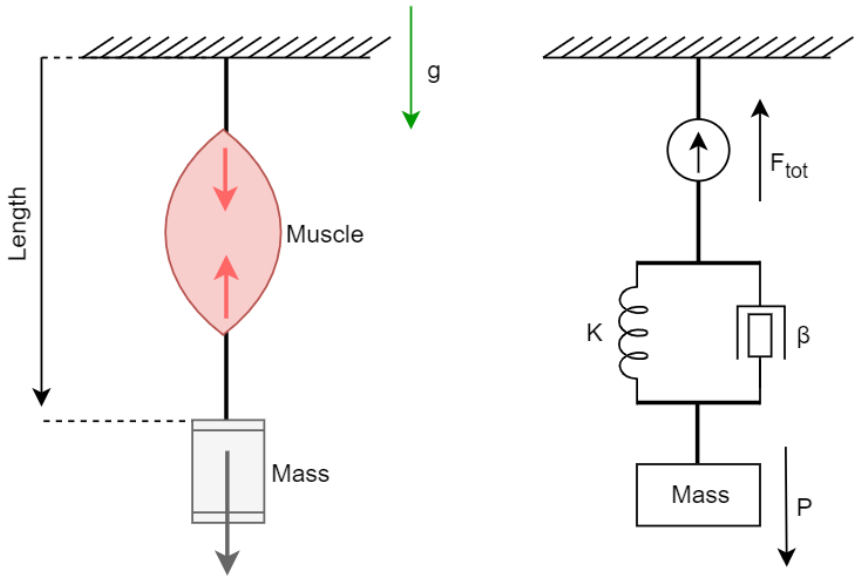

Figure 3.5: Schematics of the experiment performed to simulate the behaviour of the two models. On the left it is represented the structural idea of the configuration of the system; On the right is represented the conceptual model of each part of the structure.

The experiment taken into consideration is based on considering a modeled muscle, with the parameters of the cat Caudiofemoralis, bound to a fixed horizontal structure. A mass M is attached to the free end of the muscle itself. The whole

system is subjected to the gravitational field aligned with the vertical direction, as shown in figure 3.5. Muscle action is represented by a force generator. While the structural mechanical properties have been modeled by a spring and a damper in parallel, which parameters have been chosen arbitrarily.

By representing the two models on MATLAB's Simulink MathWorks (MathWorks), the simulation schematic of the experiment was then built for both models developed:

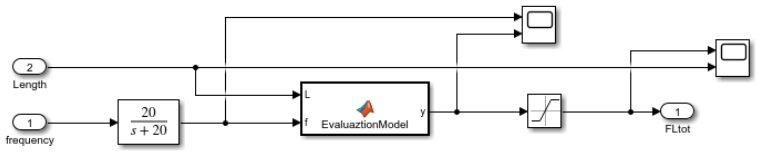

Figure 3.6: Schematic of the subsystem that contain the Evaluation model function

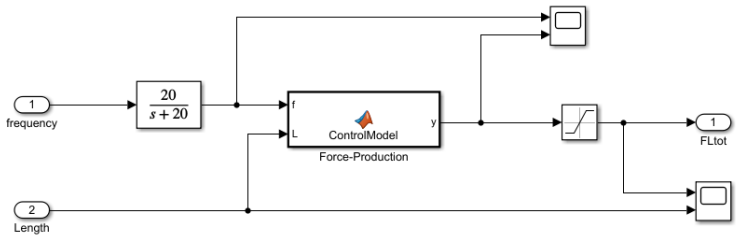

Figure 3.7: Schematic of the subsystem that contain the Control model function

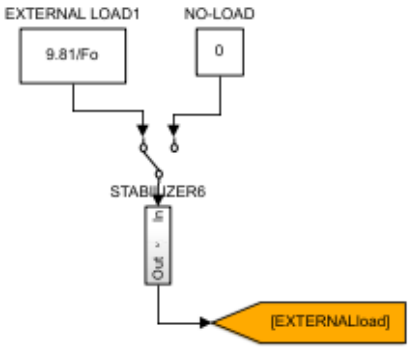

Figure 3.8: Schematic of the external load applied on the muscle

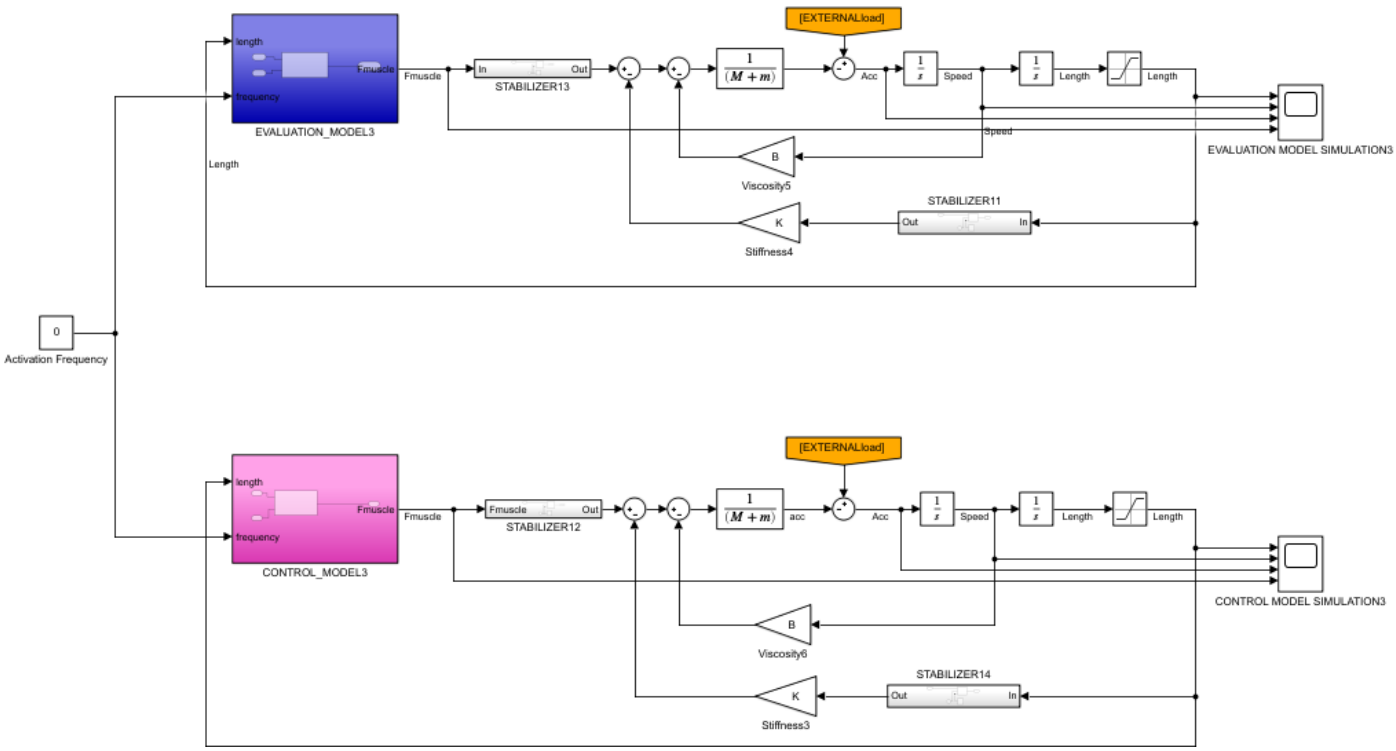

Figure 3.9: Evaluation and Control model's experiment schemes controlled by a constant Activation frequency

The schematic was found exploiting the mechanical equation that can be computed from exploiting the equilibrium of forces :

$$(M+m)\ddot{L} = P - F_{tot} + \beta\dot{L} + KL \tag{3.7}$$

where M is the external mass, m the mass of the muscle, P describes the weight, F_{tot} in this case is the total force provided by the muscle, K and β are the stiffness and the damper coefficient respectively and finally L is the length assumed by the muscle. All the quantities were normalized to Fo, which represents the maximum contractile force the muscle can produce, or Lo, defined as the length at which Fo occurs; This was done to make the overall system compatible with the Evaluation and the Control models. The models developed are based on a relationship dependent on both the frequency of excitation and the length of the muscle itself. Therefore, as can be seen from the diagram in figure 3.9, the implementation of the model requires two inputs, the length and the frequency, and one output, the force. As far as length input is concerned, this information can be fed back with the length during the simulation, which continuously provides the actual length assumed by the muscle. While the frequency of activation is the controllable input of the system. This means, that, by controlling the stimulation it is possible to change the system's balance point, and so it is, therefore, possible to change the length at which the muscle stabilizes. Furthermore, a block called 'stabilizer' can be seen in the diagram. This block imposes an additional initial behavior to the system dynamics, to permit the muscle to reach a stable isometric force value. In other words, the muscle for the first second is forced not to vary its length so that it can reach stable starting values.
The physical behavior of the system is found to be: after one second the muscle

reaches the isometric force production related to the length at which it is forced to stay and the frequency at which it is excited. Then once the bound is released, the muscle tries to contract, to impose a negative acceleration on the mass. However, the weight of the overall mass of the system will impose a stretching force on the muscle. The equilibrium position assumed, will be then the point upon which the muscle force can sustain the weight of the system.
It has been simulated then the behavior of the scheme at different frequency imposed, and the results provided by the two models were compared:

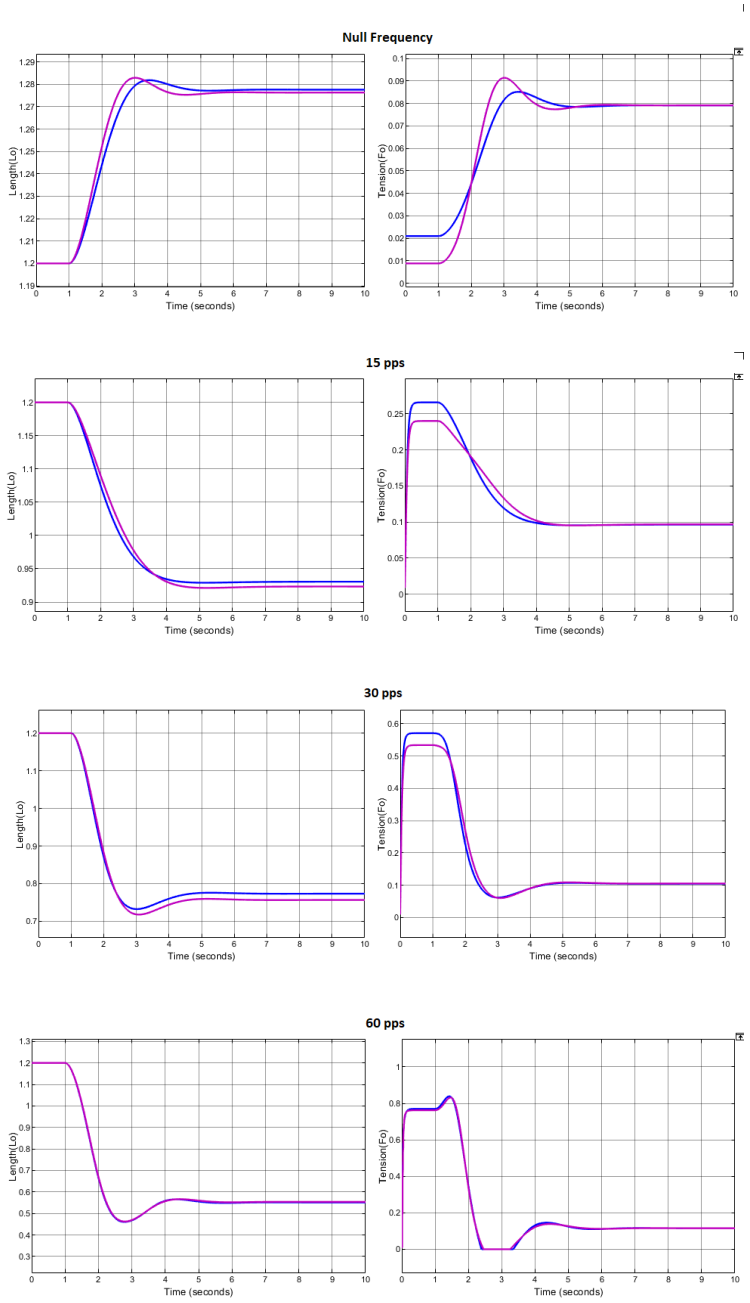

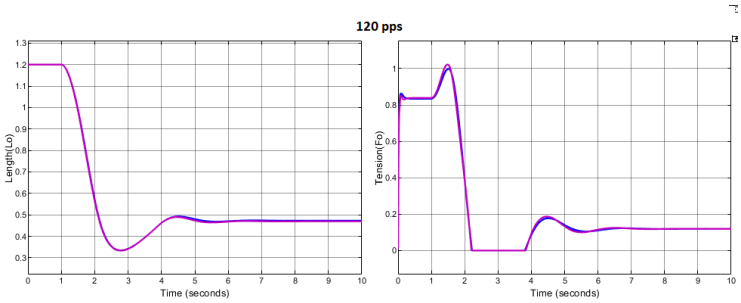

Figure 3.10: Scope of the simulation of the experiment considering an external mass M of about 0.3Kg, at different frequency of activation. It is represented in Blue the Evaluation model and in Pink the Control one. On the left it is found the length in function of the time and on the rigth is found the Tension developed by the muscle, in function of the time.

As it can be seen also from the simulation, the behavior of the two models is very similar. From the plots above, in figure 3.11, is shown the comparison between the dynamics of the two models used in the same experiments. It can be noticed that the error increases for lower frequencies and it is practically null at high frequency. Graphing the dynamics of the Error in time for both the length and the tension it results to be bounded under $18 \cdot 10^{-3} L_0$, as regarding the length error. And less than the $5 \cdot 10^{-2} F_o$; As it can be seen from the following figure:

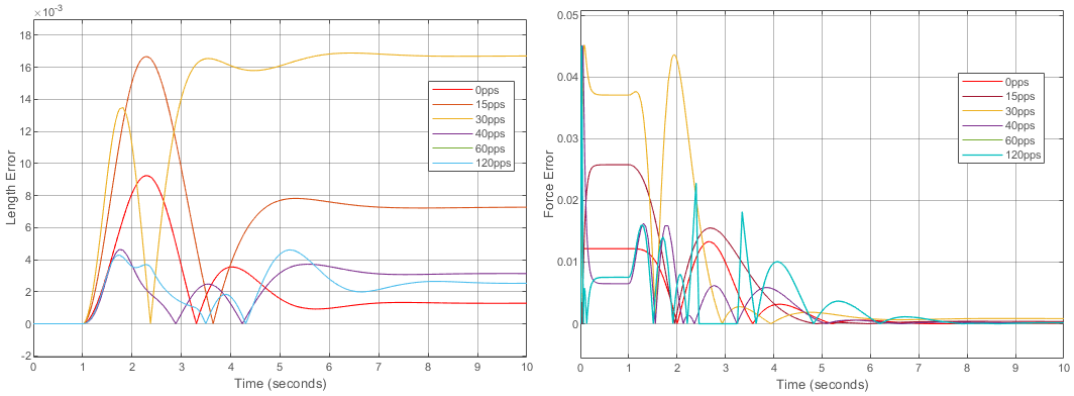

Figure 3.11: Error between the dynamics of the Evaluation model and the Control model at different frequency of activation

The results obtained from the simulations can be defined as satisfactory. Since with reference the figure 3.11, it is seen that after a transient response the muscle stabilizes at a certain length value. And by changing the activation frequency then a variation of the equilibrium would occur properly. Such a trend is well represented by the two models in a very similar way so that the deviation by the two responses can be practicably neglected.

3.4 Length Control

In order to implement a simple length control in the system described by the experiment in the previous section, a PI controller has been designed. To be able to properly tune the regulator, the system was linearized. The linearization procedure followed can be summarized by the following steps:

- Definition of a point of equilibrium. Since the model of the isometric force produced by the muscle has been expressed as a function dependent on two parameters, the muscle subjected to external forces settles at a given length of equilibrium, L_p, for a given frequency of excitation, α_p. As the frequency of excitation changes, a change in the equilibrium length will also be appreciated. The point $P = (L_p, \alpha_p)$ has been called the equilibrium point.

- Once the point P has been defined, the force generated by the muscle can be linearized through Taylor expansion in the first order of derivation:

$$F_{EM_{Lin}} = \frac{\partial F_{EM}}{\partial L}(L - L_p) + \frac{\partial F_{EM}}{\partial \alpha}(\alpha - \alpha_p) + F_{EM}(L_p, \alpha_p) \tag{3.8}$$

  In this case, it has been chosen to linearize the evaluation model arbitrarily; The same process can be carried out also for the Control model and the results would be similar.

- The equation of equilibrium of the system can be now computed using the linearized force:

$$(M + m) \cdot \ddot{L} = P - F_{EM_{Lin}} + \beta \cdot \dot{L} + K \cdot L \tag{3.9}$$

  Where M is the external mass which imposes an axial, stretching force P on the muscle; m represent the mass of the muscle and K, β are the parallel stiffness and parallel damping factor acting in series with respect to the muscle (with reference to the figure 3.5). Since the derivative is not affected by offsets, then the first and the second derivative can be considered as the variation of the quantity $(L - L_p)$. So that the equation (**??**) can be rewritten as:

$$(M + m) \cdot \frac{d^2(L - L_p)}{dt^2} = P - F_{EM_{Lin}} + \beta \cdot \frac{d(L - L_p)}{dt} + K \cdot L \tag{3.10}$$

- Assembling the state space model starts with defining two states: x_1, the deviation of the length, $(L - L_p)$, and x_2, the rapidity of variation of the deviation itself, $\frac{d(L-L_p)}{dt}$. As the input of the system, u, considered as the deviation of the frequency of activation from the equilibrium frequency selected α_p; It can be now expressed the state-space representation as:

$$\mathrm{A} = \begin{pmatrix} 0 & 1 \\ \frac{K - \frac{\partial F_{EM}}{\partial L}}{M+m} & \frac{\beta}{M+m} \end{pmatrix}; \qquad \mathrm{B} = \begin{pmatrix} 0 \\ \frac{-\frac{\partial F_{EM}}{\partial \alpha}}{M+m} \end{pmatrix}; \qquad \mathrm{C} = \begin{pmatrix} 1 & 0 \end{pmatrix};$$

  In this way the equation of the variation in time of the states and the equation of the output of the system can be written as:

$$\begin{pmatrix} \dot{x}_1 \\ \dot{x}_2 \end{pmatrix} = [A] \cdot \begin{pmatrix} x_1 \\ x_2 \end{pmatrix} + [B] \cdot u$$

$$L = [C] \cdot \begin{pmatrix} x_1 \\ x_2 \end{pmatrix}$$

- Subsequently, from the equations of states, we were led back to the transfer function of the system. Which resulted to be a second-order system with two imaginary poles. This transfer function was then multiplied with a filter of the first order which goes to model the dynamic assumed by the activation frequency during stimulation of the muscle and made the overall system more robust.
- Thanks to the linearized system represented by the transfer function found so far, then the design of the PI was possible.

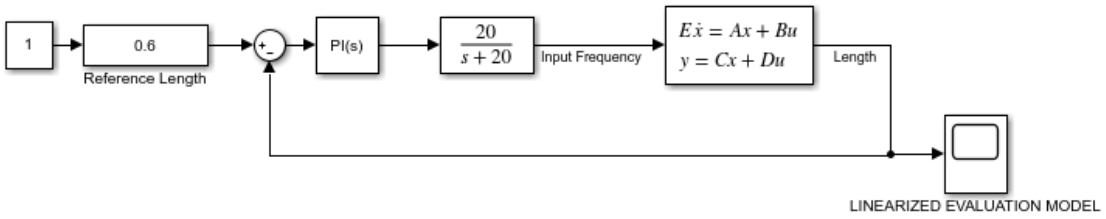

Figure 3.12: Linearized system control scheme

The PI regulator was tuned exploiting a MATLAB toolbox called 'controlSystemDesigner', which allowed the manipulation of the parameters of the controller so that the optimal design of the controller itself could be carried out.

Proportional Gain	Integral Gain
-33.1275	-132.5100

Table 3.3

The controlled response of the linearized system showed a settling time of about 4sec and good tracking of the reference length.

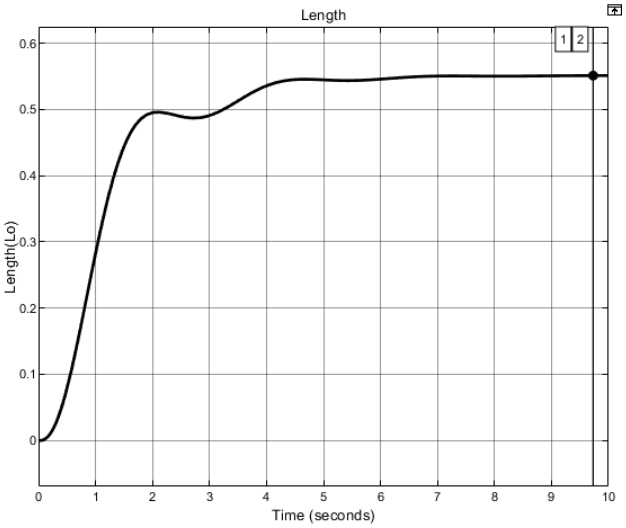

Figure 3.13: Response of the linearized system controlled by a PI regulator

The designed regulator was then inserted in the scheme of the system represented in figure 3.9 described in the previous section. The response of the non-linear system showed the same accuracy in following the reference signal in comparison to the linear one, but it also showed an overshoot of about 65% of the reference signal.

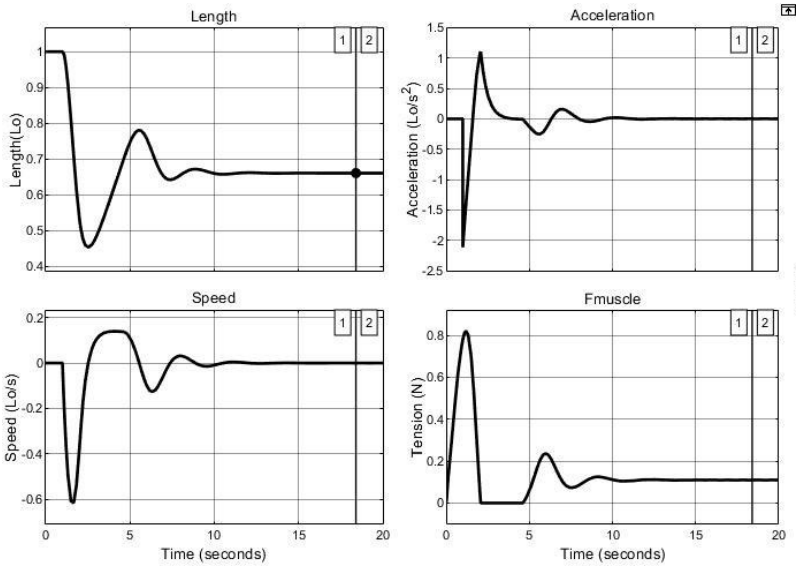

Figure 3.14: Response of the non-linear system controlled by a PI regulator

In order to overcome this drawback, it has been though to adjust the proportional gain of the PI regulator so that the overshoot could be reduced to be practicably null. The parameter of the PI controller customized for the non-linear model:

Proportional Gain	Integral Gain
-16.5638	-132.5100

Table 3.4

The trend of the final result is then shown in the figure down here.

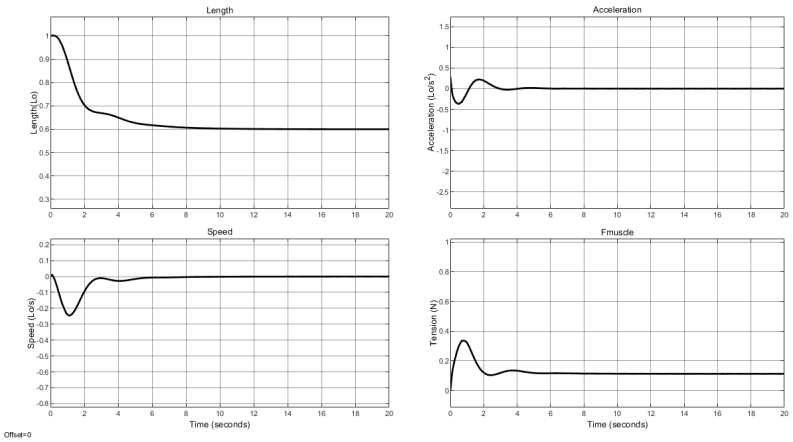

Figure 3.15: Response of the non-linear system controlled by a PI regulator with an adjustment on the proportional gain

In conclusion, due to a proper tuning of a PI regulator, which can be carried out on a linearized system, a length control of the non-linear system can be achieved with good accuracy in tracking the reference length.

Conclusion and Future Works

One of the fundamental parts in the design of a control scheme is the synthesis of a model able to describe the plant of the system. In our case, the goal we set was to understand the phenomenon of force production exploited by the muscle during active contraction and model this behavior in the view of a design of an antagonist control for the motor regulation of movement of limbs. For this purpose two models have been defined: the Evaluation model, and the Control model. The target of the Evaluation model is to describe the main characteristics of the phenomenon of force production, neglecting to yield, and recruitment of muscle fibers. Therefore, it simplifies the comprehension of muscle behavior and facilitates the computations, obtaining satisfactory results. However, the Evaluation model, as it is defined, is not implementable in the design of a controller due to its remarkable non-linearity in expression. In order to overcome such a complication, it has been developed a second prototype, called Control model. Such a model was designed as a linear product between two polynomials functions;
The approach adopted for the synthesis of the Evaluation model was to implement a curve-fitting procedure with the data found in literature from experiments belonging to other researches. The model describes the total isometric force developed by a muscle as a composition of two terms: one, called active force, is dependent on the activation frequency and the length assumed by the muscle; this component describes the overall force coming from the cycling of cross-bridges. The second component, named passive force, is found to be dependent only on the muscle length, and it represents the behavior of the mechanical structure of the entire muscle considered. The active force is described as a Normal distribution along the axis of the lengths; while the Passive force is described as a Sigmoidal function that provides a theoretical and approximate form to the overstretching behavior muscle fibers could assume. In the Control model design, the approach used was to extract the necessary data from the evaluation model and then to look for suitable polynomial functions that could satisfy the imposed linear form. Both models were designed in such a way as to be able to simulate the strength response of any muscle belonging to any animal. To this end, the two prototypes have a certain number of degrees of freedom which must then be tuned according to the nature and type of muscle considered.
Through comparisons between the developed models and the experimental data, their validity has been demonstrated. Furthermore, as regards the Evaluation model, average deviations of not more than 6% were found by analyzing the errors. On the other hand, as regards the Control model, an average error of less than 3% was calculated, in comparison with empirical data coming from cats Caudiofemoralis; While an average error of about the 15-17% was computed from a comparison with

empirical data obtained from a Gastrocnemius of a rat and a Sartorius of a frog, after a proper tuning of the degrees of freedom of the model; Shown in the Appendix. In order to obtain far more accurate results, it could be necessary to reconstruct the Control model itself so that it can be customized to the new curve assumed by the Evaluation model.
The two models also have the same trend as a function of time. Through a simulation of a simple experiment of imposed force, an error not higher than 4.5% was found between the trends traced by the two models. Furthermore, it has been shown that a length control of the mechanical system of the experiment rendered non-linear by the behavior of the muscle is made possible through a process of linearization. By tuning a PI controller, a certain dynamics was imposed on the linearized system. By proposing this length control also for the non-linear system, the results were excellent, with high accuracy in following the reference length. Through a proportional gain adjustment, the overshoot was also made very low, almost zero.
The built models can, therefore, be considered suitable to be used and implemented in the study and design of a control scheme. As a parallel work, we set ourselves the goal of also modeling the effects of reflexes in order to provide a more complete description of the muscle response under an imposed stimulation.
To make the model of extrafusal fibers more accurate and complete, muscle response may also need to be modeled under isotonic conditions. So in situations where it is present a component of muscle force dependent on the velocity of motion assumed by the muscle itself. Unfortunately, due to the lack of adequate experimental data, it was not possible to synthesize this component. Therefore, as a future goal, it has been proposed to find valid and complete experimental data that could be used as a basis to design a model of muscle's force-production even in a condition of non-zero speed.

Appendix

Comparison of the Evaluation model with data coming from other animals

In the literature there were further data from experiments conducted on different animals and on different muscles. Comparisons were therefore made between these data and the proposed evaluation model to analyze their deviation.

Data provided by G.N.Askew and R.L.Marsh

In their article G.N.Askew & R.L.Marsh (1998), G.N.Askew and R.L.Marsh analysed the tetanic stimulation response of three mice Soleus muscles. The data of both the active and passive forces were extracted from the plot represented in figure below.

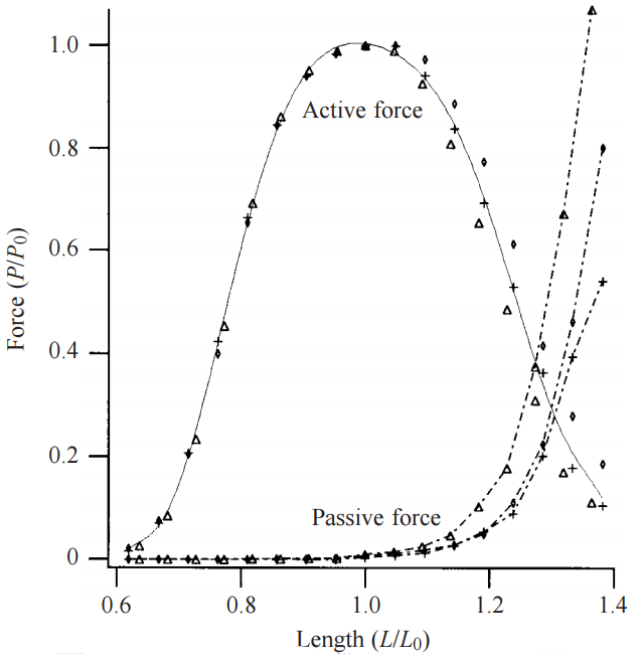

Figure 3.16: Active isometric force and passive force of three mice soleus muscles determined during tetanic stimulation. Both the two forces are found to be normalized with respect the optimal length L_0.

Active Force Validation

For the active isometric force, no distinction between the three mice data was considered, mainly because it was noticed that the measurements carried out for one mouse do not show a remarkable difference with data coming from the behavior of the muscle, belonging to a different mouse. So, practically a single set of empirical data was extracted and examined.

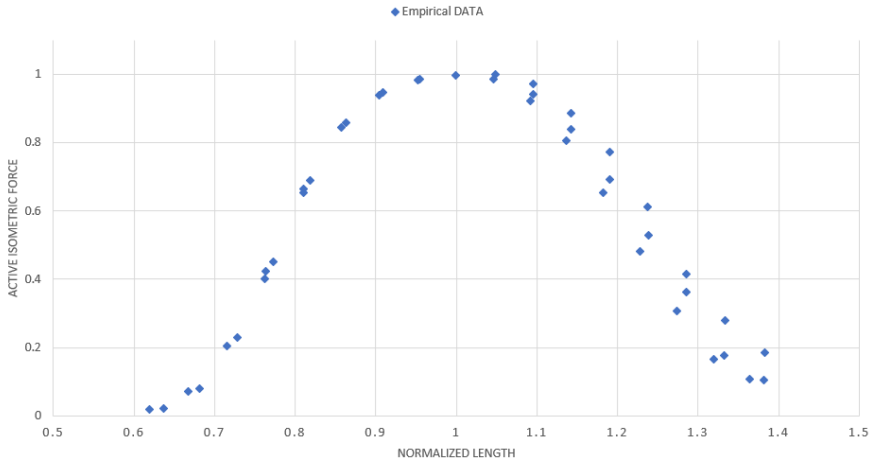

Figure 3.17: Re-plotted data of the Active Isometric Force provided by G.N.Askew and R.L.Marsh found in the figure 3.16 found in the article: I.E.Brown et al. (1999)

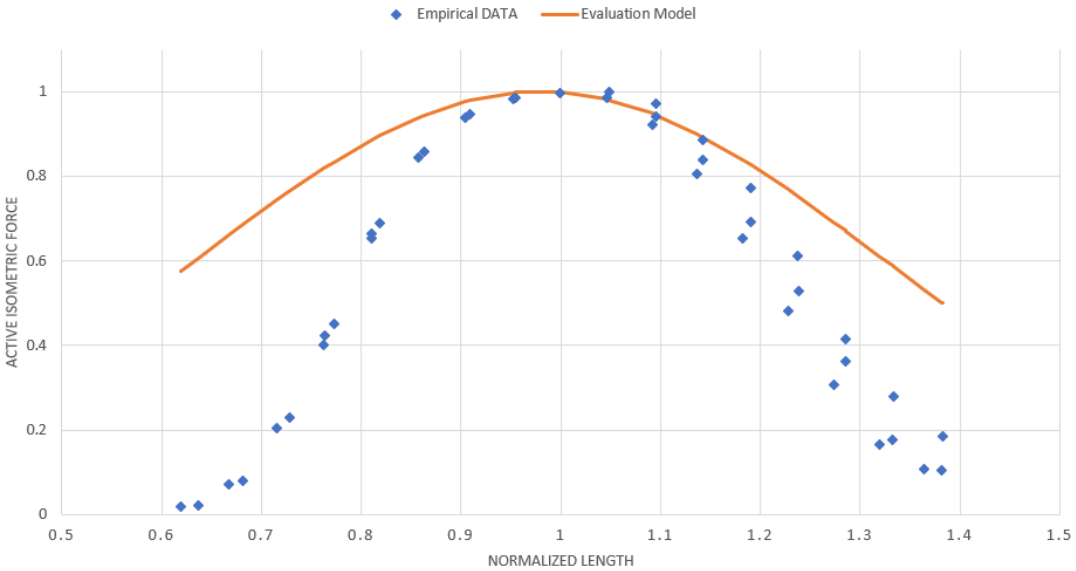

Figure 3.18: Plot comparison between the empirical data of the experiments on the Active Isometric force conducted by G.N.Askew and R.L.Marsh., shown in figure 3.17

As can be seen from the figure above (3.18) a not negligible error occurs at length distant from the optimal one. However, it is necessary to underline that this comparison, while treating normalized quantities, maintains dependence on the nature and structure of the muscle on which the Evaluation model was built. Therefore, since, the model is based on the empirical data, collected by I.E.Brown,

E.J.Cheng, and G.E.Loeb on cats' Caudiofemoralis; While the data reported by G.N.Askew and R.L.Marsh, as it has been stated at the beginning of this section, comes from three mice Soleus, then the high error is due to the inconsistency between the animal and the muscle considered by both sides. The trend of the error is shown in the following figure:

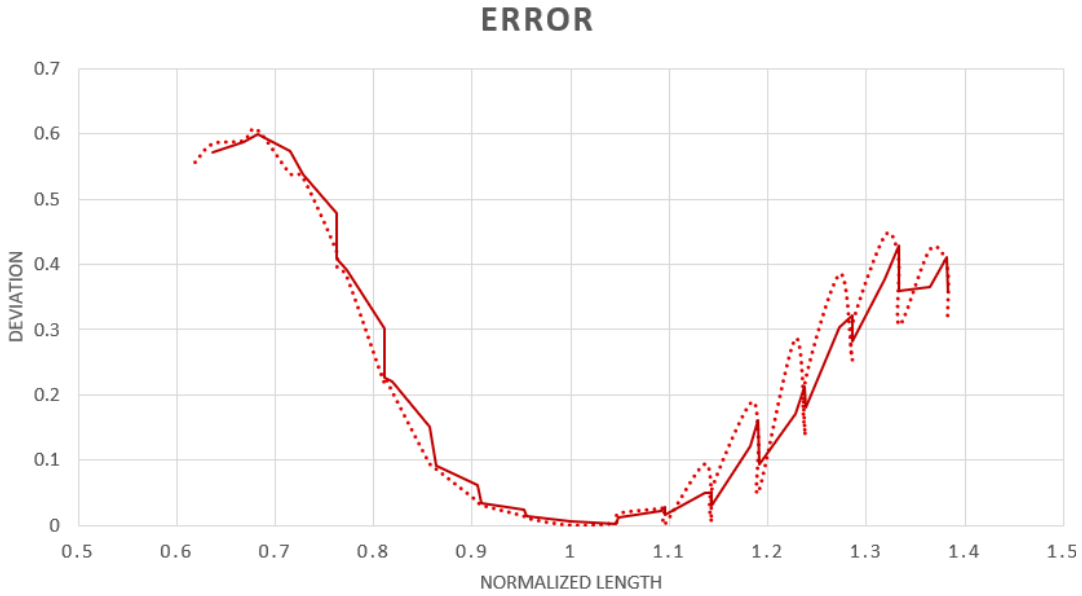

Figure 3.19: Plot showing the trend of the Deviation between the values of Active Isometric Force provided by the Evaluation model and the empirical data coming from the experiments carried out by G.N.Askew and R.L.Marsh in dotted line; While in thick continuous line it is shown the moving average of the error.

In order to provide a quantitative measure of the average error along with the interval of lengths considered, the function used to compute the average deviation was the same error function Err_{Active} defined in the subsection 2.6.1 (2.20); However, in this case, n, which represent the number of sampled data, is 42; The index j can be neglected since these experimental data are referred to the same activation frequency, and Measured_Data are the data provided by Askew and Marsh's experiments. The error function counted the 24% of error between the data and the Evaluation model. Despite this large error, it can be seen from the plot comparison 3.18 that the trend of the Evaluation model (which is known from construction to be a Normal distribution), and the trend followed by the empirical data are very similar. This consideration leads to the next step of the comparison: Optimized Parameter Tuning.

Optimized Parameter Tuning of the Active Force

Just as the Evaluation developed model has been defined, it is possible to tune its parameters, represented by the matrix C (regarding the active isometric force only), in such a way as to minimize the error with the experimental data. In order to perform the tuning of the parameter matrix, a tool of Excel was exploited, called

"Solver", that uses techniques from the operations research to find optimal solutions for all kind of decision problems.

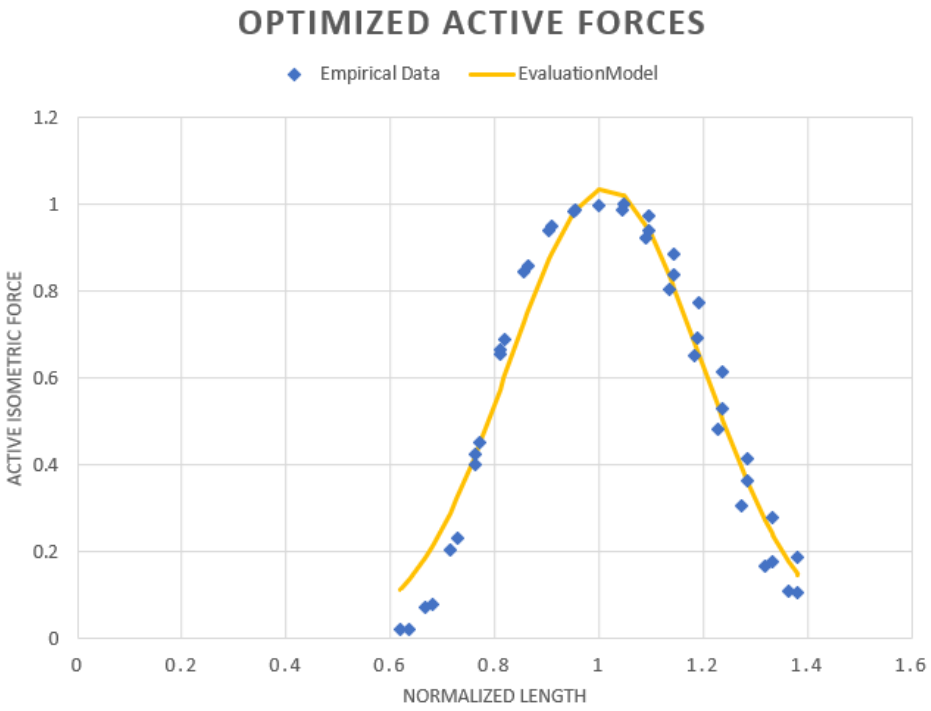

Figure 3.20: Plot comparison between the empirical data of the experiments on the Active Isometric force conducted by G.N.Askew and R.L.Marsh after the parameter optimized tuning.

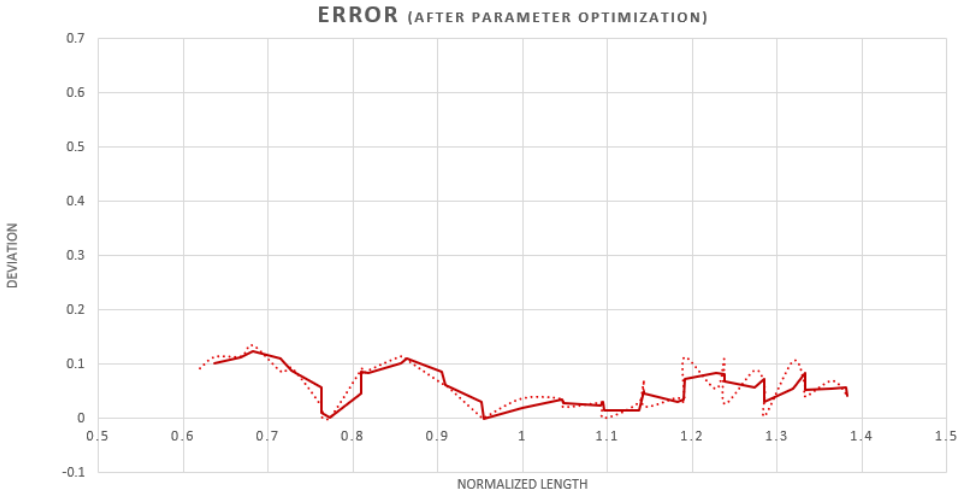

Figure 3.21: Plot showing the trend of the Deviation between the values of Active Isometric Force provided by the Evaluation model and the empirical data coming from the experiments carried out by G.N.Askew and R.L.Marsh after the parameter optimized tuning (dotted line); While in thick continuous line it is shown the moving average of the error.

After the optimized tuning of the parameters, the error computed by the function

(2.20) dropped to the 5.74%.
In conclusion, thanks to an appropriate tuning of the matrix C, it is possible to obtain a model that manages to represent the distribution of the empirical data with great accuracy. This process can also be used as validating evidence that the Evaluation model developed is valid and correct since its structure has not been altered during the optimized tuning process.

Passive Force Validation

As for the passive forces, (plot in the figure 3.16), two distinct data sets can be broadly distinguished, despite the experiment was conducted on three mice.

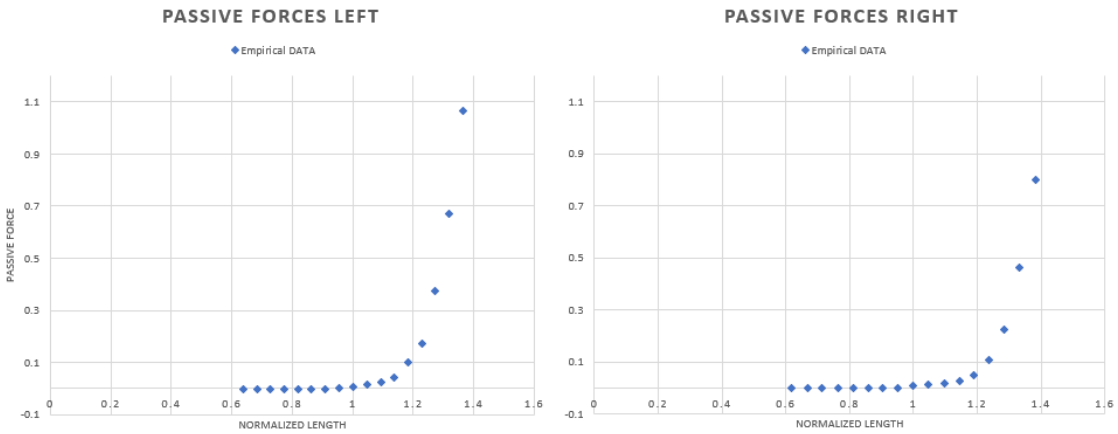

Figure 3.22: Re-plotted data of the Passive Force provided by G.N.Askew and R.L.Marsh found in the figure 3.16 found in the article: I.E.Brown et al. (1999)

It is defined as Right-passive, the set of data, collecting the behaviour of two mice soleus muscles, represented by crosses and rhombus, in the figure 3.16; And it is then defined as Left-passive, the set of non considered data from the Right-passive set, which are represented by triangles, in the same figure linked above.

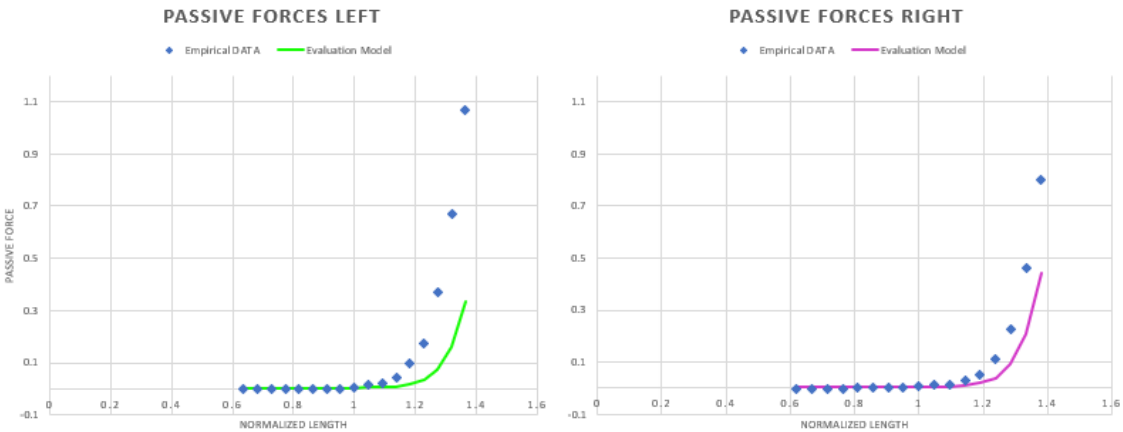

Figure 3.23: Plot comparison between the empirical data of the experiments on the Passive force conducted by G.N.Askew and R.L.Marsh., shown in the figure 3.17

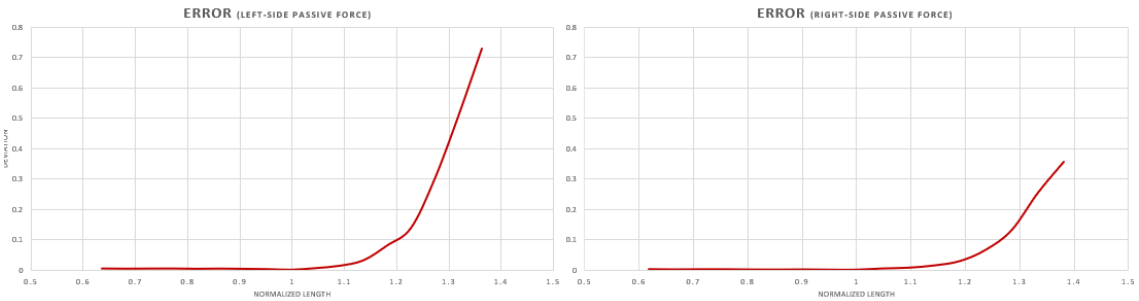

Figure 3.24: Plot showing the trend of the Deviation between the values of Passive Force provided by the Evaluation model and the empirical data coming from the experiments carried out by G.N.Askew and R.L.Marsh.

From how it can be seen, the plot comparison in figure 3.23 and from the plot representing the error trend in figure 3.24, the set of data related to the passive force of the right side shows less error. However, just considering the progression of the empirical data along the length axis, both the plots, validate the evaluation model. The error, in this case, can be computed through the function 2.21, considering n equal to 17, and as Measured_Data, both the set of data considered from G.N.Askew and R.L.Marsh experiments:

Left-Passive Error	Right-Passive Error
11.0%	5.4%

Table 3.5

The table, shown above, underlines the previously discussed circumstances, where between the two data sets, the one referred to the results obtained from experiments on two mice is the one in which the developed model is closest too. In this case, although no parameter optimization process has been used, the best average error obtained is already found to be at acceptable levels. And remembering that passive forces, because of their dependency on the structure of the muscle considered, do not normalize well, this can be defined as a remarkable result that can be added as evidence that validates the developed model.

In conclusion, looking at these results from a second point of view, it can be seen that the contractile active force, despite maintaining its shape dictated by a Normal distribution, generated by lengths at a certain distance from the optimal one varies substantially from animal to animal. This consideration explains why a parameter tuning process (matrix C in this case) is required. On the other hand, as has just been demonstrated, as far as passive force is concerned, it shows less dependence on the animal considered but is more affected by the structure and mechanical nature of the muscle considered.

Other Data

Other experimental data were found in graphs in which, however, a direct correspondence of the origin of such data was not specified. These data correspond to the stimulation of the Sartorius of a frog at a temperature of 0 ° C and the excitation of a Gastrocnemius of a rat:

Frog Sartorius Data

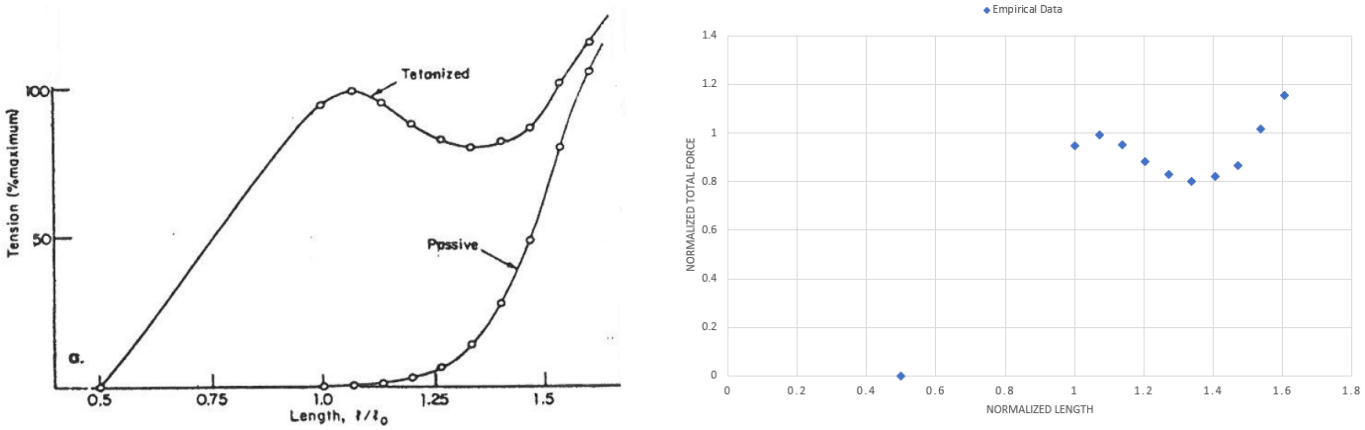

Figure 3.25: Plot containing the data referred to an experiment on a frog sartorius at 0°C in tetanus activation frequency

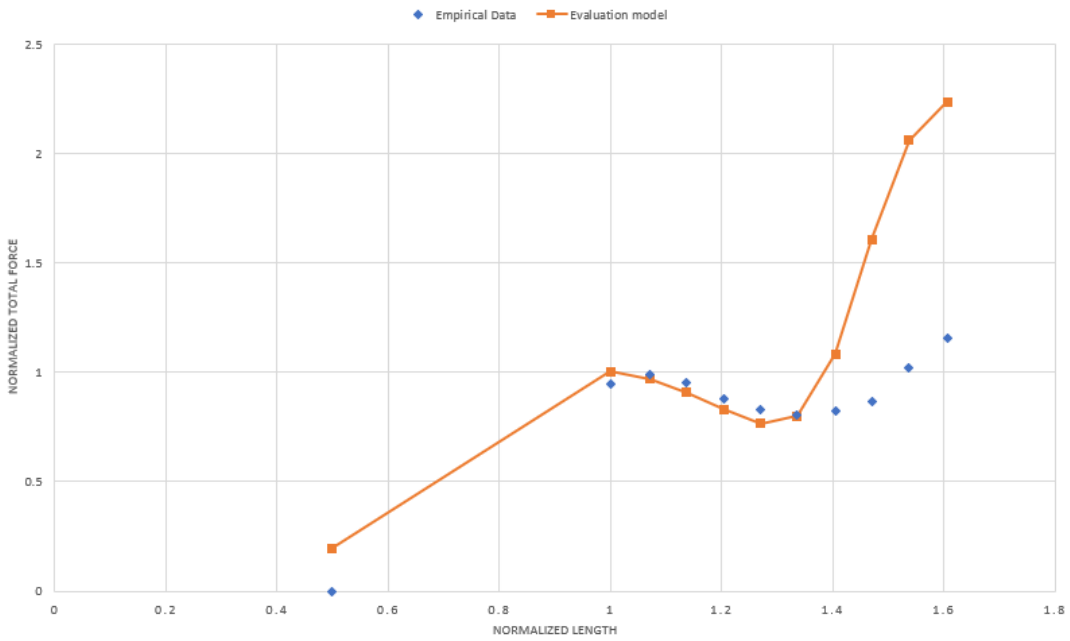

Figure 3.26: Plot comparison between the empirical data of the experiments on the Total force conducted on a frog sartorius muscle, shown in the figure 3.32

As can be seen from figure 3.26 the substantial difference in this behavior is perceived at stretch lengths where the dominant force component is the passive:

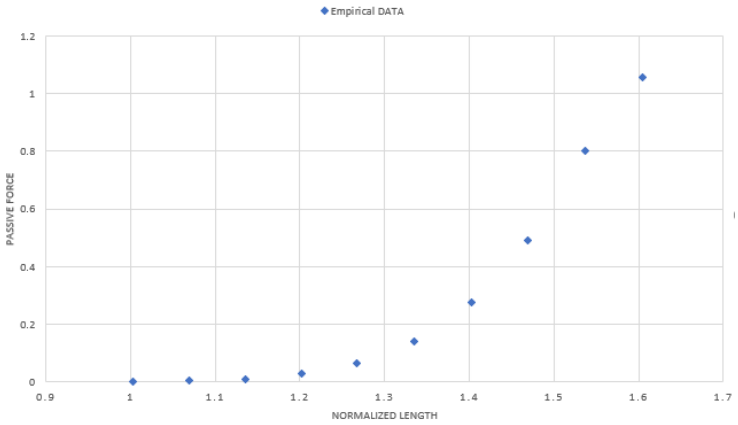

Figure 3.27: Re-plotted data of the passive force of a Frog Sartorius tetanically stimulated,taken from the left-side plot on the figure 3.32

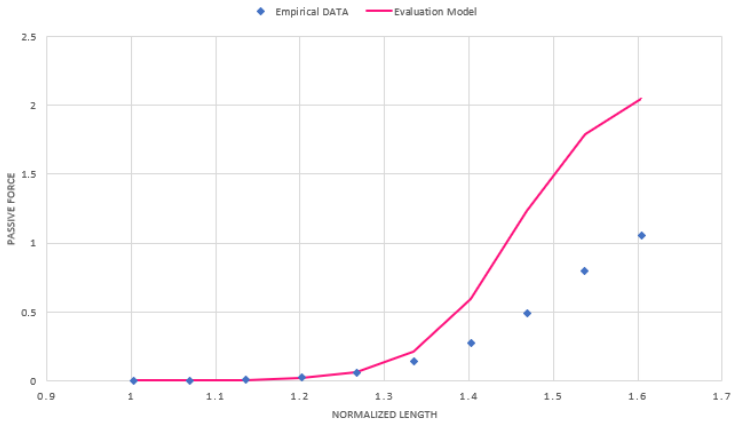

Figure 3.28: Plot comparison between the data of the passive force of a Frog Sartorius tetanically stimulated at 0°C, and the evaluation model

Therefore, as can be seen from the comparison between the experimental data and the data provided by the passive force model, the shape of the curve is almost the same; So to adapt and evaluate whether the developed Evaluation model can also simulate the behavior of the data provided, an optimized tuning process is required to set the parameters of the passive force (in this case passive stretching force) described by the vector p_l (2.5.2.1). The average error estimated was :

Total force	Passive Force
32.35%	31.26%

Table 3.6

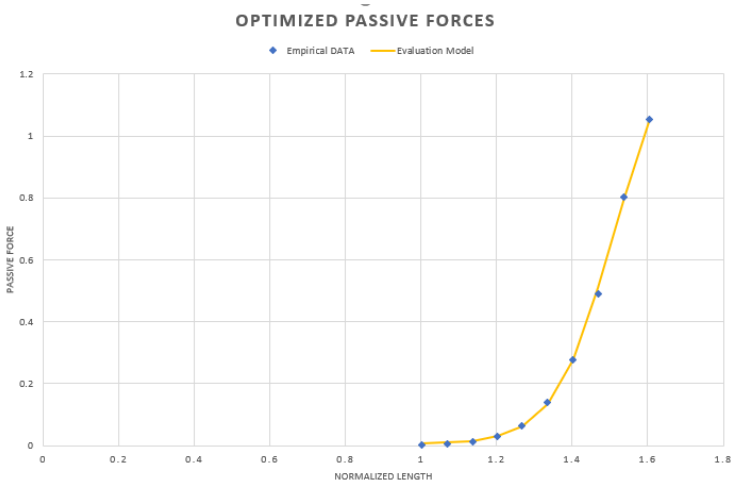

Figure 3.29: Plot comparison between the data of the passive force of a Frog Sartorius tetanically stimulated at 0°C, and the evaluation model, after a re-tuning of the model parameters

Performing also tuning of the parameter of the matrix C, related to the isometric active tension behavior, the total force in comparison with the empirical data shows an appreciable result:

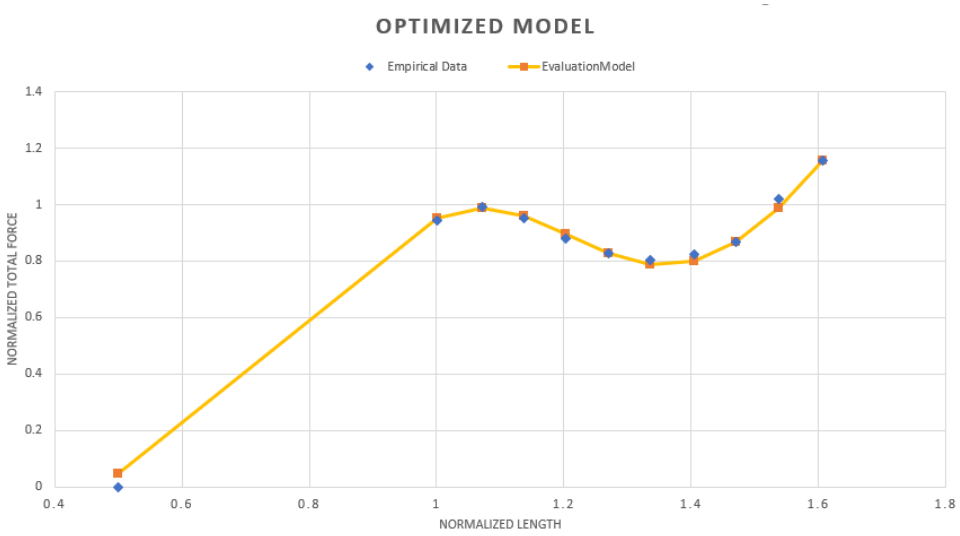

Figure 3.30: Plot comparison between the data of the total force of a Frog Sartorius tetanically stimulated at 0°C, and the evaluation model, after a re-tuning of the model parameters

In this case then, computing the error:

Total force	Passive Force
1.30%	0.39%

Table 3.7

a significant improvement can be noted, which brings the average error to almost negligible values. So then,also with regard to this comparison, the validity of the model is successfully confirmed as, after a proper tuning of the parameters, the trend of the evaluation model simulate the empirical data with a noticeable accuracy.

Rat Gastrocnemius Data

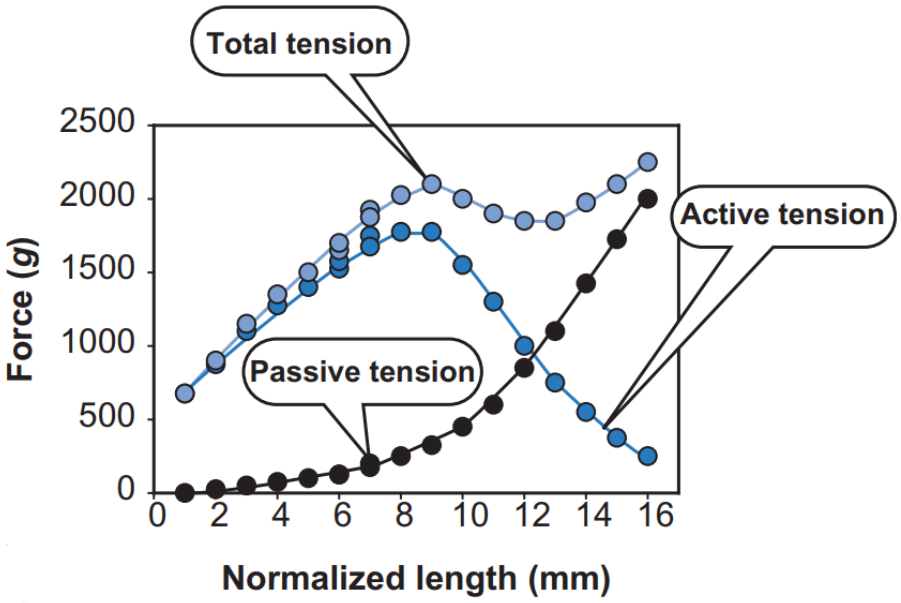

Figure 3.31: Plot containing the data referred to an experiment on a Rat Gastrocnemius under tetanus activation frequency. Figure taken from Feher (2016)

The data provided by the graph in figure 3.31 are not normalized, therefore after performing the extraction, these data were normalized according to the same criterion for which the data used in the construction of the evaluation model were normalized; So defining as L_0, the optimal length, in which the muscle reports the maximum active contractile force, lengths were normalized according to L_0 (in this case measured as 0.90mm) and normalizing the force according to the maximum active contractile force (in this case measured as 2.11g) generated by the muscle.

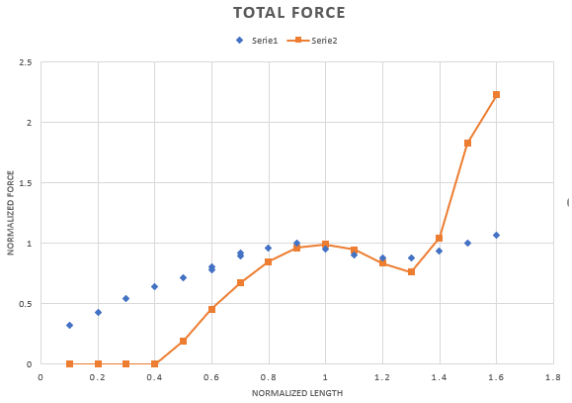

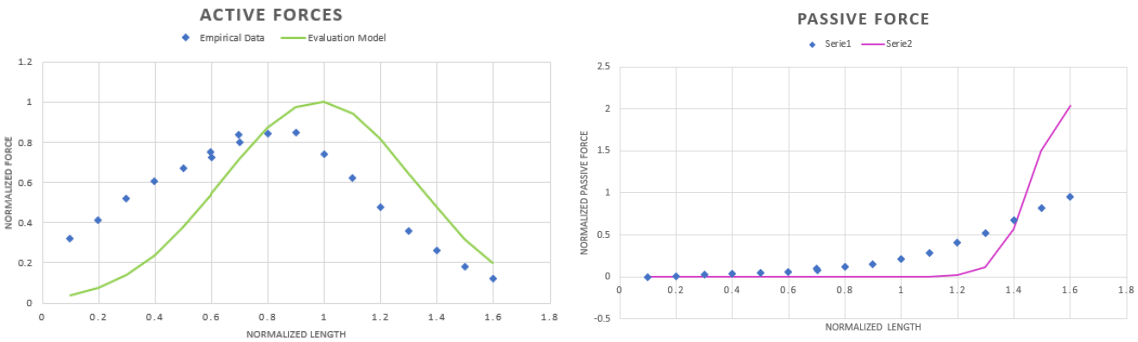

Figure 3.32: Plot comparison between the data of the total force, the active isometric force and the passive force of a Rat Gastrocnemius tetanically stimulated, and the evaluation model

As can be seen from the graphs shown above, although the trends are maintained, the error of the Evaluation model is high. However, as has been pointed out previously, this error is caused by the fact that the evaluation model was developed considering empirical data of the Caudiofemoralis of cats; It is therefore not surprising that empirical data from a rat's Gastrocnemius may show differences. By computing the average error with the equations defined in the previous comparisons, a deviation between the model and these data was assessed:

Active force	Passive Force	Total Force
23.38%	22.21%	33.84%

Table 3.8

In order to validate the Evaluation model using these empirical data, then tuning of the parameters of both the active and the passive force was performed, exploiting the Solver tool of Excel, as it was done so far for the previous validation comparisons.

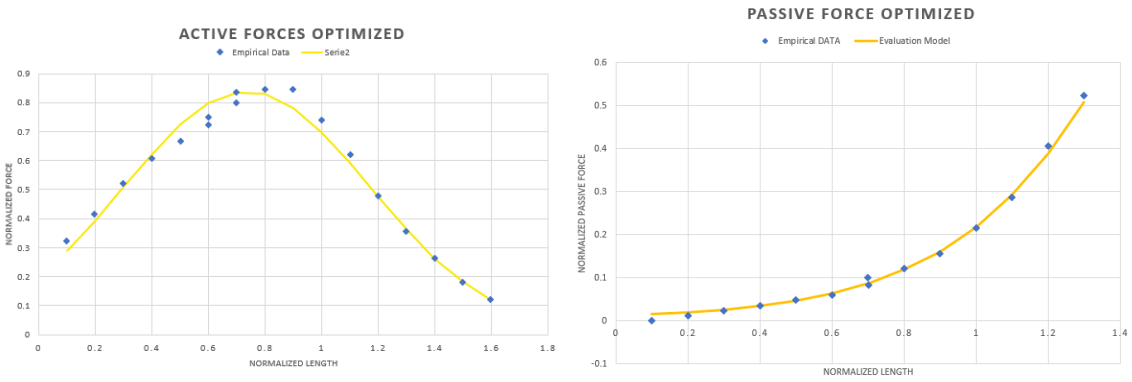

Figure 3.33: Plot comparison between the data of the total force, the active isometric force and the passive force of a Rat Gastrocnemius tetanically stimulated, and the evaluation model, after the tuning of the parameters.

As shown in the plots of figure 3.33, the trend of the model can be said to follow the experimental data with high precision, reporting average error values:

Active force	Passive Force	Total Force
2.70%	1.07%	2.65%

Table 3.9

In conclusion, it has been shown, throughout this whole section that through an appropriate parameter tuning, the developed evaluation model is capable of simulating muscle performance with an accuracy that does not exceed 3% of error. These results can, therefore, be considered satisfactory in validating the model.

Comparison of the Control model with data coming from other animals

The data considered take into account a Sartorius of a frog and a Gastrocnemius of a rat. These data were previously used to validate the evaluation model and can be found in figures 3.32 and 3.31 respectively.

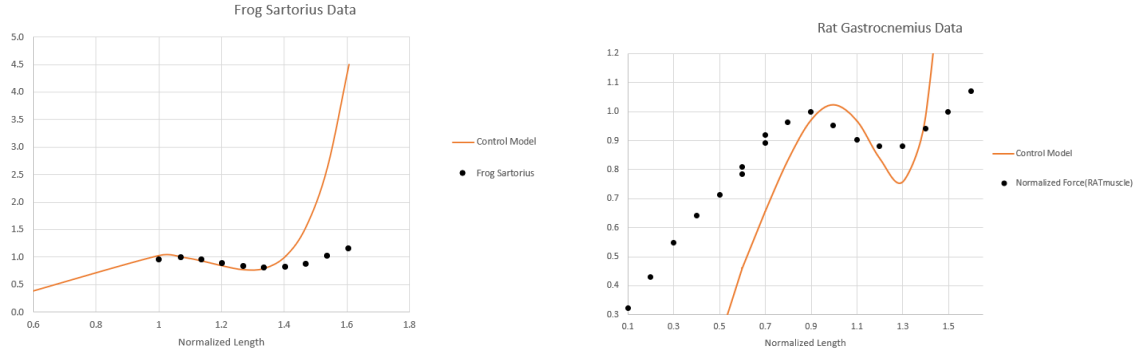

Figure 3.34: Plots comparing the trend of the Control model(orange continuous line) and the trend along the length axis of the Empirical data collected from experiment conducted on a frog Sartorius(on the left-side) and experiments conducted on a rat Gastrocnemius(on the right side).

The average error computed for these two comparison results to amount of:

Type of muscle	Frog Sartorius	Rat Gastrocnemius
Average Error in %	57.21%	45.70%

Table 3.10

In this case, the error for both data-sets turns out to be much higher than measured for the evaluation model. A plausible explanation for this result can be found in the fact that, as has also been noted for the evaluation model, it can be found the greatest erroneous peaks at high stretch lengths, therefore, caused by the passive. To confirm this hypothesis we can take advantage of the comparison previously carried out with the Brown, Cheng, and Loeb data, where it is shown that, in the length range where the behavior of the active force prevails, the error between evaluation model and control model is practically negligible. So it can be concluded that this difference of error is caused by the divergences between the passive forces of the two models, which cause a worsening in the accuracy of the control model.
Furthermore, tuning of the control model parameters is very complex and expensive in terms of computation, so much so that it is unable to obtain satisfactory outcomes, that reduce the error. It can, therefore, be concluded from these results that to obtain an accurate and simple Control model that is able to describe the behavior of different muscles belonging to different animals, it is necessary to retrace the procedure described in section 3.2 to tune the parameters through a data fitting procedure.

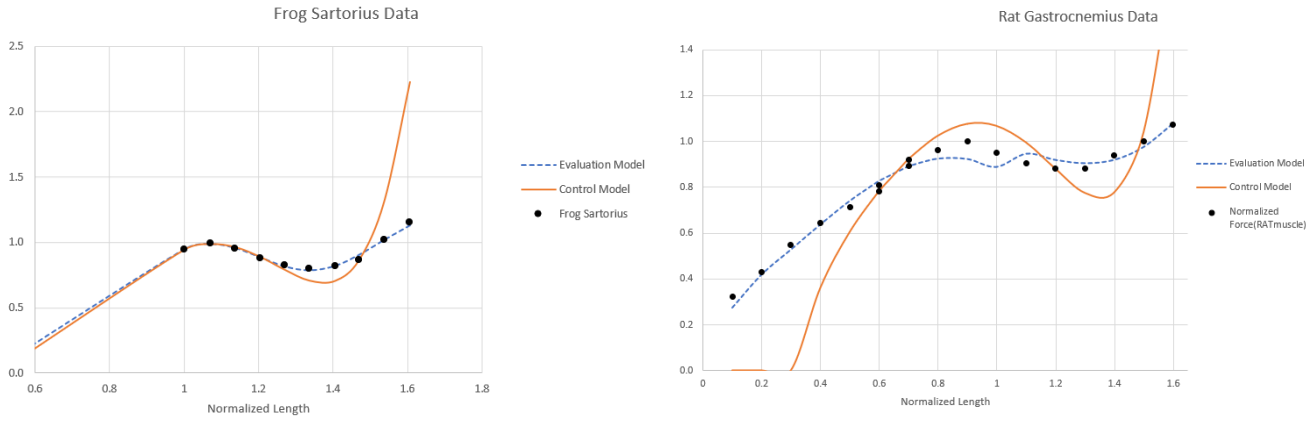

Figure 3.35: Plots result after a re-fitting procedure in order to tune the matrix H (3), and matrix R. In orange line the trend of the Control model and in black dots the empirical data are represented, and in dotted blue line the trend of the evaluation model properly tuned. (3).

Computing the average error after a tuning on the Control model:

Type of muscle	Frog Sartorius	Rat Gastrocnemius
Average Error in %	14.98%	17.33%

Table 3.11

As can be seen from the table above, the average error dropped to values less the 20%. The result obtained can be considered satisfactory for a control model whose main purpose is simplicity, which allows an implementation of the control itself, predisposed to control purposes. However, it can be of interest to understand why the re-fitting procedure did not provide better results: Despite it has been used the same number of sampled data and the same procedure in fitting the data of the evaluation model properly tuned; A different result was obtained for the three animals. This lead to the conclusion that a satisfactorily Control model can be obtained for any muscle belonging to any animal, as it has been demonstrated; But, in order to obtain an accurate Control model which shows a very low average error in comparison with the empirical data, it's is possible only, in case re-designing the Control model is performed or conducting a deep analysis of the degrees of freedom, requiring a considerable amount of computation and a big expense of time.

Bibliography

A.F.Huxley 1974, *Muscular Contraction.A review lecture*, J.Physiol, 243, 1

A.F.Huxley R.M.Simmons 1971, *Proposed mechanism of force generation in striated muscle.*, Nature(London), 233, 533

A.V.Hill 1938, *The heat of shortening and the dynamic constants of muscle*, Proc Roy Soc Lond B, 126, 136

A.V.Hill 1997, *The heat of shortening and the dynamic constants of muscle*, Proc. R. Soc. Lond., B126, 136–195

Baraghini N., 2020, *Report 3*

Biewener A., Gillis G., 1999, *Dynamics of Muscle Function During Locomotion: Accommodating Variable Conditions*, The Journal of Experimental Biology, 202, 3387

Brown I., Loeb G., 1999, *Measured and modeled properties of mammalian skeletal muscle I. The effects of post-activation potentiation on the time course and velocity dependencies of force production*, Journal of Muscle Research and Cell Motility, 20, 443

Brown I., Loeb G., 2000a, *Measured and modeled properties of mammalian skeletal muscle III. The effects of stimulus frequency on stretch-induced and force enhancement and shortening-induced force depression*, Journal of Muscle Research and Cell Motility, 21, 21

Brown I., Loeb G., 2000b, *Measured and modeled properties of mammalian skeletal muscle IV. Dynamics of activation and deactivation*, Journal of Muscle Research and Cell Motility, 21, 33

D.Purves G.J.Augustine D. e. a., 2001, *Neuroscience. 2nd edition.*

D.V.Knudson 2006, *The Biomechanics of Stretching*, Journal of Exercise Science Physiotherapy

F.Curto 2020, *Modellazione della forza isometrica muscolare: L'effetto dei riflessi muscolari sul sistema*

Feher J., 2016, *Quantitative Human Physiology. An Introduction*

G.C. Joyce P. R., Westbury D., 1969, *The mechanical properties of cat soleus muscle during controlled lengthening and shortening movements*, The journal of Physiology, 204, 461

G.N.Askew R.L.Marsh 1998, *Optimal shortening velocity (V/Vmax) of skeletal muscle during cyclical contractions: Length-Force effects and velocity-dependent activation and deactivation*, The journal of Experimental Biology, 201, 1527

Guyton A., Hall J., 2006, *Textbook of medical physiology 11th ed.*

H.S.Gasser A.V.Hill 1924, *The dynamics of muscular contraction*, Proc Roy Soc Lond B, 96, 398–437

Hill A., 1938, *The heat of shortening and the dynamic constants of muscle*, Proceedings of the Royal Society of London, 126, 136

Hogan N., 1984, *Adaptive Control of Mechanical Impedance by Coactivation of Antagonist Muscles*, IEEE Transaction on automatic Control, 29, 681

Huxley A., 1957, in Butler J., Katze B., eds, , Progress in Biophysics. McMillan Company, New York, Chapt. 7, pp 257–310

I.E.Brown E.J.Cheng G.E.Loeb 1999, *Measured and modeled properties of mammalian skeletal muscle II. The effects of stimulus frequency on force-length and force-velocity relationships*, Journal of Muscle Research and Cell Motility, 20, 627

Inc. W. R., , *Mathematica, Version 12.1*, https://www.wolfram.com/mathematica

J.M.Winters 1995, *An Improved Muscle-Reflex Actuator for Use in Large-Scale Neuromusculoskeletal Model*, Annals of Biomedical Engineering, 23, 359

MathWorks, *MATLAB R2020a*, https://www.mathworks.com/products/matlab.html

McMahon T., 1943, *Muscles, Reflexes, and Locomotion*

Rack P., Westbury D., 1969, *The effects of length and stimulus rate on tension in the isometric cat soleus muscle*, The journal of Physiology, 204, 443

Rall J., 2014, *Mechanism of Muscle Contraction*

Rohatgi A., , *WebPlotDigitizer, Version 4.2*, https://automeris.io/WebPlotDigitizer

Sweeney H., Hammers D., 2018, *Muscle Contraction*

Tsianos G., Loeb G., 2017, *Muscle and Limb Mechanics*

U.Jensen 2016, *Design Considerations and Application Examples for Embedded Classification Systems*